A SOLID STATE NMR and MS CHARACTERISATION of the CHEMICAL COMPOSITION of MIMOSA BARK EXTRACT

Thesis submitted in fulfilments of the requirements for the degree

Master of Science in Chemistry

Department of Chemistry
Faculty of Agricultural and Natural Science

University of the Free State
Bloemfontein

by

NADINE D. SENEKAL

Supervisor: Prof. J.H. van der Westhuizen
Co-Supervisors: Dr. S.L. Bonnet and Dr. D. Reid

January 2011

ACKNOWLEDGEMENTS

Firstly I thank my Heavenly Father Yahweh for His guidance and support during the last year. He has blessed me with health, perseverance and surrounded me with my wonderful family and friends and I cannot express my gratitude enough.

My thanks and appreciation to the following people as well:

Prof. J. H. van der Westhuizen as supervisor, Dr. S. L. Bonnet and Dr. D. Reid as co-supervisors for their invaluable guidance, advice, support and patience.

The University of the Free State, THRIP for financial support. Mimosa Extract Company (Pty) Ltd. for financial support and leather samples.

I spent a month with the Solid State NMR group of the Department of Chemistry at the University of Cambridge and would like to thank the Duer group, Dr. Dave Reid in particular, as well as other members of staff at the department, for their hospitality and their willingness to demonstrate the ins and outs of solid state NMR.

Prof. D. Ferreira and his team for synthesising dimers, trimers, tetramers and pentamers.

Dr. Gabré Kemp from Biochemistry, Prof. Thinus van der Merwe from FARMOVS-PAREXEL as well as Richard Turner and Asha Boodhun from the University of Cambridge, for the recording of MS data.

Mrs. Anke Wilhelm-Mouton and Mrs. Anette Allemann for the proof reading of the manuscript, countless cups of coffee and much appreciated moral support.

My father and mother, Jan and Rensche, I would like to thank profusely for raising me to respect knowledge and to regard it as a privileged gift and yet a challenge to achieve. Thank you for your love, trust, support and encouragement.

My sisters, Rensche, Laetetia and Célia, my brothers, Jan-Hendrik, Thys and Wimpie, my grandfather, Peet and especially my beloved husband Marcello, thank you for your love and support, advice and encouragement.

All my friends and the staff and fellow students at the Chemistry Department for advice and encouragement.

Nadine Senekal

DEDICATION

I would like to dedicate this work to my father, Jan Senekal.

Hierdie tesis is ‘n samevatting van my harde werk en jou inspirasie en liefde. Dankie vir die raad, moed inpraat en ongelooflike voorbeeld wat jy nog altyd vir my stel.

Contents

SUMMARY

Mimosa (*Acacia mearnsii*) also known as black wattle, and quebracho (*Schinopsis balansae, Schinopsis lorentzii*) are the major commercial sources of natural condensed tannins (proanthocyanidin oligomers) used today. Mimosa bark is harvested from commercial plantations in South Africa which, according to a survey done by the Department of Water Affairs and Forestry for 2001, cover an area of about 107 000 hectares in South Africa. Quebracho is extracted from the wood of natural forests in Brazil and Argentina. Mimosa bark is extracted with water (about 50% by weight). Tara (*Cæsalpinia spinosa*) and Italian chestnut (*Castanea sativa*) are the major commercial sources of hydrolysable tannins.

The ability of water soluble hydrolysable and condensed tannins (polyphenols) to react with proteins, presumably *via* hydrogen bonds, lies at the heart of their ability to transform raw hide into leather and their commercial application as tannin agents. It explains their existence in nature as anti-feeding agents as it renders plants indigestible to insects and herbivores. It also explains the use of milk in tea where the complexation of milk proteins with tea tannins reduces astringency. The chemistry of this process however remains uncertain. The polyphenolic nature also renders tannin extracts very susceptible to oxidation and further polymerisation and rearrangements that render the extracts even more complex. This is evident in the transformation of green tea (high flavan-3-ol content and low condensed tannin content) into Indian or black tea (low flavan-3-ol content and high condensed tannin content). The quality of red wine is to a large extent determined by the amount and composition (which changes during ageing in a poorly understood way) of its condensed tannin. The tannins react with protein receptors on the tongue to impart “mouth feel” characteristics. Wood-aged wine not only contains condensed tannins from grape skin, but also hydrolysable tannins from the wooden barrels it is aged in.

The polyphenolic nature of the aromatic rings allows reaction with electrophiles. This forms the basis of adhesive manufacturing, where formaldehyde is used to polymerise tannin extracts to form adhesives. Other commercial applications of tannin extracts include the use

as anti-foaming agents in oil drilling and the manufacturing of amine containing resins (*via* the Mannich reaction) for water purification applications (removal of heavy metals).

The production of mimosa condensed tannin is a sustainable process as trees are harvested every eight years. Tannins will become a more important source of feedstock nutrients, as crude oil, which is currently used, becomes depleted. It also creates employment in rural areas.

Higher oligomers of condensed tannins are built up by successive addition of flavan-3-ol monomer extension units *via* C-4 to C-8 or C-4 to C-6 interflavanyl bonds. Higher oligomers are impossible to purify by chromatography and other methods of analysis are required. Acid catalysed fission of the interflavanyl bonds and trapping of the monomer intermediates with toluene-α-thiol or floroglucinol followed by analysis of the trapped products with HPLC is normally used to analyse condensed tannin composition. The analysis of mimosa and quebracho tannins is however compounded by the resorcinol type A-ring in these compounds. The absence of a 5-OH group imparts stability to the interflavanyl bond against acid hydrolysis. The high temperatures thus required to hydrolyse the interflavanyl bond in mimosa and quebracho tannins leads to decomposition. Mass spectrometry and ^{13}C NMR (nuclear magnetic resonance) spectrometry in solution have also been used with varying degrees of success.

The analysis of hydrolysable tannins is even more complex than that of condensed tannins. As a result, the composition of condensed and hydrolysable tannin extracts remains uncertain, after more than 50 years of research. Of particular interest are the average chain length of tannin extracts from different sources and the composition of the constituent monomers.

In this thesis the potential of solid state NMR and electrospray mass spectroscopy to solve vexing problems in tannin chemistry was investigated. Solid state NMR is particularly useful to investigate insoluble samples, overcoming problems associated with selective extraction, chemical modifications during extraction and sample preparation and uncertainty regarding

compounds that are not extracted. Electrospray mass spectrometry complements MALDI-TOF mass spectrometry in that molecules with masses below 500 Dalton are detected.

We were able to assign all the resonances in solid state NMR of hydrolysable and condensed tannins by comparing liquid and solid state spectra of pure flavonoids and tannin extract. This allowed us to distinguish unequivocally between condensed tannins and hydrolysable tannins with a simple routine experiment, avoiding laborious chemical tests. A method was developed to identify and distinguish with confidence between quebracho and mimosa condensed tannins. This method is the only available method to identify quebracho, which is of interest to oenology (quebracho tannins are added to wine) and could hitherto only be identified chemically because it tests negatively for all the available tests for tannins.

We established that no insoluble higher oligomeric condensed tannins or tannins covalently bonded to other insoluble bark components remain in spent mimosa bark (after extraction of tannins). It promises an easy way for the wattle industry to investigate lower extraction temperatures and extraction time and the associated energy savings. A fingerprinting method for mimosa was developed and is already used by the industry (Annex A).

As the gum resonances do not overlap with the tannin resonances, the bark can be analysed directly without the requirement of manufacturing an extract. The only sample preparation required is to grind the bark (about 100mg) finely and pack the solid state NMR rotor. As carbon is magnetised *via* hydrogen, less than 30 minutes NMR time is required per sample. This provides an easy way to identify the bark of quebracho, mimosa and hydrolysable tannins. A solid state NMR spectrum of the spent bark not only indicated that no condensed tannins remain, but also supports the conclusion that spent bark consists of water insoluble gums (polymers of glucose and other sugars). We believe that this method will find application in identifying novel sources of tannins from indigenous plants.

We expanded our investigation into tanned leather and developed an easy method to determine whether leather was tanned with mimosa, quebracho, Italian chestnut, tara,

synthetic tanning material, chromium or aluminium. We believe this method can be used by the leather industry to determine tannin loading of tanned leathers.

By combining our electrospray mass spectrometry data with published MALDI-TOF mass spectrometry data we could calculate the relative composition of monomers, dimers, trimers, tetramers etc. in condensed tannin sample. These calculations were used by the mimosa and quebracho tannin industry to comply with new European Union (EU) REACH (**R**egistration, **E**valuation, **A**uthorisation and Restriction of **Ch**emical substances) legislation. Without compliance mimosa extract cannot be exported to the EU.

Sulfitation (treating mimosa and particularly quebracho extract with bisulfite) is routinely used in industry to enhance the extract's properties (e.g. increase water solubility) and products with different levels of sulfitation are commercially available. The chemical changes associated with sulfitation remain speculation. The solid state NMR indicated that the C-ring is opened during the process. The electrospray MS conclusively demonstrated the existence of condensed tannin-sulfonate molecules for the first time. The m/e values correspond with ring opening and introduction of a sulfonate group on the C-2 position.

OPSOMMING

Mimosa (*Acacia mearnsii*) ook bekend as swart wattle, en quebracho (*Schinopsis balansae, Schinopsis lorentzii*) is die hoof kommersiële bronne van natuurlik gekondenseerde tanniene (proantosianidien oligomere) wat vandag gebruik word. Mimosa bas word geoes in kommersiële plantasies in Suid Afrika wat, volgens'n opname deur die Departement van Waterwese en bosbou in 2001, 'n area van ongeveer 107 000 hektaar beslaan. Quebracho word geëkstraeer van die hout van natuurlike woude in Brazilië en Argentinië. Mimosa bas word in water geëkstraeer (ongeveer 50% per gewig). Tara (*Cæsalpinia spinosa*) en italiaanse kastaiing (*Castanea sativa*) is die hoof kommersiële bronne van hidroliseerbare tanniene.

The vermoeë van wateroplosbare hidroliseerbare en gekondenseerde tanniene (polifenole) om met proteïene, waarskynlik *via* waterstof bindings, te reageer, lê naas hul vermoë om ongebreide vel in leer te omskep, en in hul kommersiële toepassing as tannien agente. Dit verklaar ook hul bestaan in die natuur as teen-voedings agente wat plante onverteerbaar maak vir insekte en herbivore. Verder verklaar dit die gebruik van melk in tee, waar die kompleksering van melk proteïene met tee tanniene die bitterheid van tee verminder, alhoewel die chemie van hierdie proses steeds onduidelik is. Die polifenoliese aard maak tannien ekstrakte baie vatbaar vir oksidasie, asook verdere polimerisasie en herrangskikking, wat die ekstrak meer komplekseer. Dit is duidelik in die transformasie van groen tee (hoë flavan-3-ol inhoud en lae gekondenseerde tannien inhoud) na indiese of swart tee (lae flavan-3-ol inhoud en hoë tanien inhoud). Die kwaliteit van rooiwyn word tot 'n groot mate bepaal deur die hoeveelheid en samestelling (wat verander gedurende veroudering tydens 'n proses wat tot hede nog moeilik verklaarbaar is) van die gekondenseerde tanniene. Die tanniene reageer met proteïen reseptore op die tong om die kenmerkende mondgevoel te gee. Hout-verouderde wyn bevat nie net gekondenseerde tanniene van die druiweskil nie, maar ook hidroliseerbare tanniene van die houtvate waarin dit verouder word.

Die polifenoliese aard van die aromatiese ringe laat reaksies met elektrofiele toe. Dit vorm die basis van kleefmiddel vervaardiging, waar formaldehied gebruik word om tannien ekstrakte te polimeriseer om kleefmiddels te vorm. Ander kommersiële gebruike van tanniene sluit in anti-skuim agente in olie ontginning en die vervaardiging van amiene wat hars bevat (*via* die Mannich reaksie) vir water suiwerings toepassing (verwydering van swaar metale).

Die produksie van mimosa gekondenseerde tanniene is ‘n volhoubare proses aangesien die bome elke agt jaar geoes word. Dis sal ‘n belangriker bron van chemiese roumateriaal vir dierevoeding word, soos wat die huidig gebruikte ru-olie bronne uitgeput raak. Dit skep ook werksgeleenthede in landelike areas.

Hoër oligomerise gekondenseerde tanniene bestaan uit opeenvolgende eenhede van flavan-3-ol monomere *via* C-4 tot C-8 of C-4 tot C-6 inter-flavaniel bindings. Hoër oligomere kan nie met chromatografie gesuiwer word nie, en ander metodes van analise word benodig. Suur gekataliseerde splyting van inter-flavaniel bindings en die opvang van monomeriese intermediêre produkte met tolueen-α-thiol of floroglusinol, gevolg deur analise van die geïsoleerde produkte met HPLC, word normaalweg gebruik om gekondenseerde tannien samestellings te bepaal. Die analise van mimosa en quebracho tanniene word egter bemoeilik deur die resorsinol-tipe A-ring in hierdie verbindings. Die afwesighed van ‘n 5-OH groep maak die inter-flavaniel binding stabiel teen suur hidrolise. Die hoë temperature wat dus benodig word vir die hidrolise van die inter-flavaniel binding in mimosa en quebracho, lei tot ontbinding. Massa spektrometrie en ^{13}C KMR (kern magnetise resonans) spektrometrie in oplossing is ook al met wisselende grade van sukses gebruik.

Die analise van hidroliseerbare tanniene is selfs meer kompleks as die van gekondenseerde tanniene. As gevolg hiervan, bly die samestelling van gekondenseerde en hidroliseerbare tanien ekstakte onseker, selfs na 50 jaar se navorsing. Van besondere belang is die gemiddelde ketting lengte van tannien ekstrakte van verskillende bronne en die samestelling van die monomere wat dit vorm.

In dié skripsie word die potensiaal ondersoek van vaste toestand KMR en elektrosproei massa spektrometrie om die ingewikkelde probleme van die tannien industrie op te los. Vaste toestand KMR is veral geskik om onoplosbare monsters te ondersoek, probleme met selektiewe ekstraksie, asook chemiese verandering gedurende ekstraksie en monster voorbereiding en onsekerheid oor verbindings wat nie geëkstraeer is nie, te oorkom. Elektrosproei spektrometrie komplimenteer MALFI-TOF massa spektrometrie deurdat molekules met ‘n massa laer as 500 Dalton gesien kan word.

Ons kon al die resonansies in vaste toestand KMR van hidroliseerbare en gekonsentreede tanniene toeken deur die vergelyking tussen vloeibare en vaste toestand spektra van suiwer flavonoiëde en tannien ekstrakte. Dit het ons toegelaat om onomwonde te onderskei tussen gekondenseerde tanniene en hiroliseerbare tanniene deur eenvoudige roetine eksperimente, sonder langdradige chemiese toetse. ‘n Metode is ontwikkel om met sekerheid tussen mimosa en quebracho gekondenseerde tanniene te onderskei en hulle te identifiseer. Dié metode is die enigste beskikbare metode om quebracho te identifiseer, wat van belang is in wynkunde (quebracho tanniene word by wyn gevoeg). Quebracho kon tot nou toe slegs chemies geidentifiseer word, aangesien dit negatief toets in alle beskikbare toetse vir tanniene.

Ons het vasgestel dat geen onoplosbare hoër oligomeriese gekondenseerde tanniene of tanniene kovalent gebind aan ander onoplosbare bas komponente, oorbly in die gebruikte mimosa bas nie (na ekstraksie van tanniene). Dit verskaf ‘n eenvoudige metode vir die wattel industrie om die gebruik van laer ekstraksie temperature en -tye na te vors, met geassosieerde energie besparing. ‘n Vingerafdruk-metode vir mimosa is ontwikkel en word reeds in die industrie gebruik (Aanhangsel A).

Aangesien hars resonansies nie met tannien resonansies oorvleuel nie, kan die bas geanaliseer word sonder om ‘n ekstak te vervaardig. Die enigste voorbereiding behels om die bas fyn te maal (ongeveer 100 mg) en in die vaste toestand KMR rotor te pak. Aangesien koolstof via waterstof gemagnetiseer word, is minder as 30 minute KMR tyd per monster voldoende. Dit versaf ‘n maklike metode om die bas van quebracho, mimosa en

hidroliseerbare tanniene te identifiseer. ‘n Vaste toestand KMR spektrum bewys dat die gebruikte bas nie net geen gekondenseerde tanniene bevat nie, maar staaf ook die afleiding dat gebruikte bas uit water-onoplosbare harse (polimere van glukose en ander suikers) bestaan. Ons glo dat hierdie metode aangewend kan word om nuwe bronne van tanniene van inheemse plante te identifiseer.

Ons het die navorsing uitgebrei na gebreide leer en ‘n eenvoudige metode ontwikkel om te bepaal of die leer met mimosa, quebraco, italiaanse kastaiing, tara, kunsmatige brei materiaal, chroom of aluminium gebrei is. Ons glo dat hierdie metode deur die leer industrie gebruik kan word vir die bepaling van the tannien lading in gebreide leer.

Deur elektrosproei massa spektrometrie te kombineer met gepubliseerde MALDI-TOF massa spektrometrie data, kan ons die relatiewe samestelling van die monomere, dimere en trimere bereken. Hierdie berekeninge word gebruik in die mimosa en quebracho tannien industrie om te voldoen aan die nuwe Europese Unie (EU) REACH (**R**egistration, **E**valuation, **A**uthorisation and Restriction of **Ch**emical substances) wetgewing. Sonder nakoming hiervan kan mimosa ekstrak nie na die EU uitgevoer word nie.

Sulfitering (behandeling van mimosa en veral quebracho ekstrak met bisulfiet) word gereeld industrieël gebruik om die ekstrak se eienskappe te verbeter (bv. verhoogde water oplosbaarheid) en produkte met verskillende vlakke van sulfitering is kommersieël beskikbaar. Die chemiese veranderinge geassosieër met sulfitering bly spekulatief. Die vaste toestand KMR dui daarop dat die C-ring oopmaak tydens dié proses. Die elektrosproei MS bewys vir die eerste keer onomwonde die bestaan van gekondenseerde tannien-sulfonaat molekules. Die m/e waarde stem ooreen met die ring wat oopgaan en die invoeging van ‘n sulfonaat groep op die C-2 posisie.

CHAPTER 1

1. GLOSSARY

DP	– Degree of polymerisation
DP_n	- Number average degree of polymerisation
ESI	– Electrospray Ionisation
EU	– European Union
HPLC	– High pressure liquid chromatography
MALDI-TOF	– Matrix assisted laser desorption ionization – time of flight
M_n	– Number average molecular weight
MS	– Mass spectrometry
M_w	– Weight average molecular weight
NMR / KMR	– Nuclear magnetic resonance / Kern magnetise resonans
PC	– Procyanidin
PD	– Polydispersity
PD	– Prodelphinidin
REACH	– Registration, Evaluation, Authorisation and Restriction of Chemical substances
MAS	– Magic angle spinning
FSLG	– Frequency-Switched-Lee-Goldburg
RF	– Radio frequency
CP	– Cross polarization
2D	– Two dimensional
HMBC	– Heteronuclear Multiple Bond Correlation
HETCOR	– Heteronuclear correlation
DD	– Dipolar dephased

CHAPTER 2

2. LITERATURE SURVEY

2.1 Introduction

Tannins are astringent, bitter-tasting plant polyphenols that bind and precipitate proteins.[1-3] Tannins were traditionally, and are still, used to tan leather. The term "tannin" comes from an ancient Celtic word, *tan*, for oak tree.[4] Oak trees were noted as an abundant source of extracts traditionally used in converting animal hides to leather. This age-old practice was employed by the prehistoric tribes[5] to make their clothes (hides and skins) last longer. Tannin extraction from the bark of black wattle trees (*Acacia mearnsii*, South Africa) and quebracho (*Schinopsis balansae* and *Schinopsis lorentzii*, South America) is an important industry that supplies raw materials for leather tanning. The ability of tannins to complex with proteins via hydrogen bonds explains the use of tannins[5,6] for leather tanning.[7]

Tannins are responsible for much of the fragrance and flavour properties of tea, a popular worldwide beverage made from leaves of *Camellia sinensis*, a tropical ever-green plant. In Chinese tea, also known as green tea, the fresh tea leaves are heated and dried immediately after picking to destroy enzymes and preserve monomeric constituents. Chinese tea contains mainly monomers of which epigallocatechin is the most abundant.[8] The manufacturing[9,10] of black tea involves crushing the tea leaves after picking to promote enzymatic oxidation and subsequent condensation of the tea polyphenols (theaflavins and thearubigins) through a fermentation process. Addition of milk to the tea reduces the astringency by precipitating the tannins with milk proteins.

Tannins are polyphenols. Two classes of tannins are used - the so called hydrolysable tannins and the condensed tannins (proanthocyanidins).

2.2 Hydrolysable Tannins

The hydrolysable tannins (Figure 2-1) are galloyl **(1)** and hexahydroxydiphenoyl esters **(2)** and their derivatives. They are usually esters of D-glucose[4,6,7] **(3)** (sugar esters of gallic acids) and ellagitannins **(2)** (sugar esters of two gallic acid units C-C linked to each other).

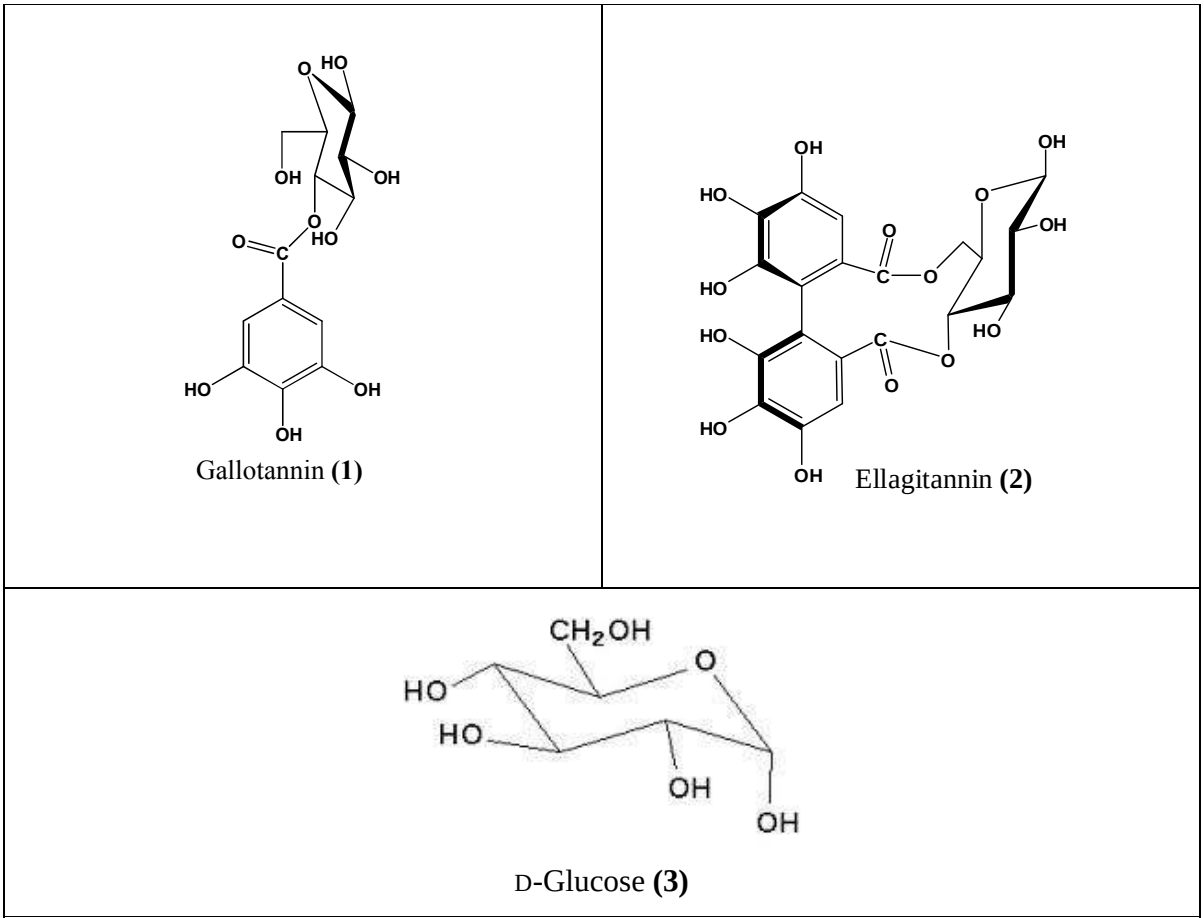

Figure 2-1: Examples of hydrolysable tannins

2.3 Condensed Tannins (Proanthocyanidins)

Condensed tannins (also called proanthocyanidins) are polymers of flavan-3-ol monomer units (Figure 2-2). The flavan-3-ol monomer units have the typical C_6-C_3-C_6 flavonoid skeleton and differ structurally according to the number of hydroxyl groups on both aromatic rings and the stereochemistry of the carbons on the heterocyclic ring.[11]

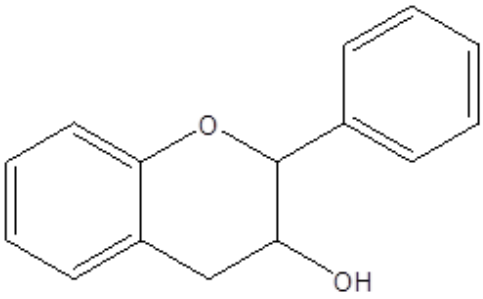

Figure 2-2: Typical flavan-3-ol building block of condensed tannin (proanthocyanidin) polymers

The isolation and elucidation of proanthocyanidin oligomers of other plants, for example Saskatoon berries (*Amelanchier alnifolia*) was done by electrospray ionization mass spectrometry, NMR spectrometry and thiolytic degradation coupled with reverse-phase liquid chromatography. The general structure is the same as that of mimosa extract. Hellstrom *et al*[12] observed that in attempting to calculate the degree of polymerisation for long polymers, the signals for the terminal units become quite small and their integration is rather suggestive than exact.

The most usual tannin interflavanyl linkages are covalent C-C bonds between C-4 of one flavanol unit and C-8 or C-6 of another (lower unit). More than 200 pure proanthocyanidin oligomers with degree of polymerisation (DP) as high as 5 (consisting of five flavan-3-ol monomers) have been isolated as pure homogeneous compounds and fully characterised.[13-18] Most proanthocyanidin polymers[19] in plants however have a much higher DP and efforts to obtain pure homogeneous condensed tannins with more than 5 monomers have failed.

Czochanska and co-workers[20] identified four parameters that are required to define the gross structure of proanthocyanidin polymers:

a) The ratio of procyanidin (PC) to prodelphinidin (PD) units. The procyanidin unit is characterised by a phloroglucinol A-ring and a 3',4'-dihydroxy B-ring. The prodelphinidin unit is characterised by a phloroglucinol A-ring and a 3',4',5'-trihydroxy B-ring.

b) The stereochemistry of the heterocyclic C-ring of the monomer units.
c) The structure(s) of the chain terminating flavan-3-ol units.
d) The number average molecular weight (M_n).

Czochanska concluded that a, b and d could be deduced from the ^{13}C NMR spectra of the polymers.

State of the art chromatography does not allow fractionation of condensed tannin mixtures into pure components that can be analysed with conventional structure elucidation techniques such as NMR. Such mixture are analysed by indirect methods.

A variety of tests has been developed to analyse the polyphenol content of tannin extracts. The most common method is the *Folic-Ciocalteau assay*[21] to determine the total phenol content. Protein precipitation gives the total condensed tannin content. This method was coupled to the use of bisulfite bleaching, giving rise to the *Davis protein precipitation assay*, also known as the *Harbertson-Adams assay*, which measures anthocyanins, tannins, small polymeric pigments and large polymeric pigments.[22]

The most useful method is *via* chemical degradation of the polymer mixture into monomer intermediates and trapping of the intermediates.[23] The interflavanyl bond between C-4 and C-6/C-8 is split with weak acid and the intermediates trapped by nucleophiles such as phloroglucinol or benzylmercaptan. Isolation, structure elucidation and quantification of the resulting phloroglucinol- or benzylmercaptan-flavan-3-ol monomers allow characterisation of the polymer. The ratio between isolated terminal- and repeat monomeric unit is used to determine the average chain length.

Czochanska *et al*[20] investigated tannin extracts of different plant sources, all based on a C4-C8/6 linked polyflavan-3-ol structure. They showed that a hydrolysable tannin can be identified with NMR by the presence of a carbonyl band around 170 ppm, due to gallate or hexahydroxybiphenyl ester moieties. They also measured the ratio of prodelphinidin to procyanidin units by using three methods, one of which was ^{13}C NMR. They mentioned that

the *cis* and *trans* C-2 unit has chemical shifts at δ = 77 ppm and δ = 84 ppm respectively. They investigated the chain-terminating flavan-3-ol units and found that a proanthocyanidin polymer terminates by one of four possible flavan-3-ol units, namely (+)-catechin, (-)-epicatechin, (+)-gallocatechin or (-)-epigallocatechin.

2.4 The Chemical Composition of Mimosa Tannin Extracts

The hot water extract of bark from commercially grown Black Wattle (*Acacia mearnsii*; previously called *Acacia mollissima*) trees is concentrated and then either spray dried to give powdered wattle extract or concentrated further to give a solid blocklike product on cooling. These chemically unmodified wattle extracts are known commercially as mimosa extract, and as *Acacia mearnsii*, ext. by ECHA (EC No. 272-777-6; CAS No. 68911-60-4). The spray dried product typically contains 5% moisture and the solid blocklike product, 15% moisture (personal communication Dr. N. P. Slabbert, Mimosa Co-Op).

More than 50 years of investigation has established the chemical composition of mimosa extract as detailed below.

The tannin fraction of the mimosa extract is classified as a condensed tannin consisting of oligomers (and polymers) of polyhydroxyflavan-3-ol monomers. The flavan-3-ol monomer units have the typical C_6-C_3-C_6 flavonoid skeleton (Figure 2-3) and differ structurally according to the number of hydroxyl groups on both aromatic rings and the stereochemistry of the carbons on the heterocyclic ring.[24]

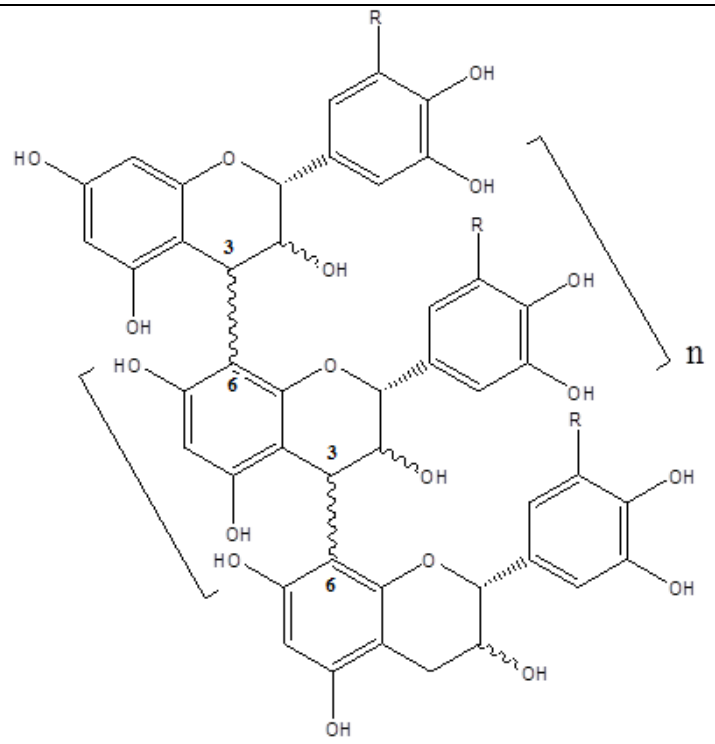

Figure 2-3: Typical flavan-3-ol skeleton of condensed tannins.

The flavan-3-ol monomers are linked by 4 → 6 and 4 → 8 covalent bonds between C-4 of one flavanol unit and C-8 or C-6 of another (lower unit) giving condensed tannin (proanthocyanidin) oligomers (Figure 2-4), where the number of monomer units (n) is greater than 1. The condensed tannins are synonymous with the proanthocyanidins.[25]

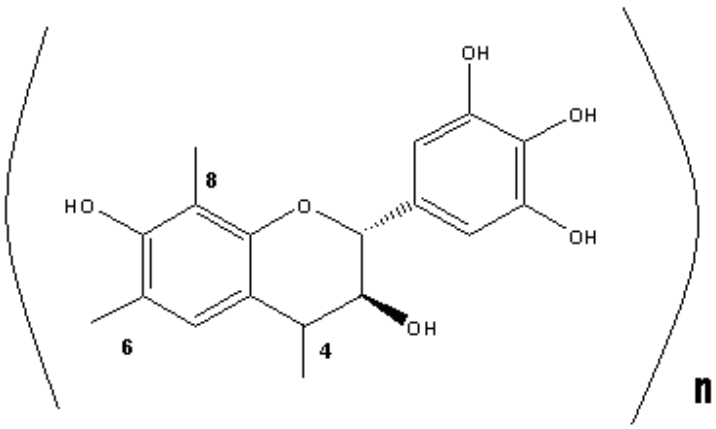

Figure 2-4: Condensed tannin molecule

By using lead acetate, Roux fractioned the black wattle extract into gums, sugars and tannins.[26,27] See Figure 2-5.

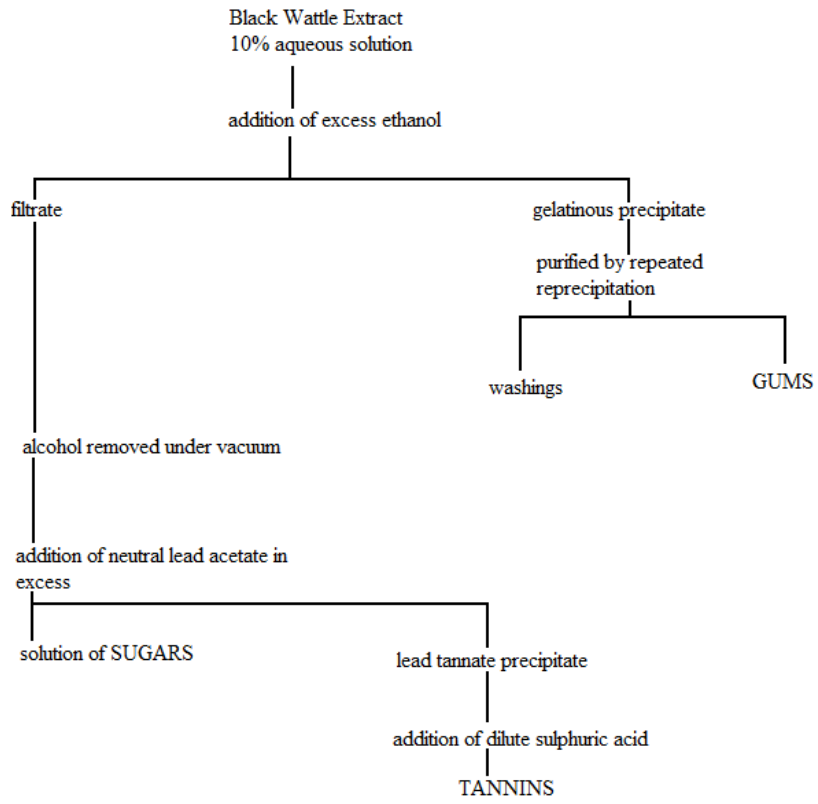

Figure 2-5: Scheme for the fractionation of mimosa extract[26]

Roux developed a standardized gravimetric assay based on precipitating gums quantitatively with absolute ethanol and condensed tannins quantitatively with lead acetate as lead tannates to quantify the amount of condensed tannins in wattle extract.[19,28] He established that wattle extract consists of 75% condensed tannins, with an average of 11% gums and 13% sugars on a dry weight basis and of 60% condensed tannins, 5-12% ethanol insoluble gums, 10% sugars and 20% water on a wet basis for the wet extract.[29]

Roux also developed a UV absorption spectrometric analytical method for wattle tannins based on absorption at 285 nm and a colorimetric method based on absorption by a ferrous

tartrate tannate complex that absorbs at 545 nm. Both these methods indicated that wattle extract contains about 76% condensed tannins and 24% non-tannins on a dry basis.[30]

Roux concluded from two dimensional paper chromatographic studies that condensed tannins in wattle extract consist of a complex mixture of proanthocyanidin oligomers of different molecular weights and that average values were obtained when determining molecular weight.[31] The results are given in Table 2-1.

Table 2-1: Molecular weight distribution of wattle and quebracho tannins[32]

	Wattle fraction C_1		Wattle fraction C_3		Quebracho extract	
Mean R_f	Tannins eluted (%)	Mol. Wt.	Tannins eluted (%)	Mol. Wt.	Tannins eluted (%)	Mol. Wt.
0'	-	-	24.3	3240	-	-
0	3.7	1442	15.7	1631	21.0	2350
0.1	20.3	1287	24.3	1606	17.1	1811
0.2	24.3	1033	22.1	1203	16.5	1362
0.3	29.7	908	13.6	933	19.7	1066
0.4	15.6	649	-	-	17.0	910
0-5+0.6	6.5	554	-	-	8.7	790
Recovery (%)	71	-	74	-	95	-
Calc. av.mol.wt.	-	971	-	1826	-	1461
Determined av.mol.wt.	-	1284	-	1507	-	1327

The fractions of wattle tannin were obtained by successive extractions of shredded fresh bark with ethyl acetate and three successive extractions with methanol. The former gave the C_1 fraction and the latter gave the C_3 fraction. The molecular weight of these fractions was determined by ebulliometry. Table 2-1 also gives the methanol extract of quebracho.

The molecular weight of black wattle tannins was derived by using the Menzies-Wright ebullioscopic technique.[33] The range was found to be of the order of 950. It is mentioned that non-polar solvents in previous experiments, to establish molecular weight, caused anomalous molecular weight values. Evelyn found that the molecular weight of the tannins varied in no particular correlation to the height of the trees.[34]

It was found that wattle tannins molecular weight ranged from 550 to 1630 Da. There was also a small fraction of a much higher average molecular weight (3240 Da). Quebracho tannin was found to be regularly distributed throughout the range from 800 to 2350 Da. The molecular weight of the quebracho tannin fractions was considerably higher compared to that of mimosa.[32]

Evelyn[35] extracted wattle bark successively with solvents of increased polarity (ethyl acetate, ethanol, methanol and water). He found that the fractions had different molecular weights and that more polar solvents extract proanthocyanidin oligomers of a higher degree of polymerization e.g. the ethyl acetate extract has a number average molecular weight (M_n) of about 1300 and the successive methanol extract a M_n of about 1500. These results support Roux's conclusion that wattle extract consists of a complex mixture of proanthocyanidin oligomers of different molecular weights.

Evelyn[36] used ebulliometry (modified Ray ebulliometer) and cryoscopy to determine the number average molecular weight (M_n) of the condensed tannins in wattle extract to be 1270 ±13. The determinations were performed on methylated or acetylated tannins (to render them soluble in benzene or bromoform and eliminate inter- and intramolecular hydrogen bonding) and calculated back to the underivatised free phenolic tannins. He found close agreement between results from ebulliometric (benzene as solvent) and cryoscopic (bromoform as solvent) methods. The number average degree of polymerisation (DPn) can be calculated from Evelyn's results, using an average flavan-3-ol monomer weight of 287, as DPn = 4.4.

Thompson and Pizzi[37] used ^{13}C NMR integration and the ratio of C-4-C-8 and C-4-C-6 interflavanoid linkages to free C-6 and C-8 sites to establish the number average degree of polymerisation of wattle tannin proanthocyanidins as DPn = 4.9. This corresponds to a M_n of between 1343 and 1406.

Covington and co-workers[38] used gel permeation chromatography to determine the number average molecular weight (M_n) as 1230, the weight average molecular weight (Mw) as 2130 and the polydispersity (PD) as 1.7 for wattle tannins.

Pasch and co-workers[39] used MALDI-TOF data (see Table 2-2) to calculate a reported DP of 5.4 for the proanthocyanidin fraction.

The interflavanyl bonds in condensed tannins are normally easily hydrolysed by dilute acid to unstable coloured anthocyanidins (hence the name proanthocyanidins). In the presence of suitable nucleophiles (e.g. benzyl mercaptan), stable monomeric adducts are formed which are analysed by HPLC to establish the composition of the condensed tannins.[40] Wattle tannins are however, resistant to acid cleavage (attributed to the absence of 5-OH substituents) and cannot be analysed reliably by this method. Mimosa extract is thus neither a procyanidin (PC) nor a prodelphinidin (PD) and thus does not fit into the Porter[20] classification. It was suggested that other methods be used to identify the constituent flavan-3-ols.[41]

MALDI-TOF mass spectrometry has shown[39] that wattle extract consists of a range of oligomeric flavan-3-ol units up to the octamer (n = 8) level (see Table 2-2). From the table it is evident that wattle tannin oligomers are permutations and combinations of mainly fisetinidol (A) (25%), robinetinidol (B) (70%) and gallocatechin (C) (5%) monomer units (Figure 2-6). Mimosa tannins are thus profisetinidins, prorobinetinidins or prodelphinidins. The data indicated a high frequency of angular trimers and tetramers.

Table 2-2: MALDI peaks for the proanthocyanidin components in commercial wattle extract.[39]

M+Na+ Experimental	M+Na+ Calculated	Unit Type				Comment
			A	B	C	
Dimers						
602	601.6		-	2	-	
Trimers						
858	857.9		2	1	-	
874	873.9		1	2	-	
		or	2	-	1	Angular structure
890	889.9		1	1	1	
			-	3	-	
906	905.9		-	2	1	Angular structure
		or	1	-	2	Angular structure
922	921.9		-	1	2	A diangular structure
Tetramers						
1147	1146.2		2	2	-	
		or	3	-	1	
1163	1162.2		1	3	-	
		or	2	1	1	
1179	1178.2		-	4	-	
		or	1	2	1	
		or	2	-	2	
1195	1194.2		-	3	1	Angular structure
		or	1	1	2	A diangular structure
1211	1210.2		-	2	2	
		or	1	-	3	
Pentamers						
1467	1466.5					
Hexamers						
1765	1754.8					
Heptamers						
2045	2043.1					
Octamers						
2333	2331.4					

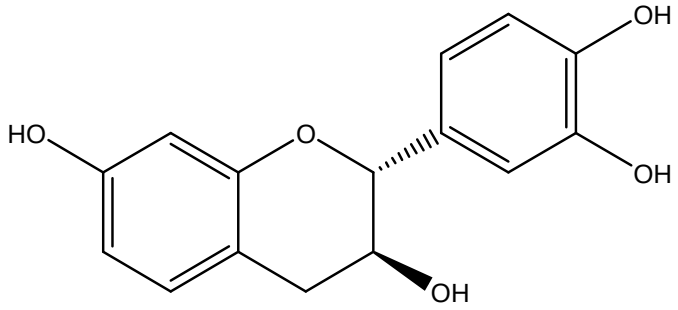

Fisetinidol

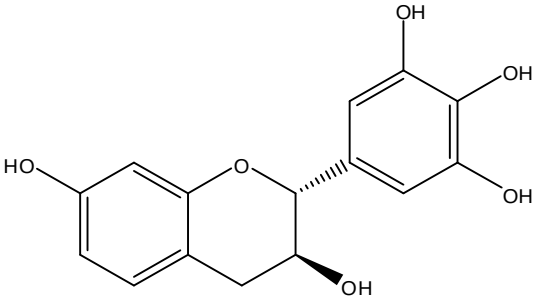

B

Robinetinidol

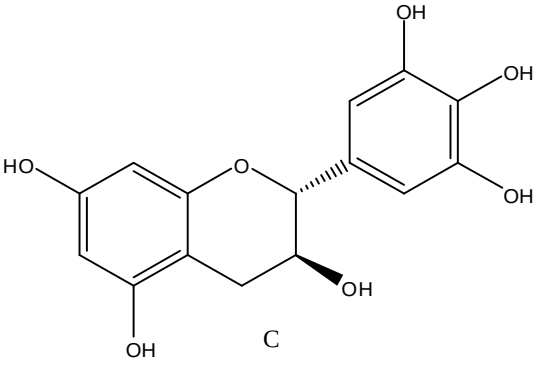

C

Gallocatechin

Figure 2-6: Flavan-3-ol monomers that constitute mimosa condensed tannins

Thompson and Pizzi[37] used ^{13}C NMR integration to establish that the A-ring of wattle tannin has on average 1.11 free OH groups (90% resorcinol and 10% phloroglucinol) and the B-ring 2.80 OH groups (20% catechol and 80% pyrogallol units). These values are consistent with an average condensed tannin oligomer molecule that consists of 20% fisetinidol, 70% robinetinidol and 10% gallocatechin monomer units.

The results of Thomson and Pizzi agree closely with the values given by Covington[38] of 25% profisetinidin (fisetinidol monomers), 70% prorobinetinidin (robinetinidol monomers) and 5% prodelphinidin (gallocatechin monomers) as typical for wattle proanthocyanidin tannins.

The non-tannin fraction of wattle extract has been found to consist mainly of sugars (sucrose, glucose and fructose) and carbohydrate gums which on hydrolysis yield predominantly galactose and arabinose.[34]

The monomers that have been isolated from mimosa tannin have been summarised by Roux and Drewes [42,43] in Table 2-3.

Table 2-3: Analogues of the main groups of flavonoids isolated and identified in wattle-bark extract

Flavonoid type	3',4',5'7-Tetrahydroxy compound	3',4',7-Trihydroxy compound
Chalcone	Robtein	Butein
Flavanone	-	Butin
Flavonol	Robinetin	Fisetin
Flavanonol	Dihydrorobinetin	Fustin
Flavan-3-ol	(-)-Robinetinidol	(-)-Fisetinidol
Flavan-3,4-diol	(+)-Leuco-robinetinidin	(+)-Leuco-fisetinidin
Tannins (mol.wt. 600-3000)	Polymeric leuco-robinetinidins	Polymeric leuco-fisetinidins

In summary, mimosa extract solids consist mainly of condensed tannins (75%) and carbohydrates (25%). Mimosa tannin is a proanthocyanidin polymer that consists of robinetinidin (70%), fisetinidin (25%) and gallocatechin (5%) monomer units. The number average molecular weight (M_n) for wattle tannin is about 1270 and the weight average molecular weight (M_w) is more than 2000. The number average degree of polymerization

(DPn) for wattle proanthocyanidin tannins has been established to be in the range of 4.4 to 5.4.

2.5 The Chemical Composition of Quebracho Tannin Extracts

The hot water extract of the heartwood of quebracho (*Schinopsis lorentzii)* trees is concentrated and then either spray dried to give powdered quebracho extract or concentrated further to give a solid / block product on cooling. These chemically unmodified quebracho extracts are generally referred to as warm water soluble quebracho extract and as *Schinopsis lorentzii* extract by ECHA (EC No. 290-224-7; CAS No. 90106-04-0)[44]. The spray dried product contains typically 6% moisture and the solid/block product, 16% moisture. The heartwood of *Schinopsis balansae* is also used.

During more than 50 years of investigation (see references below), the chemical composition of quebracho extract has been established as follows:

Quebracho is, similar to mimosa, a mixture of condensed tannin consisting of flavan-3-ol monomers, linked *via* acid labile 4→ 6 and 4→ 8 covalent bonds between C-4 of one chroman-3-ol unit and C-6 or C-8 of another (lower unit) giving polyphenol oligomers.[25]

According to Covington[38], quebracho consists of 25% robinetinidin (B) and 70% fisetinidin (A). Quebracho is thus predominantly a profisetinidin condensed tannin. Typically commercial unmodified quebracho extract consists of around 95% polyphenols and 5% carbohydrates on a dry basis (personal communication, J. Zito).

Thompson and Pizzi[37] used ^{13}C NMR (integration of the ratio of C-4 - C-8 and C-4 - C-6 interchroman linkages to free C-6 and C-8 sites), Covington and co-workers[38] used gel permeation chromatography and Pasch and co-workers[39] used MALDI-TOF data to determine the number average molecular weight (Mn) of the condensed tannin fraction in quebracho extract. These results can be used to calculate a number average degree of polymerisation (DPn) of 4-5, 6.74 and 6.25 respectively.

In summary, commercial quebracho extract solids consists of around 95% condensed tannins and 5% carbohydrates. The condensed tannin fraction is a mixture of flavan-3-ol polymers that consists of fisetinidin (about 80%) and robinetinidin (20%) monomers. The average degree of polymerization of the condensed tannin fraction of quebracho extract is 4.4 to 6.74.

2.6 References

1. Eberhardt, T. L.; Young, R. A. *J. Agric. Food Chem.***1994,** *42*, 1704–1708.
2. Hernes, P. J.; Bernner, R.; Colvie, G. L.; Goni, M.A.; Bergamanschi, B. A.; Hedges, J. I. *Geochimica et Cosmochima Acta* **2001**, *65 (18)*, 3109–3122.
3. Ham, Y. M.; Baik, J. S.; Hyun, J. W.; Lee, N. H. *Bull. Korean Chem Soc*. **2007**, *28(9)*, 1595.
4. Haslam, E. Chemistry and Pharmacology of Natural Products, *Plant Polyphenols*: Vegetable Tannins Revisited, Cambridge University Press, Sydney **1989**, 6.
5. Khanbabaee, K.; van Ree, T. *Nat. Prod. Rep.* **2001**, *18*, 641–649.
6. Haslam, E. *Phytochemistry* **1977**, *16*, 1625–1640.
7. Okuda, T.; Hatano, T.; Yazaki, K. *Chem. Pharm. Bull*. **1993**, *31*, 333.
8. Kakiuchi, N.; Hattori, M.; Nishizawa, M.; Yamagishi, T.; Okuda, T.; Namba, T. *Chem. Pharm. Bull*. **1986**, *34*, 720.
9. Yang, C. S.; Lambert, J. D.; Ju, J.; Lu, G.; Sang, S. *Toxicology and Applied Pharmacology* **2007**, *224*, 265–273.
10. Yang, C. S.; Wang, Z. Y. J. *Natl Cancer Inst*. **1993**, *85*, 13.
11. Santos-Buelga, C.; Schalbert, A. *J. Sci. Food Agric.* **2000**, *80*, 1094-1117.
12. Hellstrom, J.; Sinkkonen, J.; Karonen, M.; Mattila, P. *J. Agric. Food Chem.*, **2007**, *55*, 157.
13. Abou-Zaid, M. M. Cucumis sativus, *Phytochemistry*, **2001**, 58, 167.
14. Adamska, M.; Lutomski, J. *Planta Med.*, **1971**, *20*, 224.
15. Adinarayana, D.; Rao, J. R. *Tetrahedron*, **1972**, *28*, 5377.
16. Afifi, F. U.; Khalil, E.l Abdalla, S. *J. Ethnopharmacol.*, **1999**, *65*, 173.
17. Ahmed, A. A. *J. Nat. Prod.*, **1998**, *51*, 971.
18. Akingbala, J. O. *Cereal Chem.*, **1991,** *68*, 180.
19. Roux, D. G. Journal Society of Leather Trades' Chemists, **1952**, *36*, 210.
20. Czochanska, Z.; Foo, L. Y.; Newman, R. H.; Porter, L. J. *J.S.C. Perkin I*, **1980**, 2278.
21. Singleton, V. L.; Orthofer, R.; Lamuela-Raventos, R. M. *Methods Enzymol*., **1999,** *299*, 152-178.

22. Harbertson, J. F.; Kennedy, J. A.; Adams, D.O. *American Journal of Enology and Viticulture* **2002**, *53*, 54–59.
23. Foo, L. Y.; Porter, L. J. *J. C. S. Perkin 1* **1978**, 1186-1190.
24. Roux, D. G. in *Plant Polyphenols* Ed. by Hemingway, R. W and Laks, P. E.. Plenum Press, New York, **1992**, 7-39.
25. Haslam, E. *Practical Polyphenolics*, Cambridge University Press, Cambridge, **2005**, 24.
26. Roux, D. G. *J. Soc. Leather Trades Chem*, **1953**, 37, 274.
27. Roux, D. G. *J. Soc. Leather Trades Chem.*, **1949**, 33, 393.
28. Roux, D. G. *J. Soc. Leather Trades Chem.*, **1953**, 37, 374.
29. Roux, D. G. *J. Soc. Leather Trades Chem.*, **1957**, 41, 287.
30. Roux, D. G. *J. Soc. Leather Trades Chem.*, **1951**, 35, 322.
31. Roux, D. G. *J. Soc. Leather Trades Chem.*, **1950**, 34, 122.
32. Roux, D. G.; Evelyn, S.R. *Biochem. J.*, **1958**, *69*, 530.
33. Roux, D. G. *J. Soc. Leather Trades Chem.*, **1953**, 37, 259.
34. Evelyn, S. R. *J. Soc. Leather Trades Chem*, **1956**, 40, 335.
35. Evelyn, S. R. *J. Soc. Leather Trades Chem.*, **1958**, 42, 282.
36. Evelyn**,** S. R. *J. Soc. Leather Trades Chem.*, **1954**, 38, 142.
37. Thompson, D.; Pizzi, A. *Journal of Applied Polymer Science*, **1995**, *55*, 107.
38. Covington, A. D.; Lilley, T. H.; Song, L.; Evans, C. S. *JALCA*, **2005**, *100*, 325.
39. Pasch, H.; Pizzi, A.; Rode, K. *Polymer*, **2001**, *42*, 7531.
40. Matsuo, T.; Itoo, S. *Agric. Biol. Chem.*, **1981**, *45*, 879.
41. Schofield, P.; Mbugua, D. M.; Pell, A. N. *Animal Feed Science and Technology*, **2001**, *91*, 21.
42. Roux, D. G. Leather Industries Research Institute, *The Chemistry of Condensed Tannins*, 614.
43. Drewes, S. E.; Roux, D. G. *Biochem. J.*, **1963**, *87*, 167.
44. Regulation (EC) No 1907/2006 of the European Parliament and of the Council of 18 December 2006 concerning the Registration, Evaluation, Authorization and Restriction of Chemicals (REACH), establishing a European Chemicals Agency, amending Directive 1999/45/EC and repealing Council Regulation (EEC) No 793/93 and Commission

Regulation (EC) No 1488/94 as well as Council Directive 76/769/EEC and Commission Directives 91/155/EEC, 93/67/EEC, 93/105/EC and 2000/21/EC

CHAPTER 3

3. THEORY OF SOLID STATE NMR

3.1 Introduction

High-resolution solid state NMR spectra can provide the same type of information that is available from corresponding solution state NMR spectra, but the main advantage is that the sample in question need not be soluble or in a crystalline form, and the approach can be used to study molecules larger than 100 kD. Samples are evaluated in the absence of solvents and are packed directly in their powdered form and analysed.

Some atomic nuclei possess nuclear spin, the angular momentum of the nucleus, and thus have a magnetic moment. The direct magnetic dipole-dipole interaction between two atoms with non-zero spin gives rise to dipolar coupling, and the magnitude of the interaction is dependent on the internuclear distance and the orientation of the vector connecting the two spins with respect to the external magnetic field. In solution state NMR these orientation-dependent anisotropic effects are largely averaged out by the rapid isotropic tumbling (Brownian motion) of the molecules. This produces a spectrum appearing as a series of well defined, narrow lines corresponding to very sharp transitions. In solids the orientations of the atoms are fixed and the anisotropic effects give rise to broad line shapes in the solid state NMR spectra, resulting in the overlap of resonances and a decrease in resolution. In order to suppress these effects several techniques have been developed including magic angle spinning (MAS), and heteronuclear and homonuclear dipolar decoupling techniques, such as the Lee-Goldburg technique. However, experiments where the anisotropic nuclear spin interactions are not suppressed can give useful information on the structural parameters, dynamics and chemistry of compounds in the solid state.

3.2 Magic Angle Spinning (MAS)

In the late 1950's Andrew[1] and Lowe[2] independently succeeded in suppressing the anisotropic dipolar interactions by placing the rotor at an angle of 54.71º (magic angle) to the

magnetic field of spin (B_0). Spinning speeds are required to be at a rate equal to or greater than the magnitude (in Hz) of the anisotropic interaction (width of the spectrum of a static sample) in order to avoid the appearance of spinning sidebands in the resultant NMR spectra. Routinely, MAS is used to remove the effects of homo- and heteronuclear dipolar coupling, chemical shift anisotropy and to narrow the lines from quadrupolar nuclei. To fully understand why MAS is successful it is required to look at chemical shielding, dipolar coupling and Lee-Goldburg decoupling.

3.3 Chemical Shielding

The signal frequency that is detected in NMR is proportional to the magnetic field applied to the nucleus. However, the motions of the electrons around the nucleus produce a small magnetic field at the nucleus which usually acts in opposition to the externally applied field (chemical shielding interaction). Chemical shift is the frequency of absorption for a nucleus relative to the frequency of absorption of a molecular standard, e.g. tetramethylsilane. In solid state NMR under sufficiently fast magic angle spinning the directionally dependent character of the chemical shielding is removed, leaving the isotropic chemical shift.

Molecular orientation effectively creates different magnetic environments by the electrons circulating about the nuclei in different ways depending on crystal orientation. The shielding interactions' dependence on orientation is proportional to:

$$3cos^2\theta - 1 \qquad (1)$$

Where θ is the angle between the internuclear axis and the applied magnetic field B, and θ effectively takes on all possible values when working in the solid state. The sample is spun about an axis which is tilted at an angle of θ_R in relation to the applied field B. Now the molecular orientation dependence becomes proportional to an average:

$$(3cos^2\theta - 1) = \tfrac{1}{2}(3cos^2\theta_R - 1)\,(\,3cos^2\beta - 1) \qquad (2)$$

Where θ_R is the angle between the applied field (β_0) and the spinning axis and β the angle between the spinning axis and the principal *z*-axis (internuclear axis). In a powder sample the angle β takes on all possible values like θ does, but in a rigid solid sample it is fixed for a given nucleus. Elimination of line broadening is due to the variability of the angle θ_R by the operator. When this angle is set to the magic angle of 54.71^0, equation 1 becomes zero and hence the average, equation 2, becomes zero as well.

3.4 Dipolar Coupling

Dipolar coupling is the result of the interactions of local magnetic fields originating from the spin of a nucleus when a magnetic field is applied to it. This effect acts on other spins creating different local environments. It is highly dependent on the distance between nuclei and orientation of the vector connecting the two nuclear spins relative to the applied magnetic field, as it is a direct through-space interaction as seen in Figure 3-1.

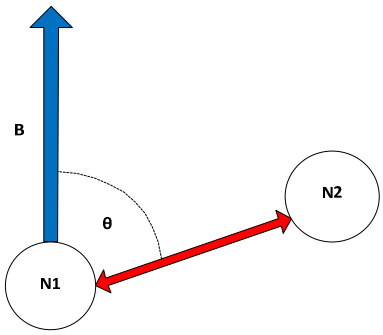

Figure 3-1: Dipolar coupling Vectors

The dependence on orientation is the same as with the shielding interaction, as in equation 1. Therefore line broadening due to dipolar coupling is eliminated by MAS just as it is for chemical shielding. As mentioned above, the rate of spin needs to be equal to or greater than the coupling strength. The strength of the dipolar interaction is proportional to:

$$\gamma_1 \gamma_S \, 1/r^3 \qquad (3)$$

Where γ is the gyromagnetic spin ratio of spin 1 and *r* is the internuclear distance. In some experiments ^{1}H – ^{13}C heteronuclear coupling is required and not ^{1}H – ^{1}H homonuclear coupling. However, MAS at moderate speeds cannot remove all the ^{1}H – ^{1}H dipole interactions and heteronuclear coupling is eliminated more effectively than homonuclear coupling. In this case Lee-Goldburg decoupling is necessary.

3.5 Lee-Goldburg Decoupling

Lee-Goldburg decoupling solves the problem described above by removing homonuclear dipolar coupling. It is a multiple-pulse sequence which imposes artificial motion on the spin operators, while leaving the special operators intact. It explicitly applies off-resonance 360^{0} RF pulses constantly during the decoupling period. In the case of solid state 2D experiments, specifically during the evolution time and the contact pulse.

The effective magnetic field (B_{eff}) is set at the magic angle relative to the applied field by offsetting the pulses from resonance with a frequency of Δω. Phase errors are reduced during t_1 by changing the offset Δω regularly to above or below the resonance frequency. This is called Frequency-Switched-Lee-Goldburg (FSLG). Homonuclear dipolar coupling is averaged to zero. This requires the effective magnetic field (B_{eff}) to be greater in frequency units than the dipolar coupling. Usually this is not a problem as

$$B_{eff} = \sqrt{\omega_1^2 + \Delta\omega^2} \qquad (4)$$

Here ω_1 is the amplitude of the RF pulse and Δω is the offset from resonance of the RF pulse. Thus the strength can easily be modified by increasing the amplitude ω_1.

3.6 Cross Polarisation

Cross Polarisation (CP) is the transfer of polarization (magnetization which is perpendicular to the applied field) from abundant nuclei (such as ^{1}H or ^{19}F) to dilute or rare nuclei (such as ^{13}C or ^{15}N) and / or inherently insensitive nuclei with low γ, via the dipolar coupling between them, so as to enhance the signal to noise (S / N) ratio {γ (protons) / γ (X nucleus)} and to

increase relaxation time (Figure 3-2) between two experiments, thereby decreasing the recycle time between scans because the repetition time depends on proton T_1 and not on the X nucleus. The reasons why protons usually have shorter T_1 is because T_1 depends on the product of the γ values of the two nuclei and γ (proton) times γ (proton) is 4 times larger than γ (proton) times γ (C^{13}). Another reason is the dipolar interaction between two spins which decreases according to approximately $1/r^6$. In most organic solids there are many protons close to each other, but a carbon can have a maximum of three protons in its vicinity. The decreased recycle delays follow from the fact that abundant spins are strongly dipolar coupled. Hence they are subject to big magnetic fields originating from motion. Rapid spin-lattice relaxation is now achieved at the abundant nuclei. The recycle delay is dependent on the T_1 of protons, fluorine, etc. Firstly a $\pi/2$ pulse is implemented only on the proton channel and after this the resultant polarization is transferred to the assigned nucleus (X).

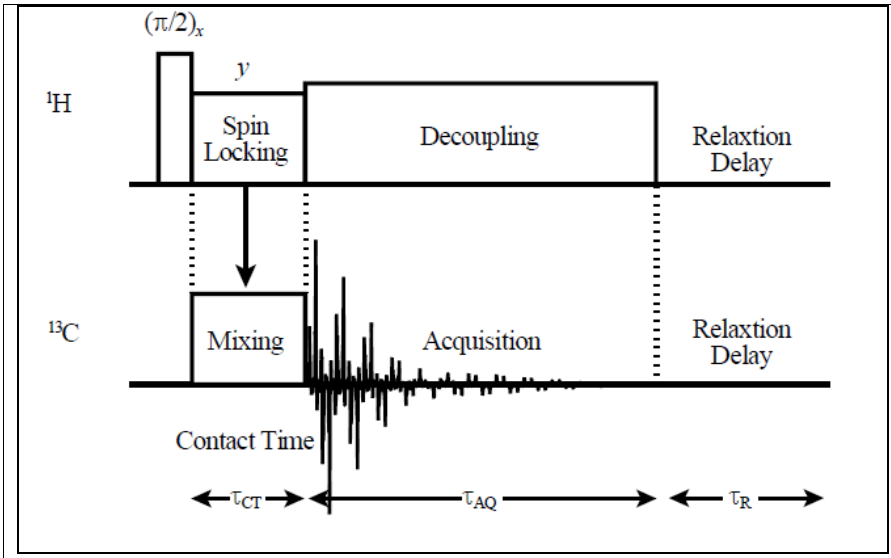

Figure 3-2: Diagram showing contact- , acquisition- and relaxation time

3.7 Hartmann-Hahn Condition

The **Hartmann-Hahn** condition needs to be set properly for cross polarization to be efficient. This involves using RF-pulses on both the high γ and the low γ to set their nuclear energy levels equal to one another. Now the energy levels can mix, allowing diffusion of

transverse spin magnetisation from the generator-nucleus to the other nucleus. The Hartmann-Hahn condition is:

$$\gamma_Z B_1(Z) = \gamma_X B_1(X) \qquad (5)$$

Where γ is the gyromagnetic ratio of the nucleus specified and B_1 is the effective field on the nucleus when an RF pulse is applied. If the parameters for the Hartmann-Hahn condition are set properly, magnetisation for both nuclei occurs at the same rate, allowing transfer of the abundant spin polarization to the dilute spin.

Cross polarization is applied together with magic-angle spinning (CP-MAS NMR) as it works efficiently while samples are being spun rapidly, at a specified rate, at a position equal to the magic angle to enhance the signal sharpness.

3.8 Heteronuclear Correlation

During a heteronuclear correlation (HETCOR for short) experiment, a two dimensional spectrum is produced by using the dipolar coupling between nuclei. For the experiments in this study the nuclei used were ^{1}H and ^{13}C. This type of experiment is similar to a HETCOR HMBC in solution state, which shows the correlation of the proton to carbon interaction and bonding. An important difference is that the solution state HMQC defines connectivity on the basis of through-bond J-coupling, whereas the solid state HETCOR defines ^{1}H – ^{13}C proximities on the basis of closeness in space. A HETCOR shows the correlation in space of protons to carbons and vice versa. As in cross polarization, a higher signal to noise ratio is achieved by increasing scans. Rapid spin-lattice decay is also a benefit of HETCOR. Another benefit is that HETCOR can be used to separate proton peaks more clearly from the usual broad peak in solid state NMR experiment. It must be mentioned that this higher resolution is influenced by homonuclear spin diffusion. Correlation occurs when magnetisation is transferred from the protons closest to the carbon during the contact time creating a cross-peak. Protons, however, all transfer magnetisation amongst themselves in a so-called proton-bath effect, giving rise to every proton potentially sharing magnetisation with every other proton. This effect causes a carbon-proton peak to broaden considerably as

magnetisation from all other protons is added to it. This hampers the accurate determination of the chemical shift of specific protons. Because the heteronuclear coupling ability between protons and carbons to create cross-peaks is much weaker, it would be removed by slower MAS rates than the spin diffusion. This prevents the removal of the spin diffusion with MAS by using extremely high spinning speeds. Lee-Goldburg decoupling, as described above, is preferentially used to remove the spin diffusion.

3.9 References

1. Andrew, E. R.; Bradbury, A.; Eades, R. G. *Nature* 1958, 182, 1659.
2. Lowe, I. J. *Phys. Rev. Lett* 1959, 2, 285–287.
3. http://nmr900.ca/instrument_e.html.
4. Duer, M. J. Introduction to Solid state NMR spectroscopy, *Wiley-Blackwell,* 2004.
5. Shurko, R. *Introductory Solid State NMR Notes*, 2009, http://mutuslab.cs.uwindsor.ca/schurko/ssnmr/.

CHAPTER 4

4. ANALYSIS and CHARACTERISATION of CONDENSED (MIMOSA and QUEBRACHO) and HYDROLISABLE (TARA and CHESTNUT) TANNINS in EXTRACTS, BARK and LEATHER with SOLID STATE NMR

4.1 General Introduction

Mimosa (*Acacia mearnsii* formerly *mollissima*) and quebracho (*Schinopsis balansae* and *Schinopsis lorentzii*) are the major commercial sources of natural condensed tannins used today. Mimosa bark is harvested from commercial plantations in South Africa covering an area of more than 120 000 hectares. Quebracho is extracted from the wood of natural quebracho forests in Brazil and Argentina. About 50% by weight of mimosa bark is extracted with water as condensed tannins. The composition of this extract remains uncertain, after more than 50 years of research (Roux started publishing from 1949).[1]

The soluble polymeric forms of condensed tannins from a large variety of plant sources have been extensively studied and characterised.[2,3,4] The condensed tannin fraction is generally extracted with acetone-water (30:70) and fractionated with Sephadex LH-20.[5] The fractions are then studied with ^{13}C nuclear magnetic resonance and chemical degradation. Degradation involves weak acid catalysed fission of the interflavanyl bonds, followed by trapping of the monomer intermediates with toluene-α-thiol or phloroglucinol and analysis of the trapped products with HPLC.[6-8]

Present knowledge suggests that condensed tannin higher oligomers are built up by the successive addition of flavan-3-ol monomer extension units *via* the C-4 to C-8 or C-4 to C-6 interflavanyl bond in the same way that the dimers are formed from monomers.[9]

The situation with mimosa and quebracho tannins is compounded by the resorcinol type A-ring in these compounds. The absence of a 5-OH group imparts stability to the interflavanyl bond against acid hydrolysis. The high temperatures thus required to hydrolyse the interflavanyl bond in mimosa and quebracho tannins leads to decomposition. This renders the classical method to analyse condensed tannins *via* acid hydrolysis of the interflavanyl bond followed by trapping of intermediates with toluene-α-thiol or phloroglucinol and analysis of the trapped intermediates with reverse phase HPLC, unreliable.

Mimosa tannin was reported to consist of robinetinidol (Figure 4-1) (75%), fisetinidol (Figure 4-2) (30%) and gallocatechin / delphinidin (Figure 4-3) (5%) monomers.[9] The gallocatechin has a reactive phloroglucinol A-ring and is assumed to allow branching in the oligomer. Quebracho consists predominantly of fisetinidol monomers and therefore presumed to be less branched than mimosa.[9]

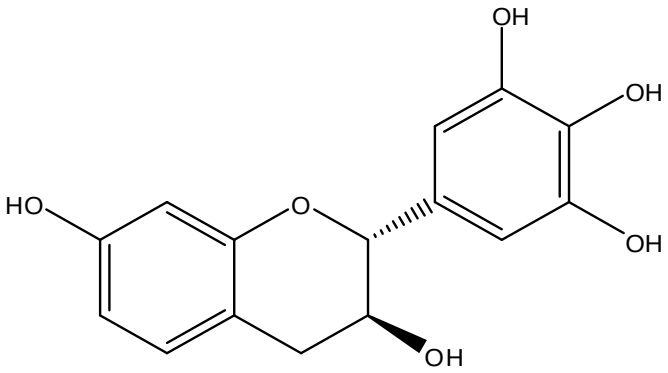

B

Figure 4-1: Robinetinidol

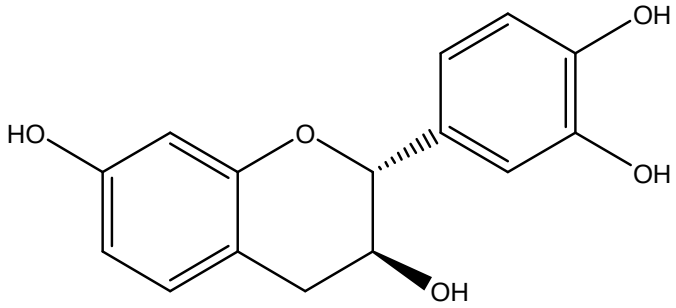

Figure 4-2: Fisetinidol

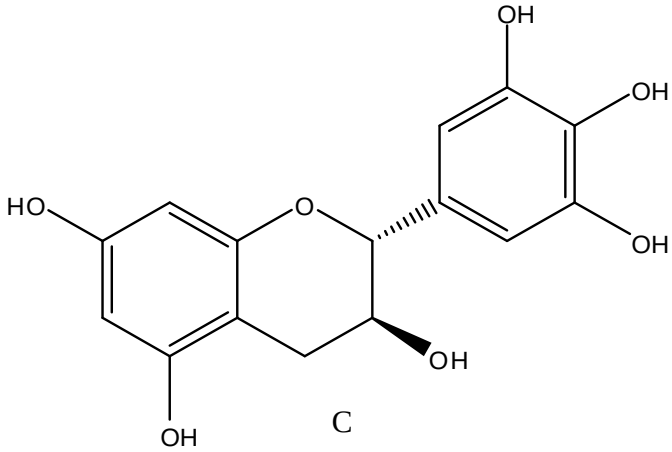

Figure 4-3: Prodelphinidin / gallocatechin

Quebracho tannin is thus considered to be predominantly a profisetinidin (PF) (resorcinol type A- and catechol type B-ring) and mimosa predominantly a prorobinetinidin polymer (PR) (resorcinol type A-ring and pyrogallol type B-ring) (See Figure 4-4).

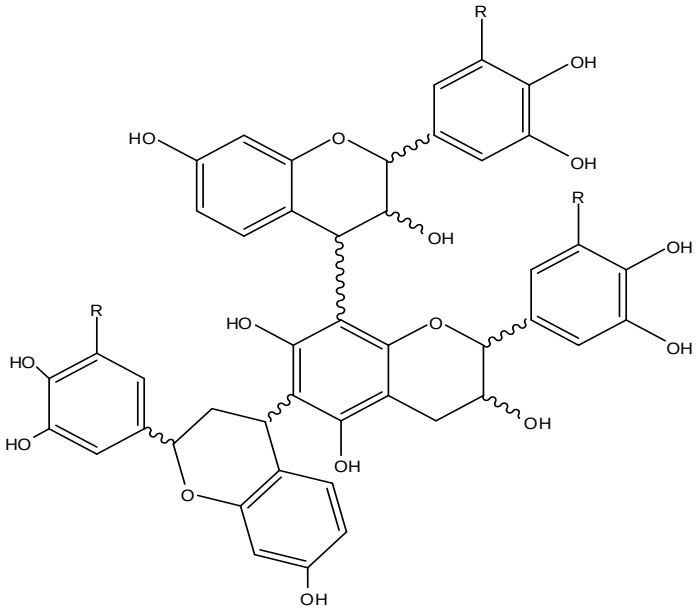

Figure 4-4: General structure of mimosa and quebracho trimer

Solid state NMR is performed directly on solid samples in the absence of a solvent. Despite the use of finely ground powders and high spin rates, the perfect homogeneity associated with conventional solution state NMR is not achieved. Also, in the poorly crystalline solid materials such as condensed tannin extracts, each atom experiences a range of chemical environments characterized by slightly different chemical shifts. In solution state NMR rapid molecular motion averages chemical shifts to single values, but this averaging is generally not present in solids. Resultant broad line shapes result in signal overlap and loss of resolution.

Developments such as magic-angle spinning (MAS), cross polarization (CP) of signal from sensitive protons to less sensitive carbons, heteronuclear dipolar decoupling and dipolar dephasing techniques have however transformed ^{13}C solid state NMR into a powerful tool to investigate insoluble or poorly soluble materials. The technique is particularly suitable for polymer analysis and routine quality control.

Despite great interest in the composition of condensed tannins, there have been few studies making full use of the information available from ^{13}C solid state NMR spectroscopy. Lorenz and coworkers[11] investigated Canadian (*Picea mariana* [Mill.] B.S.P.) litter, German spruce litter (*Picea abies* [L. Karst.]) and humus with ^{13}C solid state NMR. They attributed resonances in the 100 to 150 ppm region to condensed tannins.

Gamble and coworkers[12] used ^{13}C solid state NMR to study biological degradation of condensed tannins in *Sericea lespedeza* (*Lespedeza cuneata*) by the white rot fungi *Ceriporiopsis subvermispora* and *Cyathus stercoreus.* Resonances in the 90 to 160 ppm region were attributed to the aromatic moieties of condensed tannins.

4.2 Experiment 1: Determination of optimum cross polarisation (CP) contact time

4.2.1 Introduction

The cross polarization contact time (P15) of an NMR experiment is the time during which magnetization is transferred from the abundant nucleus (^{1}H) to the dilute nucleus (^{13}C). Since quaternary carbons have no directly attached hydrogen atoms, they receive magnetization from the proton bath only and thus need a longer contact time to be polarized. The length of the contact time should be chosen such that all types of carbons have sufficient time to polarize yet not so long as to lose significant magnetization due to the proton bath.[13] An optimal contact time was established by starting with a P15 time of 2500 μs and lowering the value until the quaternary carbons attached to the hydroxyl groups showed sufficient intensities.

4.2.2 Results and Discussion

The quaternary carbons (no attached hydrogen atoms) at 143 ppm and 153 ppm were monitored as their signals take longer to intensify compared to protonated carbons with fast polarization rates. The spectra of epicatechin-4β-8-catechin (B1), was used to determine the contact time and the spectra of contact times equal to 2500 μs, 1000 μs, 500 μs, 200 μs, 100 μs and 50 μs are shown in Figure 4-5. Thereafter the spectra for all oligomers were done at contact times of 500 μs and 1000 μs, respectively.

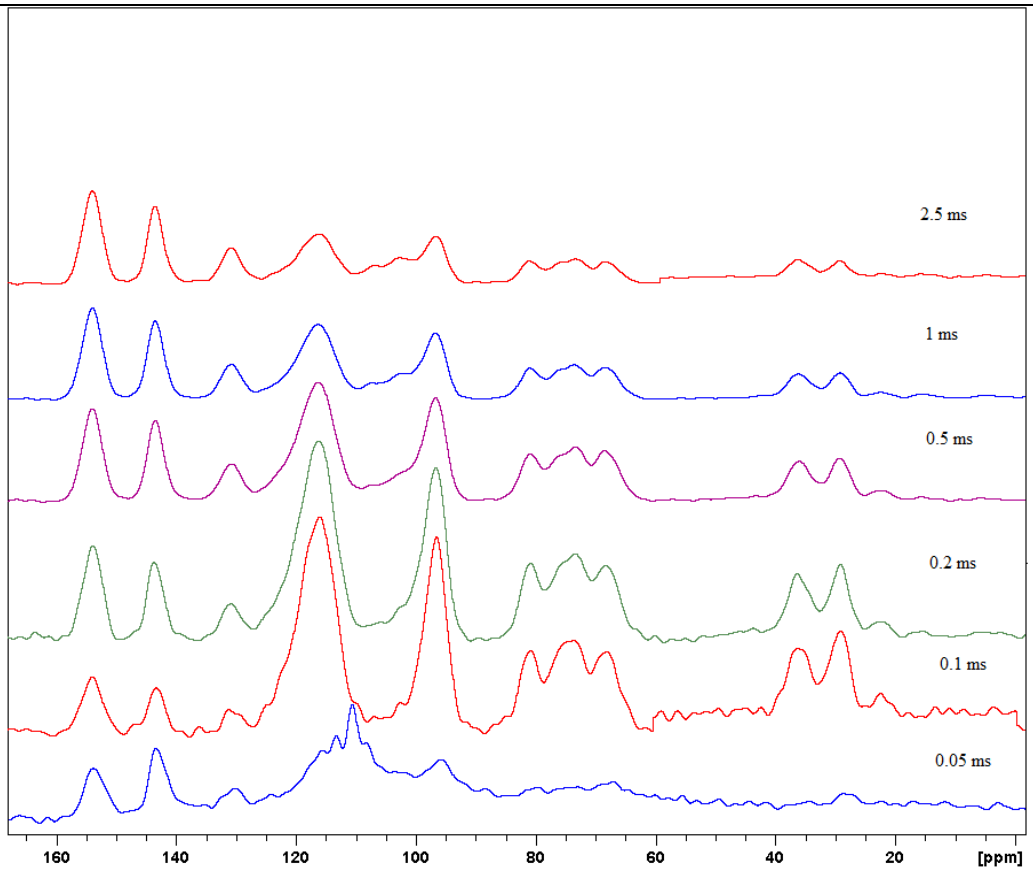

Figure 4-5: Influence of alternate contact time on Cross Polarization of a dimer (B1)

By comparing the different calculated chain lengths from the two contact times as in Table 4-1, it can be seen that the deviation from the optimal, known chain length value was less for a contact time of 500 μs. The data taken with a contact time of 500 μs was therefore used in all other discussions.

It is clear from these spectra that the resonances from the quaternary carbons intensified relative to the other peaks in the spectrum as the contact time was lengthened each time, until a cross polarization contact time of 500 μs. At P15 times higher than 500 μs there was no further significant improvement in the resolution of these quaternary peaks indicating that sufficient time was allowed for the transfer of magnetization to these carbons.

Table 4-1: Determination of optimal contact time					
Oligomer	Expected chain length	500 μs		1000 μs	
		Actual	Deviation	Actual	Deviation
B1	2	2.12	0.12	2.14	0.14
B2	2	1.95	0.05	1.92	0.08
B4	2	1.83	0.17	1.72	0.28
Trimer 1	3	2.81	0.19	2.86	0.14
Trimer 2	3	2.21	0.79	2.21	0.79
Tetramer	4	3.44	0.56	3.20	0.80
Pentamer	5	4.16	0.84	4.40	0.60

4.2.3 Conclusion

The optimal P15 time to use in ^{13}C solid state NMR is 500 μs.

4.3 Experiment 2: Assignment of ^{13}C resonances in the solid state NMR of mimosa and quebracho condensed tannins with dipolar dephasing techniques

4.3.1 Introduction

To put our resonance assignments on a firmer footing we performed dipolar dephasing experiments.

By selecting a suitable time for dipolar dephasing, only quaternary carbons (no attached hydrogen atoms) are detected, due to the faster decay of protonated carbon signals. The high-power decoupler is turned off for a short while (*d*2) after cross polarization and then turned on again for data acquisition.[14] During the *d*2-delay, the dipolar interactions between protons and carbons induce fast dephasing of signals. Due to the close proximity of attached protons, protonated carbons are dephased faster resulting in the disappearance of these peaks from the ^{13}C solid state NMR spectrum. These experiments are usually conducted with variable *d*2-delay times (*d*2 = 0 to120 µs) to establish an optimal value for these times. The degree of substitution in aromatic rings can thus be estimated. Dipolar dephased (DD) spectra were generated by inserting a delay period of 100 µs without ^{1}H decoupling between the cross-polarization and acquisition portions of the CP-MAS pulse sequence.

4.3.2 Results and Discussion

The spectra showing the dipolar dephased NMR of mimosa and quebracho are shown in Figure 4-6 and Figure 4-7 respectively.

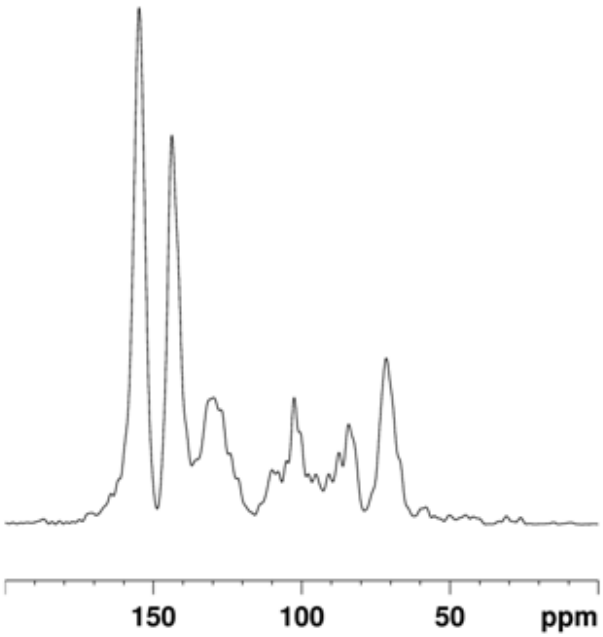

Figure 4-6: Dipolar dephased (d2 = 100us) solid state NMR of mimosa.

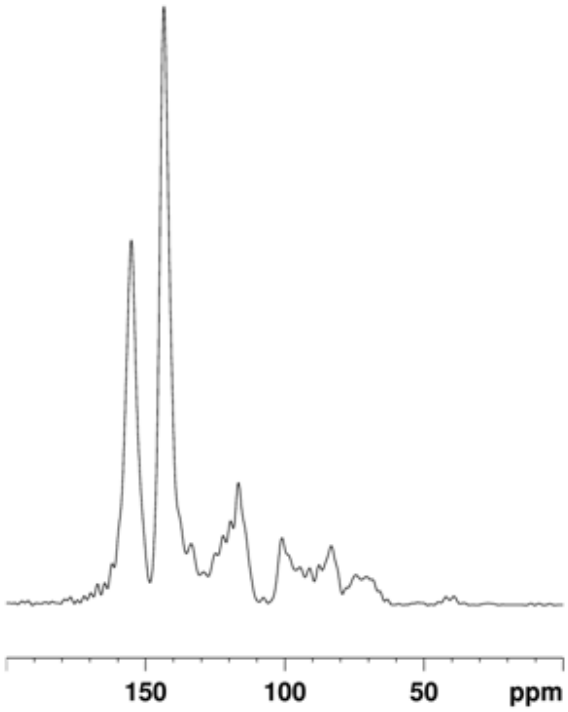

Figure 4-7: Dipolar dephased (d2 = 100us) solid state NMR of quebracho extract

4.3.3 Conclusion

From these experiments we can conclude that resonances below 90 ppm represent carbons attached to hydrogen. The resonances above 140 ppm represent quaternary carbons (carbons not attached to hydrogen), probably C-OH carbons. The resonances between 90 and 140 represent overlapping quaternary and C-H bonded carbons.

4.4 Experiment 3: Using ^{13}C solution state NMR chemical shifts to assign ^{13}C solid state NMR resonances

4.4.1 Introduction

It was unclear whether ^{13}C liquid state NMR chemical shifts could be used to assign ^{13}C solid state resonances. The hypothesis was to take a known compound with previously assigned and accepted resonances and analyse the sample with solid state NMR. The resonances in solid state would then be compared to the resonances in solution state. The degree of deviation or similarity would give an indication if this method can be reliably extrapolated to apply to unknown compounds in solid state NMR. During this experiment, the catechin monomer was used as it had been previously assigned in acetone-d_6.[3,15]

4.4.2 Results and Discussion

A sample of amorphous catechin was finely ground and a ^{13}C solid state NMR was recorded. (Figure 4-8) The spectrum for catechin dissolved in acetone-d_6 is given in Figure 4-9. Table 4-2 compares the ^{13}C NMR chemical shifts of the solid sample with a sample dissolved in acetone-d_6.

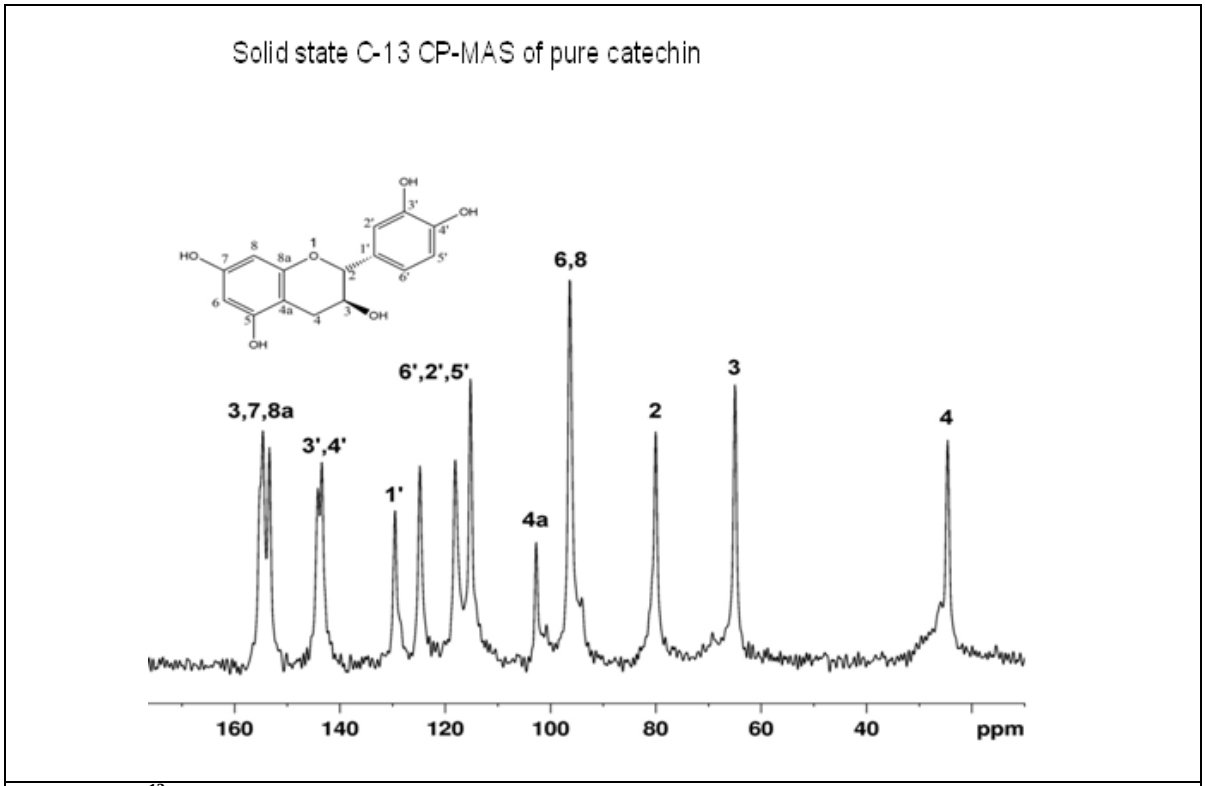

Figure 4-8: ^{13}C solid state NMR of amorphous catechin

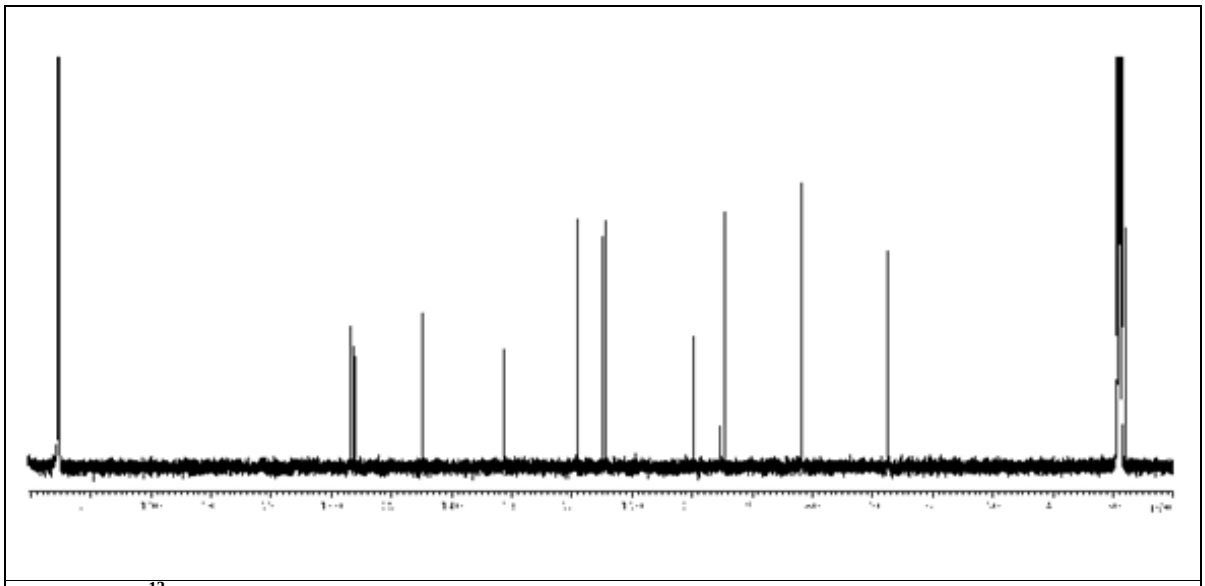

Figure 4-9: ^{13}C solution state NMR of Catechin in acetone-d_6

Table 4-2: Comparison of the ^{13}C solid state and solution state (acetone-d_6) NMR spectra of catechin		
Carbon number	Chemical shift in the solid state	Chemical shift in solution (acetone-d_6)
2	81	82
3	65	67
4	24	38
4a	102	99
5	155	156
6	96	100
7	155	156
8	96	94
8a	155	157
1'	130	131
2'	115/118/124	114
3'	144	145
4'	144	145
5'	118/118/124	119
6'	124/118/124	125

4.4.3 Conclusion

There is a close correlation between ^{13}C solid state and solution state NMR chemical shifts. This implies that conventional solution state chemical shifts can be applied to assign solid state resonances.

The work of Lorenz and co-workers[11] and Czochanska and co-workers[3,] can thus be applied directly to interpret ^{13}C solid state NMR spectra of condensed tannins. The chemical shifts of proanthocyanidin polymers (both procyanidin PC [containing a phloroglucinol A-ring and catechol B-ring] and prodelphinidin PD [containing a phloroglucinol A-ring and pyrogallol B-ring] type tannins) as published by above mentioned authors are shown in Table 4-3 and Table 4-4.

Table 4-3: Chemical shift assignment for ^{13}C solid state NMR of tannins in spruce litter (Lorenz and co-workers)[11]	
13C chemical shift (ppm)	Assignment
0-50	Alkyl C
50-60	Methoxyl C
60-93	O-alkyl C
93-112	di-O-alkyl C and some aromatics
112-140	Aromatic C
140-165	Phenolic C
165-190	Carboxyl C

Table 4-4: ^{13}C solution state NMR chemical shifts of proanthocyanidin polymers compared to ^{13}C solid state NMR chemical shifts of catechin (Czochanska and co-workers)3		
Carbon number	Polymers (acetone-d_6 - water)	Solid state catechin
C-4 (terminal)	28-29	25
C-4 (repeat)	37-38	
C-3 (terminal)	66-68	65
C-3 (repeat)	73	
C-2 (2,3-*cis*)	77	
C-2 (2,3-*trans*)	84	80
A-ring C-H (6 and 8)	96-97	96
A-ring quaternary (4a)	100-102 (107 in PD)	103
B-ring C-H (2' and 6' of PD)	108-109	
B-ring C-H (2',5' and 6' of PC)	115-116 (120 for 6')	115, 118, 125
B-ring quaternary (1')	131-132	130
B-ring (4' C-OH of PD polymers)	133	
B-ring C-OH (3', 4' of PC and 3',5' of PD)	145-146	144
A-ring C-OH (5, 7 and 8a)	157	155 (d)

4.4.3.1 ^{13}C solid state NMR of mimosa tannin extract (ME) versus the ^{13}C solid state NMR of catechin

The ^{13}C solid state NMR spectrum of mimosa extract compared to the spectrum of the monomer catechin showed great similarity. (Table 4-5 and Figure 4-10) However, since mimosa consists of various oligomers (has various monomers making up the structure) compared to catechin being a monomer, the ^{13}C solid state NMR spectrum of mimosa shows much broader peaks due to the overlap of resonances. Also present in the ^{13}C solid state NMR spectrum of mimosa are resonances associated with the pyrogallol type B-ring of robinetinidin. For instance, the peak at 145 ppm can be assigned to a prorobinetinidin / prodelphinidin C-3□ or C-5□ or to a fisetinidin C-3□ or C-4□. In the case of catechin, the 144 ppm peak is assigned to C-3□ and C-4□ only. The stereochemistry of catechin is known and therefore the assignments for the 2-C and 3-C peaks can be made without any doubt as 82 ppm and 67 ppm. In the case of mimosa, the stereochemistry is unknown due to the fact that different monomers combine in several unknown sequences to create a chain of unknown length. Here the 2-C peak for a *trans* configuration around the 2-3 bond has a chemical shift of 82 ppm but that for the 2-C peak with a *cis* conformation around the same bond has a chemical shift of 73 ppm. The 3-C peak is broken up into a terminal peak, appearing at 62 ppm and a repeat peak, appearing at 73 ppm. The same happens with the C-4 peak and the terminal peak is shown at 26 ppm and the repeat peak at 39 ppm.

Table 4-5: ^{13}C Chemical shift values for mimosa and catechin			
Mimosa		Catechin	
Carbon Number	Chemical shift	Carbon Number	Chemical shift
2 (2,3-*trans*)	80	2	82
2 (2,3-*cis*)	72		
3 repeat	72		
3 terminal	63	3	67
4 repeat	40	4	38
4 terminal	30		
4a	102-113	4a	100
5	155	5	156
6	102-113	6	95
7	155	7	156
8	102-113	8	94
8a	155	8a	157
1'	133	1'	131
2'	118	2'	114
3'	146	3'	145
4' pyrogallol	133	4'	145
4' catechol	146		
5' catechol	118	5'	119
5' pyrogallol	146		
6' pyrogallol	102-113	6'	114
6' catechol	118		

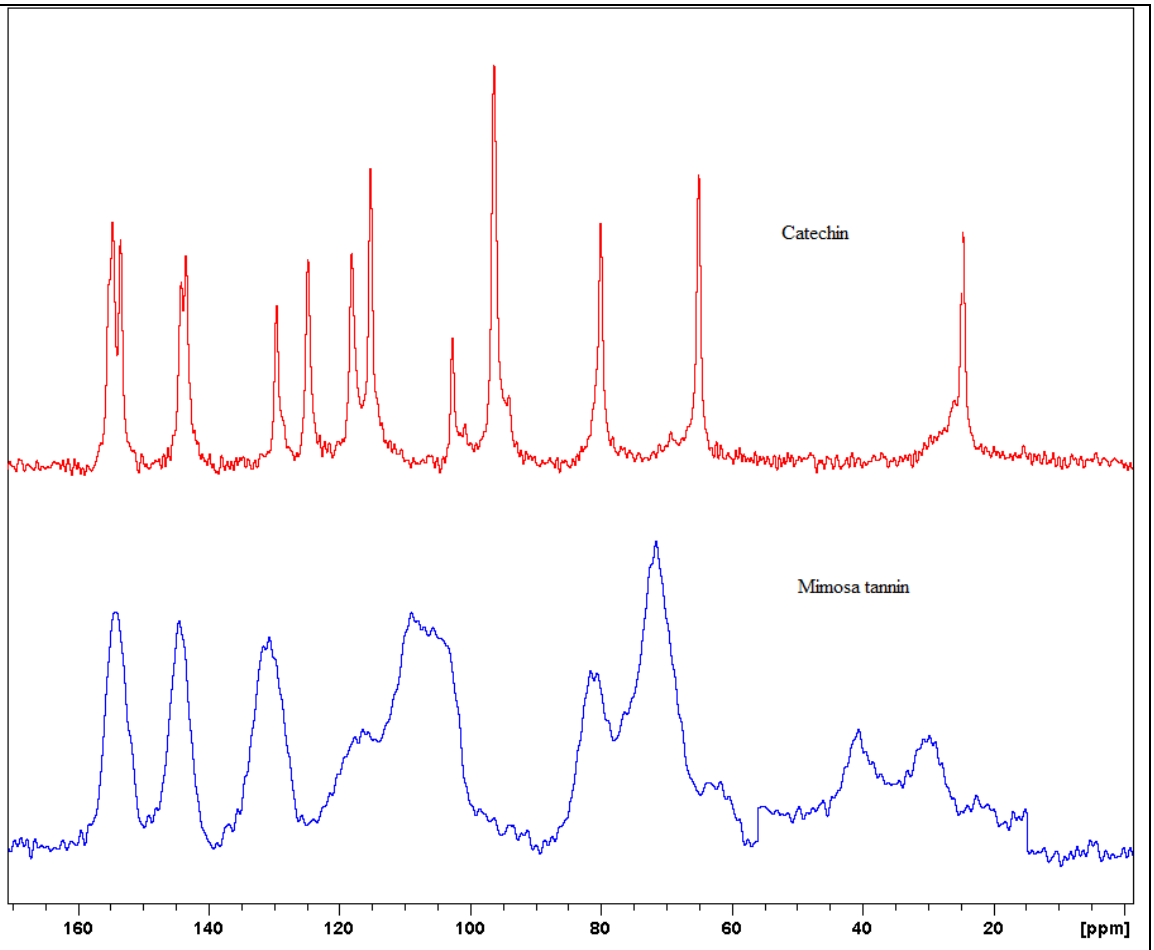

Figure 4-10: ^{13}C solid state NMR of catechin monomer and mimosa tannin

4.5 Experiment 4: ^{13}C Solid state NMR spectra of mimosa and quebracho condensed tannin.

4.5.1 Introduction

The ^{13}C solid state NMR spectra of quebracho and mimosa have not been obtained, assigned or compared in the literature (according to our knowledge). Apart from the scientific and commercial interest in the information on the structure that a solid state NMR investigation may yield, the industry did not have a quick and easy method to distinguish between these two extracts.

4.5.2 Results and Discussion

Solid state ^{13}C NMR spectra of commercial spray dried quebracho (ATN) and normal mimosa (ME from Mimosa Extract Company (Pty) Ltd) extracts with cross-polarization and magic-angle spinning (CP-MAS NMR) were obtained. Chemical shifts are reported relative to the methylene signal from solid glycine at 43.1 ppm, with the reference frequency set using tetramethylsilane (0 ppm).

The experimental procedure for the NMR experiments' conditions (frequency, contact time, magic angle spinning rate) are discussed in paragraph 6.2.

Figure 4-11 shows the solid state ^{13}C CP-MAS spectra of spray dried mimosa and quebracho tannin samples. Figure 4-12 shows all the peaks assigned. In general it can be observed that quebracho shows a distinct identifying peak at 115 ppm which is assigned to the fisetinidin catechol B-ring. This peak is absent in mimosa, which has a distinctive peak at 105 ppm assigned to the robinetinidin pyrogallol B-ring. These two peaks establish a fingerprint for mimosa and quebracho tannins. They also illustrate the difference in the B-ring nature of the two tannins.

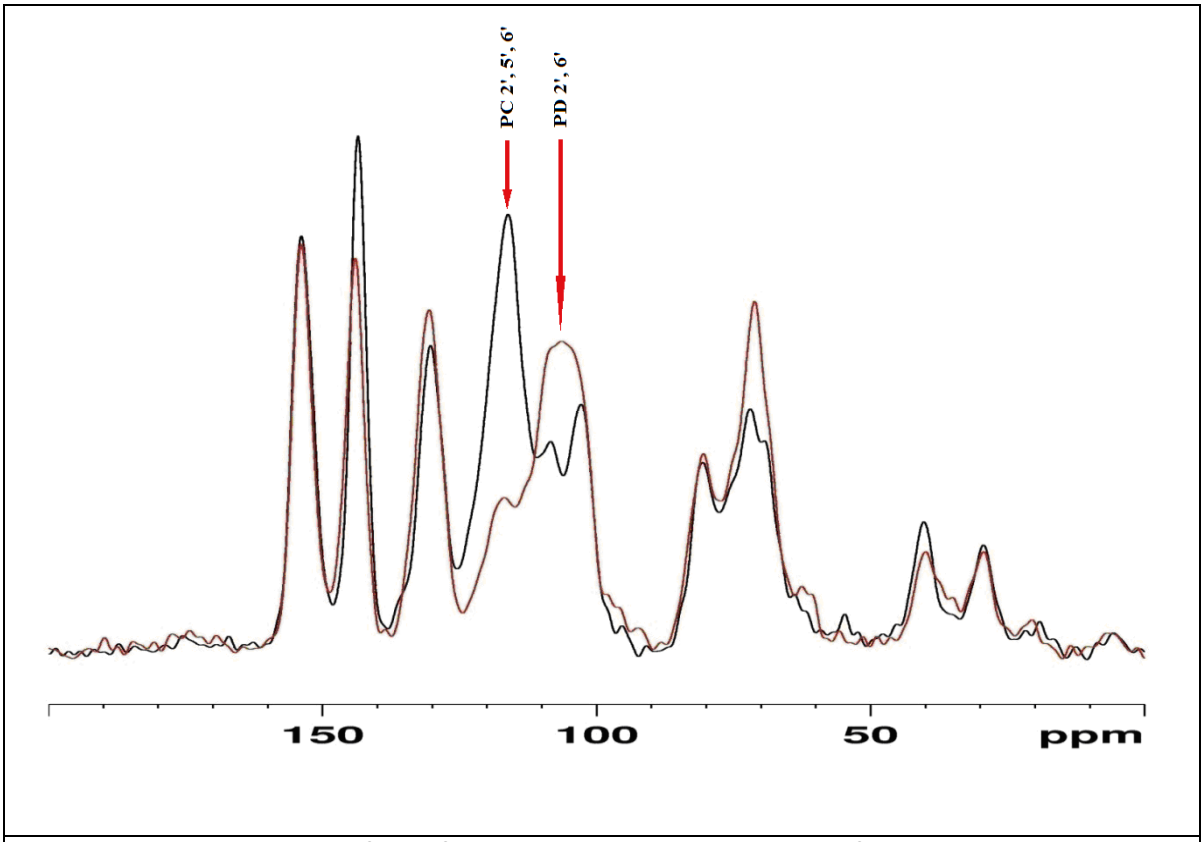

Figure 4-11: Solid state NMR of unsulfited mimosa (ME) (in red) and unsulfited quebracho (ATN) (in black)

The following further observations are made:

a) The major peak at 115 ppm in the quebracho (ATN) sample (black) is assigned to the PF B-ring (2',5' and 6' C-H). The major peak at 105 ppm in the mimosa (ME) sample (red) is assigned to the PR / PD pyrogallol B-ring (2' and 6' C-H). Solid state NMR thus provides a quick method to distinguish between quebracho and mimosa and confirms the predominant PR / PD nature of mimosa and PF nature of quebracho.

b) Minor peaks at 102 and 108 ppm in ATN (black) are assigned to the A-ring C-H and C-4' respectively. The corresponding peaks in the ME sample (A-ring C-H and C-4') are hidden below the big PR peak assigned above.

c) The peak at 116 ppm in the mimosa sample is assigned to the PF B-rings that also occur in mimosa.

d) The peak at 80 ppm in both quebracho and mimosa is assigned to C-2 with 2,3–trans relative stereochemistry.

e) The peak at 70 ppm is assigned to C-3. It is unclear why the C-3 peak of mimosa (red) is bigger than C-3 of quebracho (black). This indicates unknown impurities, probably waxes.

f) The terminal C-4 at 28 ppm and repeat C-4 at 40 ppm is of potential major significance. Reliable integration of these peaks would give an accurate terminal / repeat unit ratio. This would allow the establishment of an accurate average degree of polymerisation (DP) value. Unfortunately sugar and gums (about 25 % of the mimosa extract) also resonate in this region and purified tannins would be required.

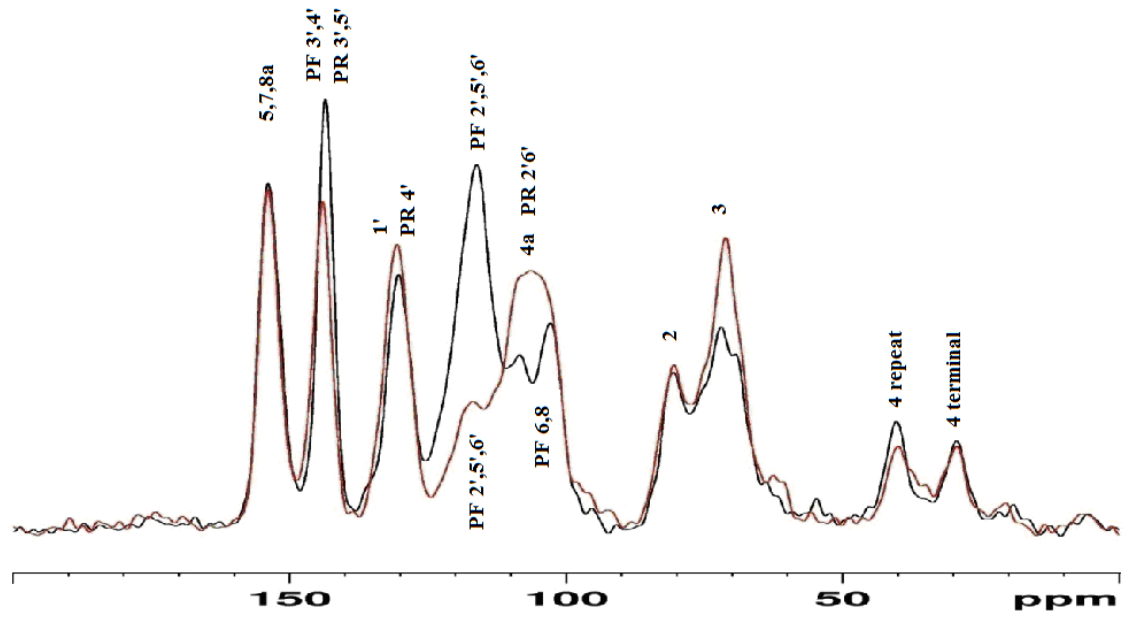

Figure 4-12: ^{13}C NMR of mimosa (ME) (red) and quebracho (ATN) (black), showing all the assigned peaks

4.5.3 Conclusion

Solid state NMR unambiguously differentiates between mimosa and quebracho extract. As seen in Figure 4-11, quebracho shows a distinct identifying peak at 115 ppm which is assigned to the fisetinidol catechol B-ring. This peak is absent in mimosa, which has a

distinctive peak at 105 ppm assigned to the robinetinidol (gallocatechin) / pyrogallol B-ring. These two peaks establish a fingerprint for mimosa and quebracho tannins. They also illustrate the difference in the B-ring nature of the two tannins.

The terminal C-4 at 28 ppm and repeat C-4 at 40 is potentially of major significance. In contrast with ^{13}C solution state NMR where the terminal C-4 and repeat C-4 have a low intensity and require many scans to become observable, these peaks are prominent in ^{13}C solid state NMR. Reliable integration of these peaks would give an accurate terminal / repeat unit ratio. This would allow the establishment of an accurate average degree of polymerisation (DP) value. Existing methods to determine DP give conflicting results. The ratio between these two peaks promises the first reliable indication of the average chain length of polymers.

4.6 Experiment 5: The ^{13}C solid state NMR spectra of hydrolysable tannins

4.6.1 Introduction

Tannins are classified into condensed tannins (proanthocyanidins) and hydrolysable tannins. In contrast to condensed tannins that are oligomers of flavan-3-ols, hydrolysable tannins are galloyl (**1**) and hexahydroxydiphenoyl (**2**) esters (Figure 4-13), most often with D-glucose (**3**) and derivatives (for example quinic acid [**4**]). Italian chestnut and tara are examples of hydrolysable tannins.

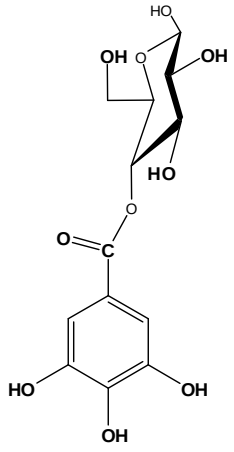

Gallotannin **(1)**

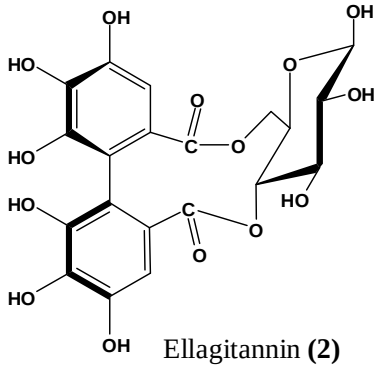

Ellagitannin **(2)**

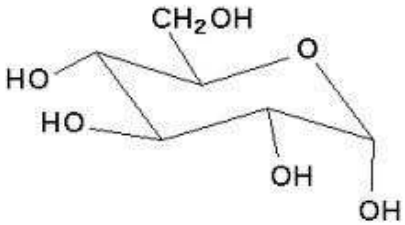

D-Glucose

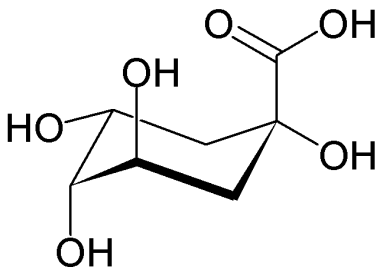

Quinic acid

Figure 4-13: Hydrolysable tannins building blocks

A previous report[16] on the ^{13}C solid state NMR of tannic acid, which is an example of a hydrolysable tannin, indicated that peaks are expected at 139 ppm and 119 ppm (C-4 and C-1, respectively, of the aromatic ring).

4.6.2 Results and Discussion

The following tannins were obtained and analysed with solid state NMR:

a) South African mimosa spray dried (ME)
b) Chinese mimosa (*Albizzia julibissin*)
c) Quebracho (ATN)
d) Tara from Peru (*Caesalpinia Spinosa*)
e) Yugan from China (*Boswelia frereana*)
f) Chestnut from Italy (*Castanea sativa*)

The results are summarized in Figure 4-14. Condensed tannins and hydrolysable tannins can clearly be distinguished by the absence of the 155 ppm C-OH resonance associated with the aromatic A-ring in condensed tannins and the presence of the 170 ppm ester carbonyl resonance in hydrolysable tannins.

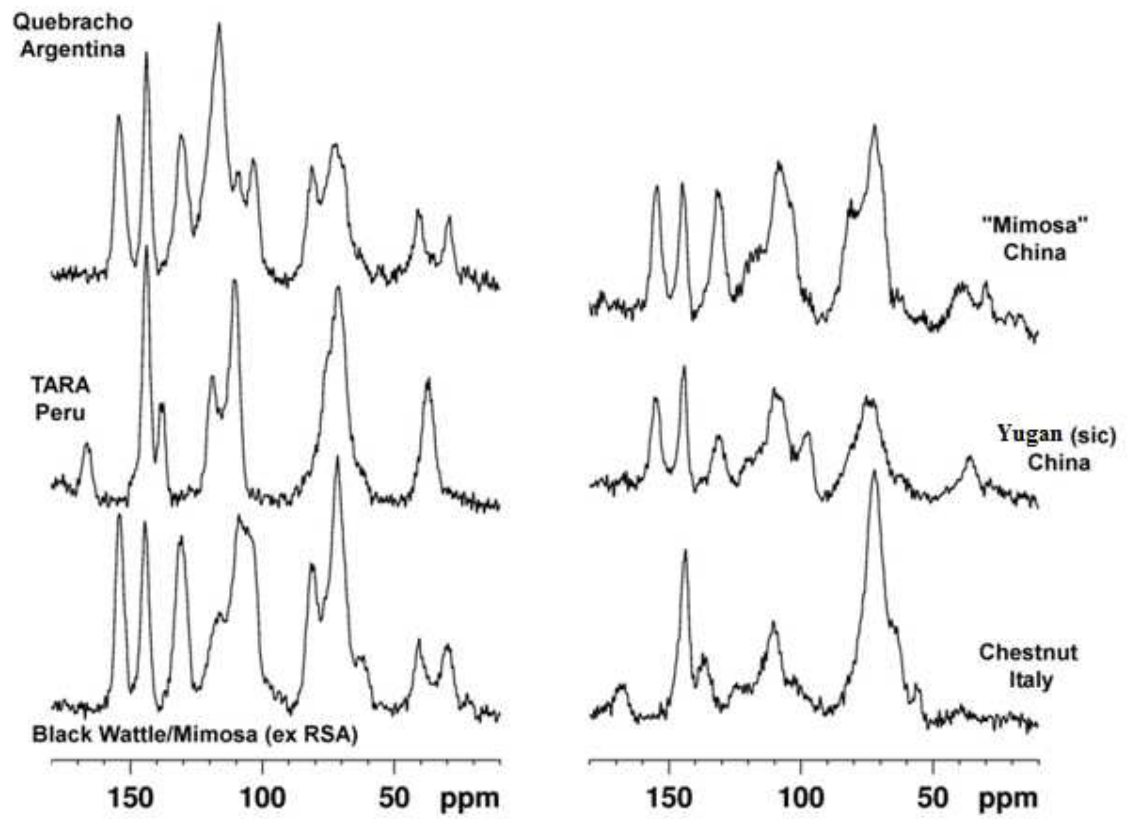

Figure 4-14: ^{13}C solid state NMR of South African mimosa spray dried (ME), Chinese mimosa, quebracho (ATN), tara from Peru, yugan from China and Italian chestnut.

The following observations are made:

a) South African- and Chinese mimosa are similar; both are dominated by robinetinidin / prodelphinidin pyrogallol-type B-rings which show a major peak around 105 ppm. Chinese mimosa seems to have a smaller terminal peak at C-4 (25 ppm), indicating a larger degree of polymerization.
b) Quebracho has profisetinidin catechol-type B-rings which show major peaks around 115 ppm.

c) Yugan has a smaller A-ring C-OH peak, no C-2 (2,3-*trans*) peak at 80 ppm and a single C-4 peak at about 30 ppm. It can be identified by a characteristic peak at 95 ppm. This peak does not occur in any of the other tannins.
d) Tara does not have an A-ring C-OH peak (155 ppm), has a single large C-4 peak at 36 ppm, a medium peak at 120 ppm (PC) and a large peak at 110 ppm (PD). Tara and Italian chestnut show similarities. Italian chestnut has an almost absent smaller C-4 at 38 ppm whilst that of tara is prominent (benzylic C-H). Both have a large aliphatic C-OH at 70 ppm. Tara has is a resonance at about 45 ppm which is absent in chestnut.
e) Yugan exhibits a possible 2,3-*cis* stereochemistry and has fewer terminal carbons around 20 ppm, indicating a longer polymer chain.
f) The 35 ppm peak in tara is the two CH_2-groups of the quinic acid (Figure 4-13).

4.6.3 Conclusion

^{13}C solid state NMR can be used to distinguish between condensed and hydrolysable tannins. Tara Peru and Italian chestnut are clearly hydrolysable tannins. Diagnostic is the absence of A-ring carbons (155 ppm) and the presence of a carboxyl resonance (170 ppm).

From the mass spectrometry data (Plate 5-16 on page 170) we know that chestnut is a glucose-gallic acid oligomer and tara is a quinic acid-gallic acid oligomer. This allows us to assign the resonance at about 45 ppm in the tara solid state spectrum (Figure 4-14) (this resonance is absent in chestnut) to the CH_2 carbons in the quinic acid moiety (Figure 4-13).

The ^{13}C solid state NMR of yugan, shows it is clearly a hydrolysable tannin as indicated by mass spectroscopy (Plate 5-17, page 172). At this stage we cannot explain the resonance at 158 which indicates a condensed tannin. Yugan differs from the condensed tannins as follows:

a) The resonance at 33 ppm, is between that of a terminal (*ca.* 28 ppm) and repeat (*ca.* 38 ppm) condensed tannin terminal unit. We see the same in tara and attribute

it to the quinic acid CH_2 groups. This is the region where sugar and gum resonances interfere with our carbon tannin spectrum.

b) The resonance at 80 ppm that corresponds with CH_2 with a *trans* hydrogen (on C-3) is absent.

The 158 ppm resonance in the yugan spectrum is probably due to the quinic acid carbonyl that has shifted from 168 ppm for unexplained steric reasons. Yugan is not commercially available from China and not of commercial interest anymore. It however indicates the requirement that spectral analysis should be done with care. Ideally solid state NMR and mass spectrometry should be used together.

4.7 Experiment 6: The effect of sulfitation on mimosa and quebracho tannins

4.7.1 Introduction

Sulfitation is used to increase tannin extraction yield from bark. It also enhances tannin in formaldehyde adhesive applications by lowering viscosity and enhancing water solubility. It increases water retention by the adhesive resin that allows slower adhesive film drying.[17,18] It is postulated that by opening the C-ring and changing the A-ring from a methoxyphenol to a hydroxyphenol (Figure 4-15), the reactivity of the A-ring towards formaldehyde is increased.

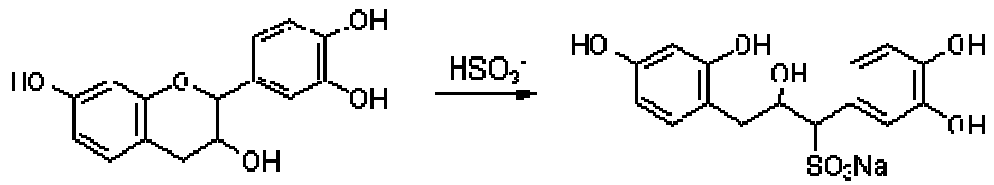

Figure 4-15: The postulated opening of the pyran ring during sulfitation of bark extracts

Foo *et. al.*[19] claimed that sulfitation breaks the interflavanyl bond. The sodium epicatechin-(4β)-sulphonate (Figure 4-16) was isolated upon treatment of loblolly pine bark with sodium hydrogen sulfite at pH 5.5 and 100º C for 20 hours. They attributed small quantities of the C-ring opened product **3** (Figure 4-17) to the reaction of the terminal unit with sulfite.

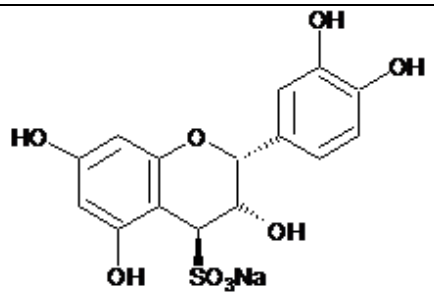

Figure 4-16: Structure of isolated sodium epicatechin-(4β)-sulphonate

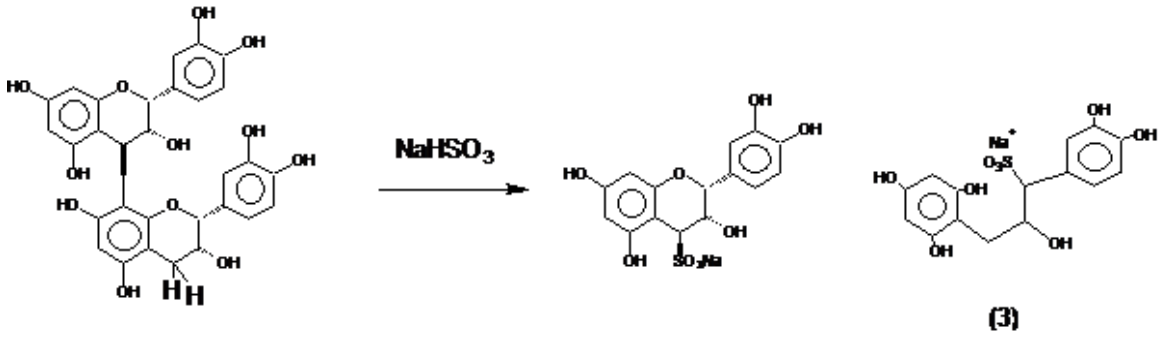

Figure 4-17: Reaction yielding the pyran ring-opened product

Foo[19] identified an upfield shift for C-2 from about 79 ppm to 76 ppm upon sulfitation of C-4 and used this to assign the sulfonate *trans* to the 3-hydroxy group of compound **3** (γ-*gauche* effect).[20] The sulfited carbons resonate at 60 ppm (C-4) and 71.4 ppm (C-2 in **3**).

Sulfitation enhances the commercial properties of mimosa and particularly quebracho tannins. It involves treating the commercial extract with various levels of bisulfite. Despite widespread industrial use, two important questions persist:

a) The chemical changes associated with sulfitation remains uncertain. It is generally assumed that the heterocyclic C-ring opens and a sulfonic acid group is introduced into the benzylic 2-position. The sulfonic acid group will be very acidic (it should have a pKa value similar to *p*-toluenesulfonic acid). This will enhance the water solubility of condensed tannins. It will also lead to acid catalysed decomposition of the polymer upon heating and removal of water from the extract. It has been postulated that sulfited extracts have shorter average chain lengths. The low pKa interferes with chromatography and the composition of sulfited extracts have not been reported yet.

b) It is uncertain how much of the bisulfite the extract is treated with actually reacts with the condensed tannin polymers. In the absence of suitable analytical methods to separate bisulfite from condensed tannins, this cannot be determined.

4.7.2 Results and Discussion

Solid state ^{13}C NMR spectra of unsulfited (ME), medium sulfited (FS) and heavily sulfited (WS) mimosa samples were obtained using standard cross polarization (CP) MAS techniques. The spectra are shown in Figure 4-18 and Figure 4-19.

Figure 4-18 shows that unsulfited (ME) and sulfited extracts (WS and FS), can be distinguished. It does not distinguish WS from FS though. Unsulfited mimosa has an identifying peak at approximately 81 ppm (based on solution state ^{13}C NMR chemical shifts (Table 4-3). This peak, which represents the C-2 carbons of 2,3-*trans* units, disappears during sulfitation. This is attributed to the fact that sulfitation opens the C-ring by introducing a sulfonic acid group on C-2. Isomerisation from 2,3-*trans* to 2,3-*cis* stereochemistry will however have the same effect. These spectra suggest that the C-ring of mimosa is opened upon treatment with bisulfite. There does not seem to be a big difference between medium and heavily sulfited mimosa extract, despite the fact that their physical properties differ. This suggests that all changes are not observed by ^{13}C solid state NMR due to overlap of broad resonance peaks.

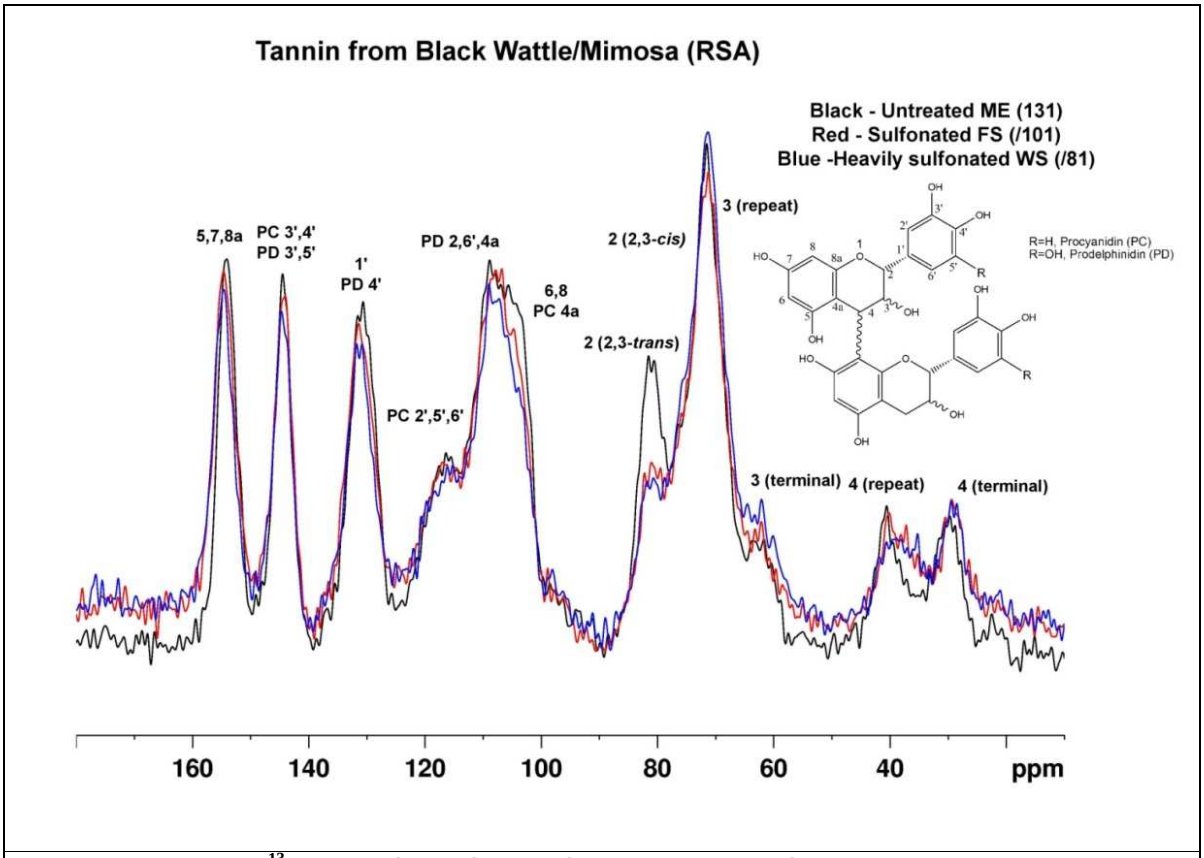

Figure 4-18: CP-MAS ^{13}C NMR of unsulfited, sulfited and heavily sulfited mimosa

Figure 4-19 shows that the sulfitation of quebracho, like mimosa, leads to the disappearance of the C-2 peak at 80 ppm. This indicates ring opening (introduction of a sulfonic acid group at C-2) or isomerisation to the 2,3-*cis* isomer. The peak at 70 ppm increased significantly, whereas in mimosa, it increased only slightly. This can be ascribed to the fact that quebracho has fewer impurities (5% sugars and gums) than mimosa (25% sugars and gums) due to the fact that mimosa is a bark extract and quebracho is a heartwood extract. Sugars and gums resonate at 70 ppm.

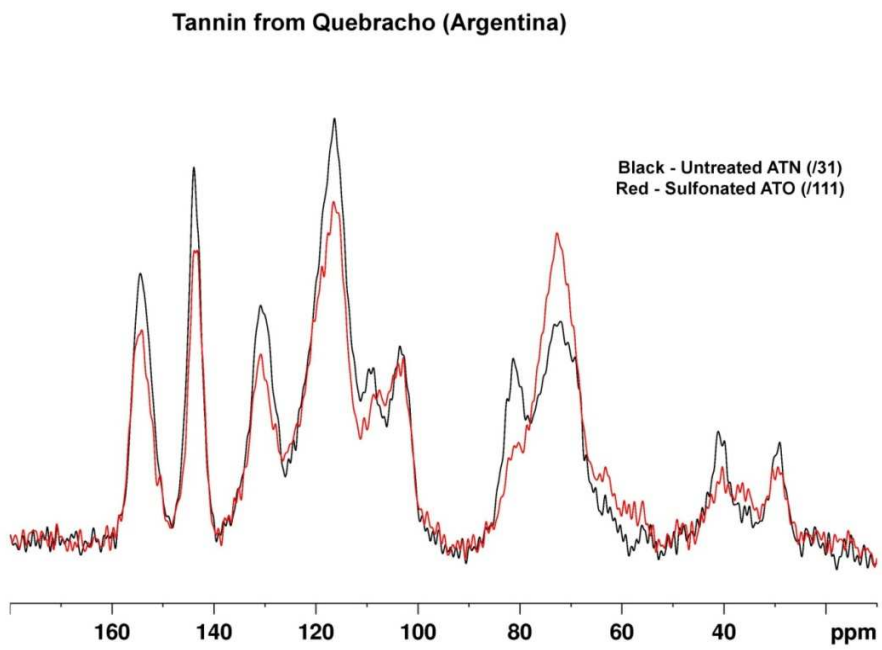

Figure 4-19: CP-MAS ^{13}C NMR of unsulfited and sulfited quebracho

4.7.3 Conclusion

^{13}C solid state NMR can be used as a fingerprint technique to distinguish between sulfited and unsulfited quebracho and mimosa tannin. It cannot distinguish between medium and heavily sulfited extracts. It supports the assumption that sulfitation opens the heterocyclic C-ring and introduces a sulfonic acid group at C-2.

Our ^{13}C solid state NMR results do not support Foo's conclusion regarding the upfield shift upon sulfited and unsulfited quebracho and mimosa tannin.[19] The resonance at 80 ppm disappears, indicating sulfitation at C-2. The sulfited species in the mass spectra in the next chapter (Chapter 5) corresponds to a ring-opened product.

Foo[19] worked with loblolly pine bark that consists of predominantly epicatechin monomers with a 5-OH group that renders the interflavanyl bond labile.[20] We worked with mimosa and quebracho tannins that consist predominantly of robinetinidol and fisetinidol monomers. The

absence of a 5-OH group renders the interflavanyl bond stable and sulfitation at C-2 with ring opening becomes feasible

4.8 Experiment 7: Determination of the average degree of polymerisation (average chain length / number of monomers) in condensed tannin dimers, trimers, tetramers and pentamers

4.8.1 Introduction

One of the most vexing questions in tannin chemistry is the average chain length or average molecular weight of the tannin. A variety of methods have been applied, including ebulliometry, mass spectroscopy and ^{13}C NMR. [21,22,23] None of these methods are unambiguous.

Salient in the ^{13}C solid state NMR spectra of mimosa and quebracho extracts are the prominent resonances at *ca.* 28 and 38 ppm associated with the C-4 carbon of the heterocyclic C-ring. In the terminal flavan-3-ol monomer units the heterocyclic C-4 is benzylic with two hydrogens attached and resonates at 28 ppm. The repeat flavan-3-ol monomer units have double benzylic heterocyclic C-4 carbons that resonate at 38 ppm. This provides an opportunity to determine chain length *via* comparing the ratio between the intensities or areas of the peaks at 28 and 38 ppm, respectively.

The areas under the peaks were taken to be directly proportional to the number of carbons contributing to the size of the peak. The following formula for chain length was postulated:

$$Chainlength = \frac{repeat + term}{term} = \frac{I(38\,ppm) + I(28\,ppm)}{I(28\,ppm)} \qquad \text{(Equation 1)}$$

The hypothesis was investigated using synthetic oligomers and extrapolated to extracts from commercial wattle and fresh bark.

4.8.2 Results and Discussion

The following synthetic dimers, trimers, tetramer and pentamer were investigated:

- Epicatechin-4β-8-catechin (B1) Figure 4-20
- Epicatechin-4β-8-epicatechin (B2) Figure 4-21
- Catetechin-4α-8-epicatechin (B4) Figure 4-22
- Catetechin-4α-8-catechin-4α-8-epicatechin (T1) Figure 4-23
- Epicatechin-4β-8-epicatechin-4β-8-epicatechin (T2) Figure 4-24
- Epicatechin-4β-8-epicatechin-4β-8-epicatechin-4β-8-epicatechin (tetramer) Figure 4-25
- Epicatechin-4β-8-epicatechin-4β-8-epicatechin-4β-8-epicatechin-4β-8-epicatechin (pentamer) Figure 4-26

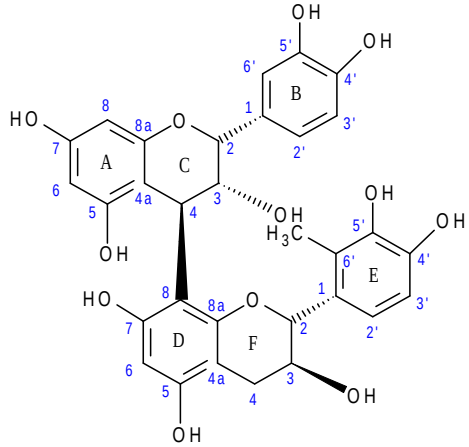

Figure 4-20: B1: Epicatechin-4α-8-catechin

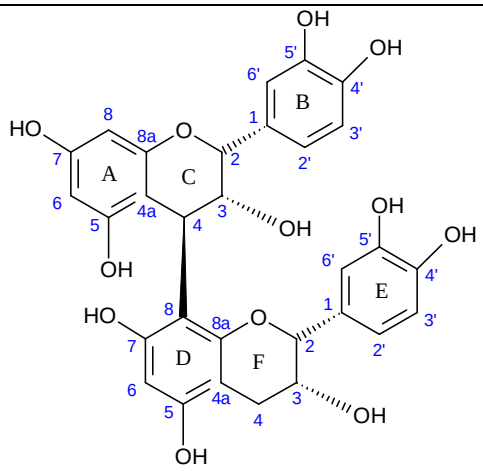

Figure 4-21: B2: Epicatechin-4β-8-epicatechin

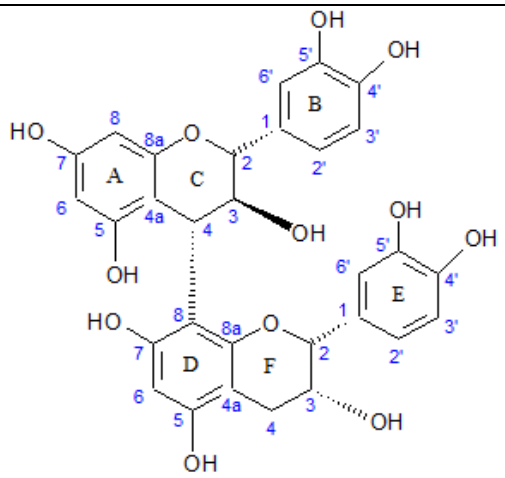

Figure 4-22: B4: Catetechin-4α-8-epicatechin

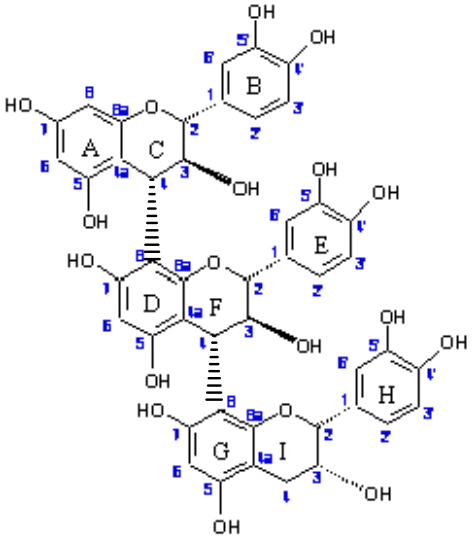

Figure 4-23: T1: Catetechin-4α-8-catechin-4α-8-epicatechin

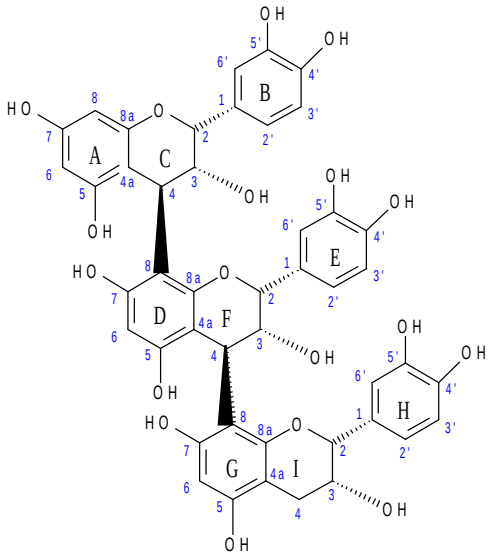

Figure 4-24: T2: Epicatechin-4β-8-epicatechin-4β-8-epicatechin

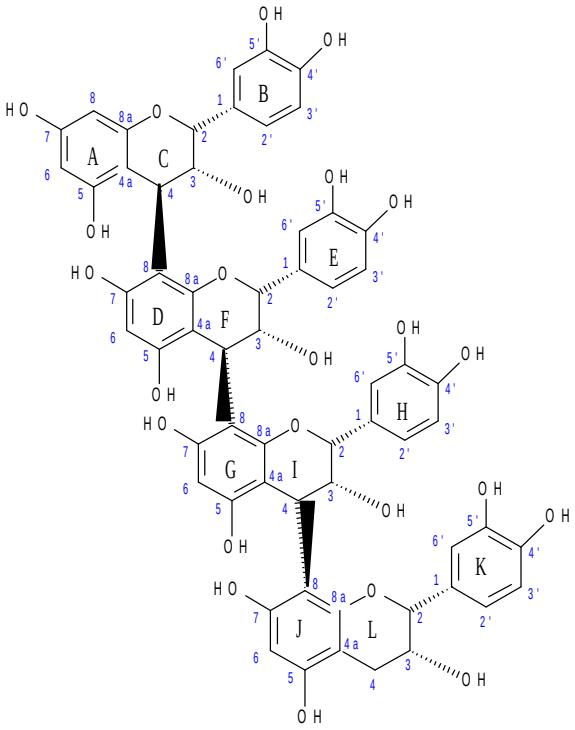

Figure 4-25: Tetramer: Epicatechin-4β-8-epicatechin-4β-8-epicatechin-4β-8-epicatechin

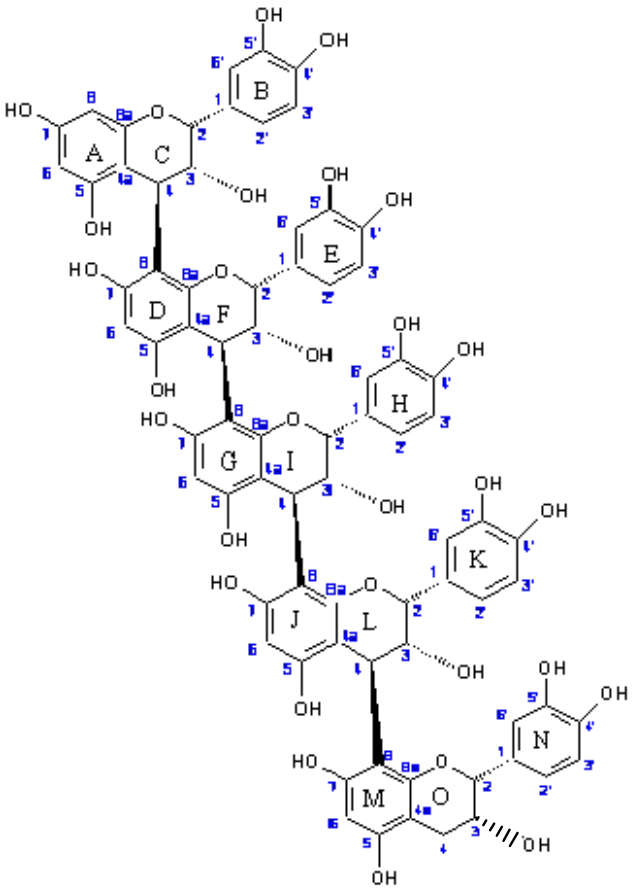

Figure 4-26: Pentamer: Epicatechin-4β-8-epicatechin-4β-8-epicatechin-4β-8-epicatechin-4β-8-epicatechin

Figure 4-27 shows the solid state NMR spectra of a dimer, trimer, tetramer and pentamer. Whilst the chemical shift of all resonances remains the same, the intensity varies as follows:

a) The ratio between the peaks at 28 and 38 ppm becomes smaller as the chain length increases;
b) For the tetramer and pentamer, resonances appear at 20 and 170 ppm. These are not compatible with the synthetic structures and are assumed to be impurities;
c) The resonance at 67 ppm is absent in the tetramer and pentamer.

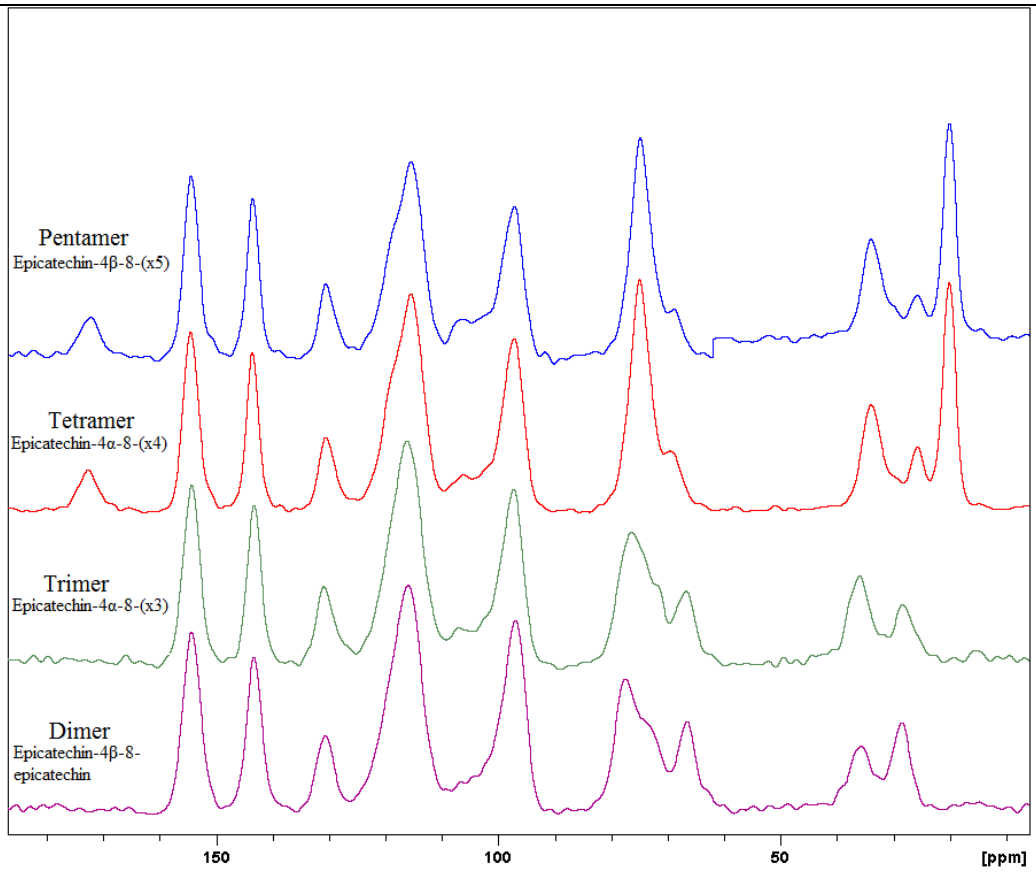

Figure 4-27: 13C solid state NMR spectra of known oligomers

Figure 4-28 and Table 4-6 compare the theoretical chain length (based on the number of monomers in the synthetic product) to the chain length calculated from the ratio of the peak areas at 28 ppm and 38 ppm from Equation 1 depicted above.

Some mass discrimination seems to take place. As the chain length increases, the number of monomers calculated from the ratio of the areas under the peaks at 28 ppm and 38 ppm are less than the actual number of monomers in the compound. It is uncertain whether the impurities observed at 20 ppm and 170 ppm in the spectra of the tetramer and pentamer play a role. It is also possible that some decomposition of the tetramer and pentamer has taken place. It is notoriously difficult to purify these higher oligomers. The 5-OH group in the model compound also renders the interflavanyl bond unstable and it is also possible that some decomposition of the tetramer and pentamer takes place since it is known that oligomers bigger than pentamers

decompose rapidly once benzyl protection has been removed (verbal communication from Prof. D.Ferreira, Department of Pharmacognosy, University of Mississippi).

Table 4-6: Deviation from the expected chain length of known oligomers

Chain length	Expected	Observed	Deviation
Dimer	2	1.921	0.079
Trimer	3	2.786	0.214
Tetramer	4	3.392	0.608
Pentamer	5	4.329	0.671

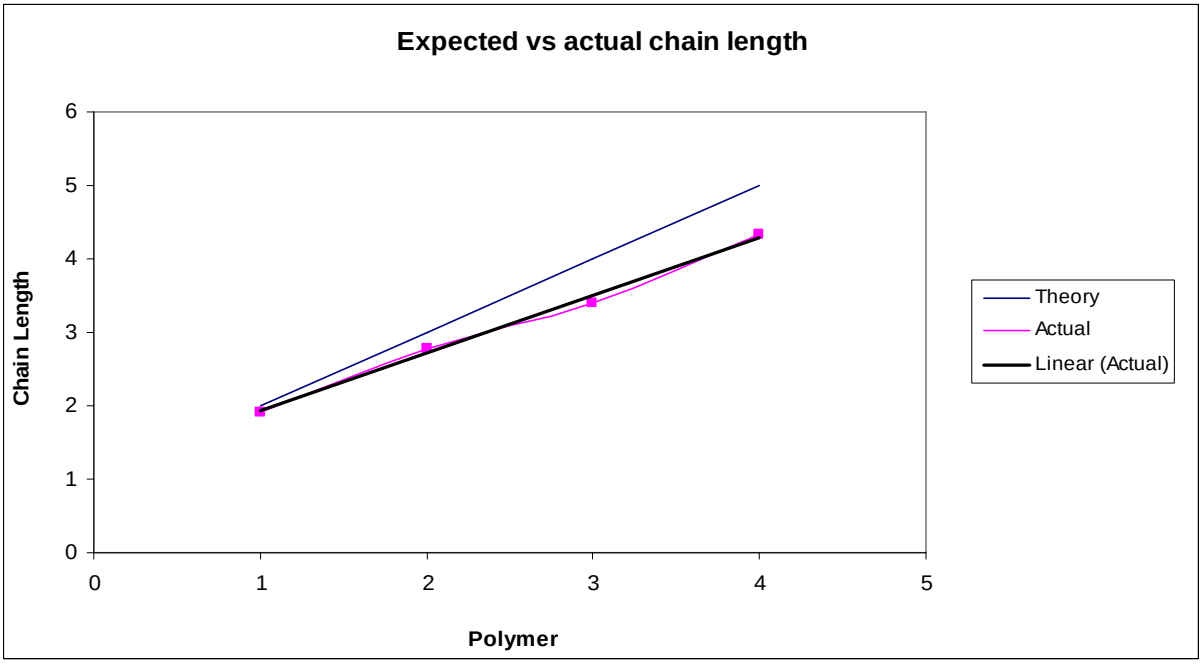

Figure 4-28: Graph of the expected versus known chain length of oligomers

Potentially more interesting is the disappearance of the 68 ppm resonances in the spectra of the tetramer and pentamer, associated with C-3. We postulate that the dimers and trimers occur in different configurations different from the tetramer and pentamer in the solid state and that this influences the chemical shift of C-3.

Applications of equation 1 to the lead-acetate precipitate of stick bark (Figure 4-29) and the lead-acetate precipitate of spray dried mimosa (Figure 4-30) gave an average chain length of 2.9 and 3.4 respectively. These should be treated with caution as the acetate methyl group signals with the 28 ppm resonance of the terminal C-4. Precipitation of condensed tannins using a lead salt, with a counter-ion that does not resonate in the 28 ppm to 38 ppm region, should be explored.

Monomers and dimers cannot tan leather, because they are too small to act as a bridge between different collagen strands and are washed out with water and solutions used in tanning. Ebulliometry and other studies suggest a tetramer average chain length for mimosa condensed tannins.[22]

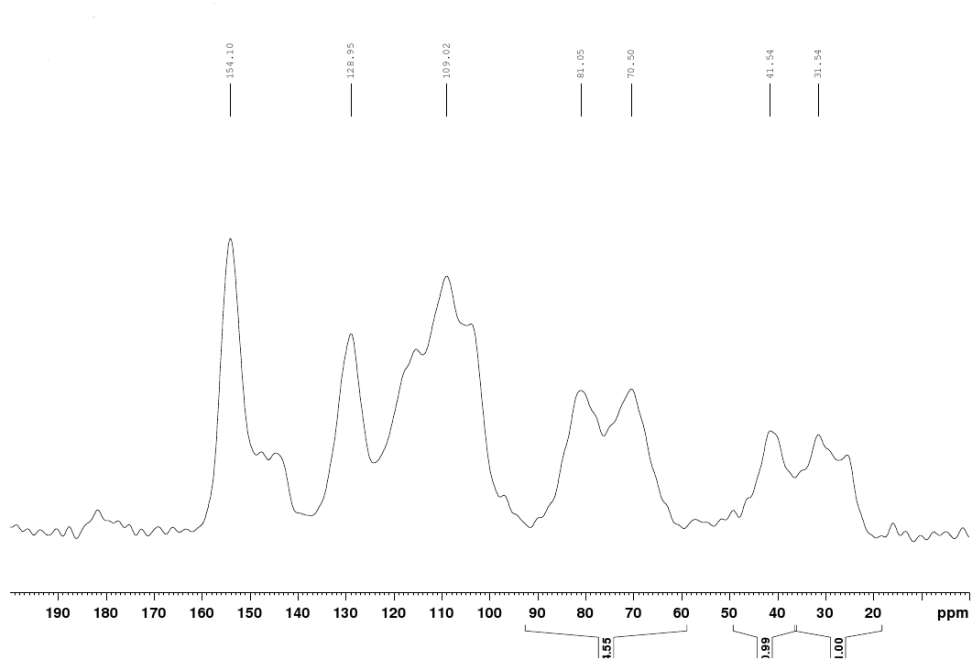

Figure 4-29: ^{13}C Solid state NMR of lead-acetate precipitated tannins from stick bark of mimosa

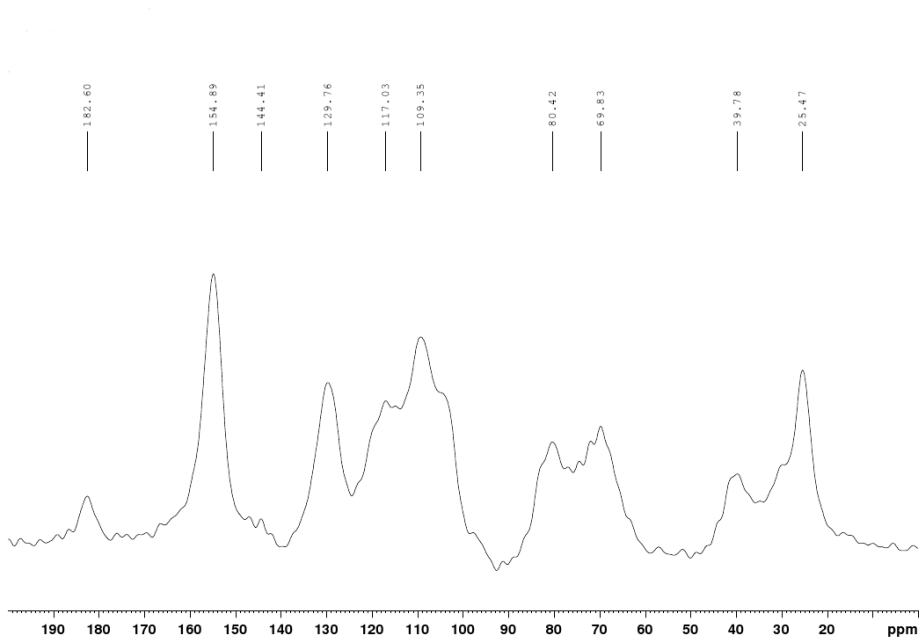

Figure 4-30: ^{13}C Solid state NMR of lead-acetate precipitated tannins from commercial spray dried mimosa

4.8.3 Conclusion

Theoretically the ratio between the terminal- and repeat unit can be used to estimate average chain length of condensed tannin extracts. Results so far are however disappointing and the chain length determined with solid state NMR does not agree with the values obtained with other techniques.

4.9 Experiment 8: Fractionation of mimosa condensed tannins via precipitation of gums with ethanol and precipitation of tannins with lead acetate

4.9.1 Introduction

An aqueous solution of mimosa condensed tannins is traditionally fractionated as follows:

a) The gums are precipitated by the addition of ethanol;
b) The tannins are then precipitated from the supernatant of the ethanol extract, by addition of lead acetate;
c) Sugars remain in ethanol solution.

4.9.2 Results and Discussion

After fractionation of a mimosa sample, as described above, ^{13}C solid state NMR spectra of commercial spray dried mimosa extract (Figure 4-31), the gums precipitated with ethanol (Figure 4-32), the ethanol supernatant containing sugars and condensed tannins (Figure 4-33), and the lead acetate precipitated condensed tannins (Figure 4-34), were recorded.

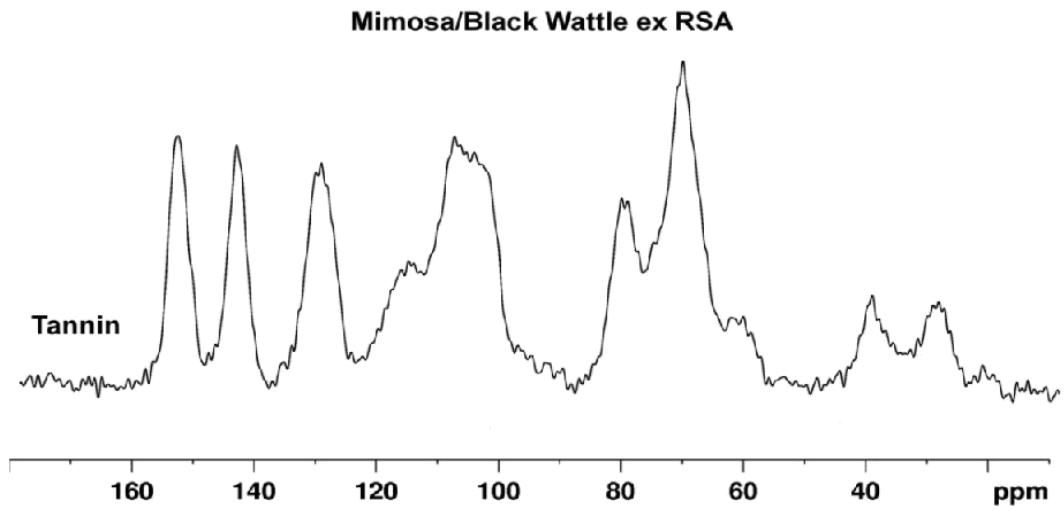

Figure 4-31: 13C Solid state NMR of spray dried Mimosa extract (ME)

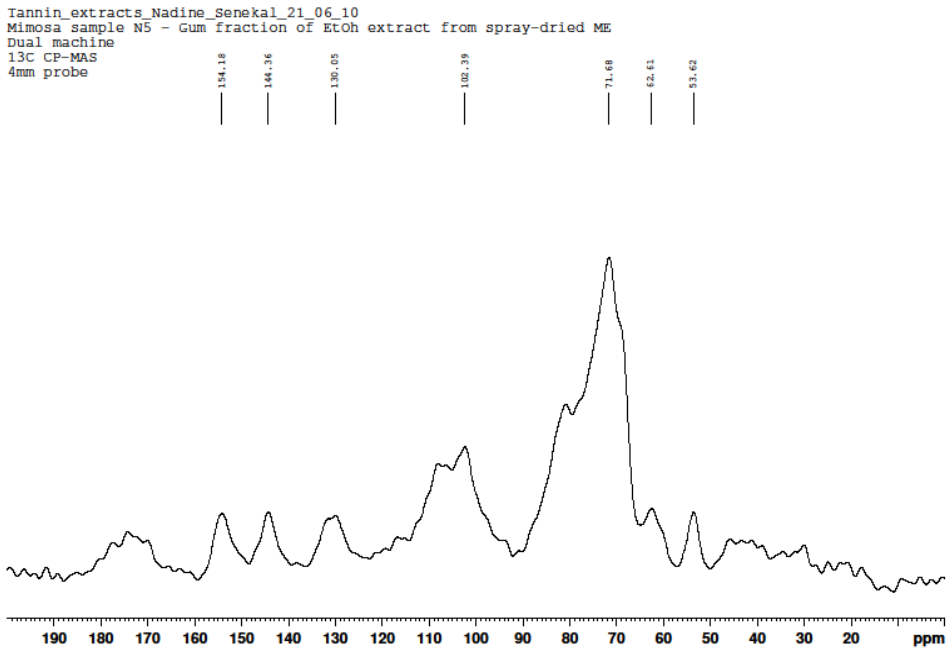

Figure 4-32: Gums precipitated with ethanol from an aqueous solution of ME

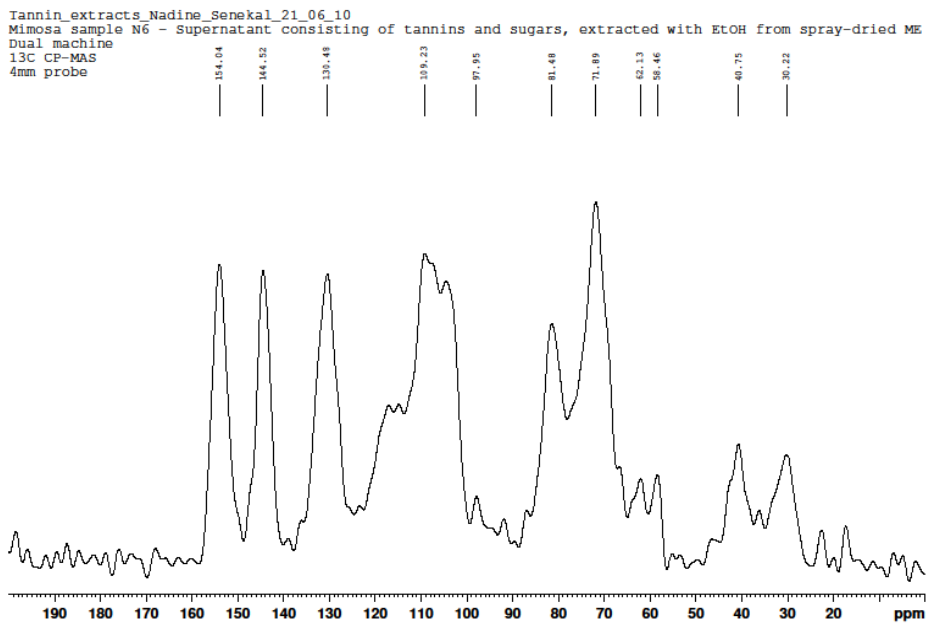

Figure 4-33: Supernatant consisting of sugars and condensed tannins

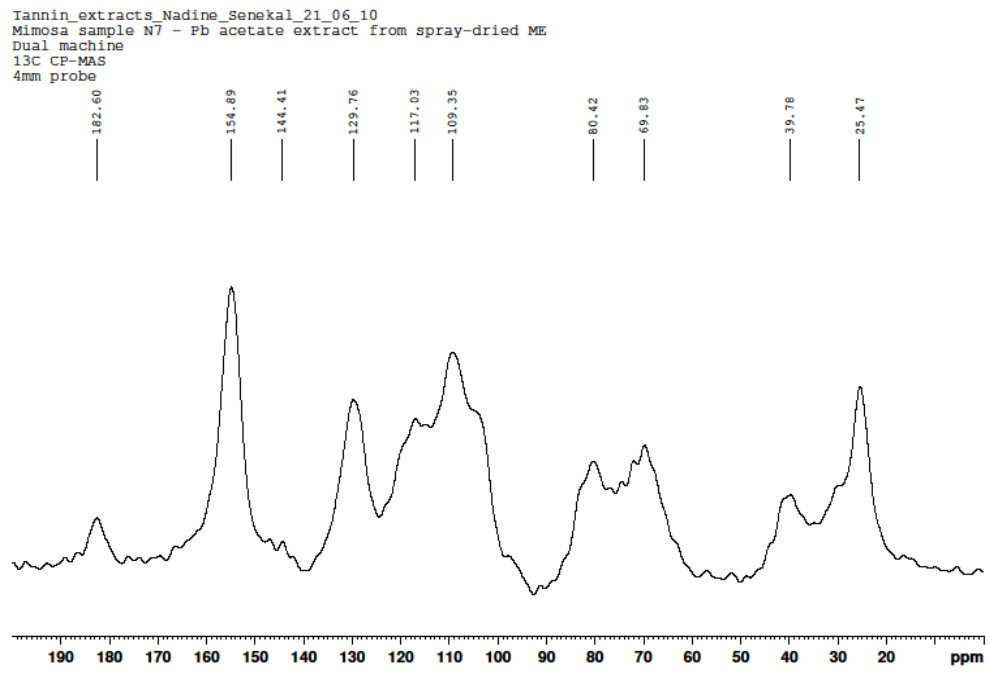

Figure 4-34: Lead-acetate precipitate from ethanol extract of ME consisting of condensed tannins

Figure 4-32 represents the water soluble and ethanol insoluble gum fraction. The gums resonate exclusively in the region assigned to carbohydrates and the spectrum correlates closely with that of cellulose (middle spectrum in Figure 4-35 and Figure 4-36) agreeing with the general assumption that the gums are carbohydrate monomers.[24,25] We know from the literature[26] that the average molecular weight of mimosa tannin is about 90 000 Da. The large resonance at 71 ppm in Figure 4-32 (spray dried mimosa tannin) thus represents gums (polymers of carbohydrates) and it overlaps with the condensed tannin C-3 resonance. Some aromatic resonances associated with condensed tannins remain in the gum fraction. The ethanol precipitate should be repeatedly washed with water in future experiments to establish whether these resonances represent tannins that are covalently bonded to gums or impurities.

Figure 4-33 (condensed tannins and ethanol soluble sugars) still has a prominent carbohydrate resonance at 71 ppm. The resonances at 28 ppm and 38 ppm represent the C-4 of terminal and repeat condensed tannins constituent monomers.

Figure 4-34 (lead acetate precipitate of condensed tannins) shows that the 1:1 ratio of the 70 ppm (C-3) and 80 ppm (C-22) resonances support the absence of interfering carbohydrate resonances. The presence of lead acetate is clearly evident from the carbonyl resonance at 160 ppm and the methyl resonance at 25 ppm.

The resonance at *ca*. 140 ppm, associated with C-3', C-4' and C-5', disappears, due to complexation of the *ortho*-OH groups (cathechol or pyrogallol rings) with lead. The A-ring has OH groups in meta-positions only and does not complex with lead.

4.9.3 Conclusion

The possibility of lead being paramagnetic and hence having certain influences on the resonance of the extract is being investigated and is considered as future work. The magnetization of other metals combining with mimosa extract has been investigated and is discussed in paragraph 4.13.

4.10 Experiment 9: The tannin content of spent bark

4.10.1 Introduction

It is of scientific and commercial interest to understand how much tannins remain in bark and other plant material after exhaustive extraction. Sir Robert and Lady Robinson concluded in the 1930's that the greater proportion of proanthocyanidins in plants issues occur as insoluble higher oligomers and polymers.[27,28] They classified proanthocyanidins on the basis of solubility in three classes:

a) those that are insoluble in water and the usual organic solvents,
b) those readily soluble in water but not extracted from the water extract with ethyl acetate, and
c) those that can be extracted from an aqueous solution with ethyl acetate

Hillis and Swain (1959),[29] Bate-Smith (1975)[30] and Porter (1989)[2] also came to the conclusion that only a small fraction of proanthocyanidins in plants belongs to class 1 and 2 and that the majority of proanthocyanidin oligomers remain unextracted. It was postulated that readily soluble proanthocyanidins (classes 2 and 3) represented only the "tip of the iceberg" and that the insoluble fraction forms the base of the "metabolic iceberg"[31,p34] and are thus not reflected. These conclusions were supported by the development of a red colour upon treatment of spent bark with dilute acid (the so-called proanthocyanidin test).[32]

4.10.2 Results and Discussion

Samples of mimosa bark, mimosa tannin extract and spent bark (what remains after water soluble tannins have been extracted) were obtained and analysed with ^{13}C solid state NMR. The spectra of spent Mimosa barks compared to bark from which the tannin has not been extracted and industrially prepared mimosa tannin extract is shown in Figure 4-35. The peaks in Figure 4-35 marked with "T" represent the tannins, "C" represents water insoluble carbohydrates (gums) and "L" represents lipids.

The tannin peaks in mimosa bark and mimosa tannin extract are similar. The spent bark spectrum clearly lacks the tannin resonances which are observed in the unextracted bark. This means that mimosa bark and tannin spray dried extract have a similar chemical composition. The absence of aromatic resonances associated with condensed tannins in the 110 to 160 ppm region proves that spent bark contains no condensed tannin and that condensed tannins are exhaustively extracted with warm water. As discussed elsewhere (paragraph 4.9), the water soluble carbohydrates in mimosa extract consists of an ethanol soluble fraction and a fraction that can be precipitated with ethanol. This fraction has an estimated molecular weight of about 90 000 Dalton. We can thus conclude from the spectra that spent bark consists predominantly of carbohydrate gums with an average molecular weight of more than 90 000 Dalton. It is well known that lipids appear as sharp resonances in solid state NMR due to free rotation (see Chapter 3). Small quantities of lipids are thus present in bark and spent bark.

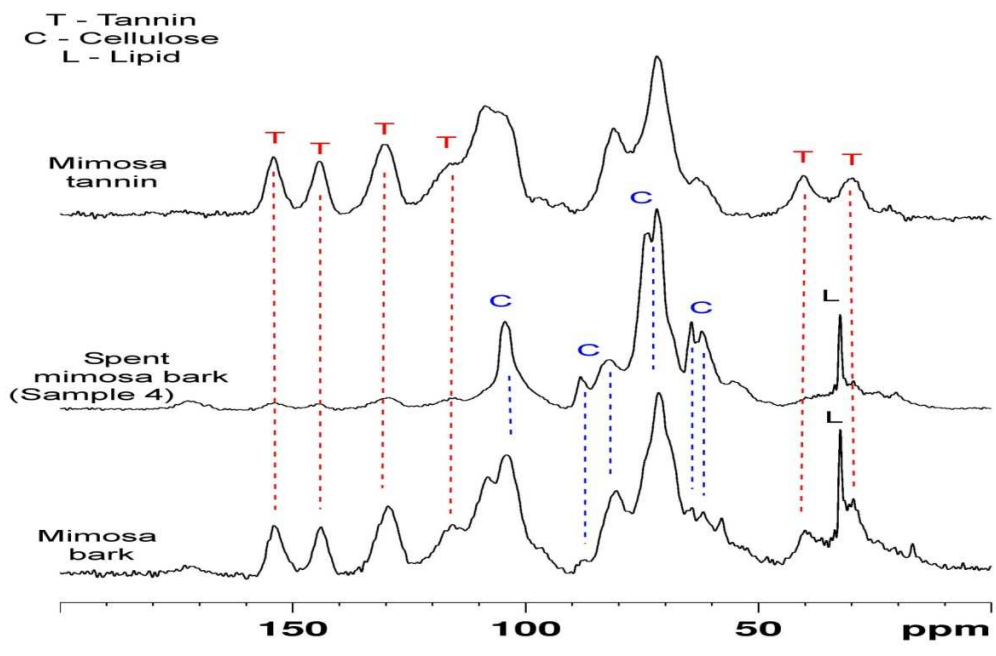

Figure 4-35: Solid state NMR of mimosa bark, spent bark and mimosa extract

Figure 4-36 shows a solid state ^{13}C CP-MAS spectrum of pine plywood. This is assumed to consist of cellulose high molecular weight polymers. The similarity of this spectrum with that of

spent bark in Figure 4-35 supports our conclusion that spent bark consist of cellulose polymers with a molecular weight of more than 90 000 Daltons.

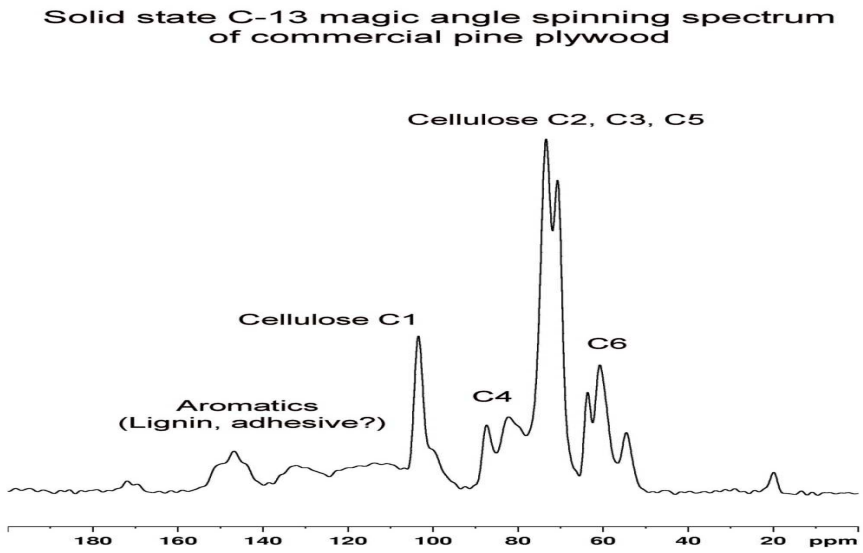

Figure 4-36: Solid state NMR of pine plywood (cellulose)

4.10.3 Conclusion

^{13}C solid state NMR proves that spent bark (bark extracted with hot water) consists of cellulose and contains minimal quantities of condensed tannins. The hypothesis by Robinson and Robinson and others (see paragraph 4.10.1) that during extraction of tannins with water and other less polar solvents from plant material, large insoluble oligomers remain behind, is thus clearly wrong in the case of mimosa tannins.

Because the yield of mimosa extract is about 50% of bark weight, this observation may imply that the procedure to yield tannins is exaggerated. The question can be asked whether less water at lower temperatures can be used industrially to produce mimosa tannins from bark. This will decrease the energy, both to heat water before extraction and to evaporate the water after extraction. The same may apply to quebracho tannins that are extracted at 130° C in autoclaves.

4.11 Experiment 10: Comparison of the solid state ^{13}C NMR of B1, B2 and B4

4.11.1 Introduction

Czochanska and co-workers[3,11] established that C-2 of condensed tannins with 2,3-*cis* stereochemistry resonates at 77 ppm and with 2,3-*trans* stereochemistry at 84 ppm in solution. C-3 of the terminal unit resonates at 67 ppm and that of a repeat unit at 73 ppm. C-4 of the terminal unit resonates at 38 ppm and that of the terminal unit at 28 ppm. In view of earlier comparisons between ^{13}C solid state and liquid state NMR spectra these spectra of the dimers B1, B2 and B4 were further investigated.

4.11.2 Results and Discussion

The ^{13}C solid state NMR spectra of epicatechin-4α-8-catechin (B1), epicatechin-4β-8-epicatechin (B2) and catechin-4α-8-epicatechin (B4) are given in Figure 4-37, Figure 4-38 and Figure 4-39 and summerised in Table 4-7.

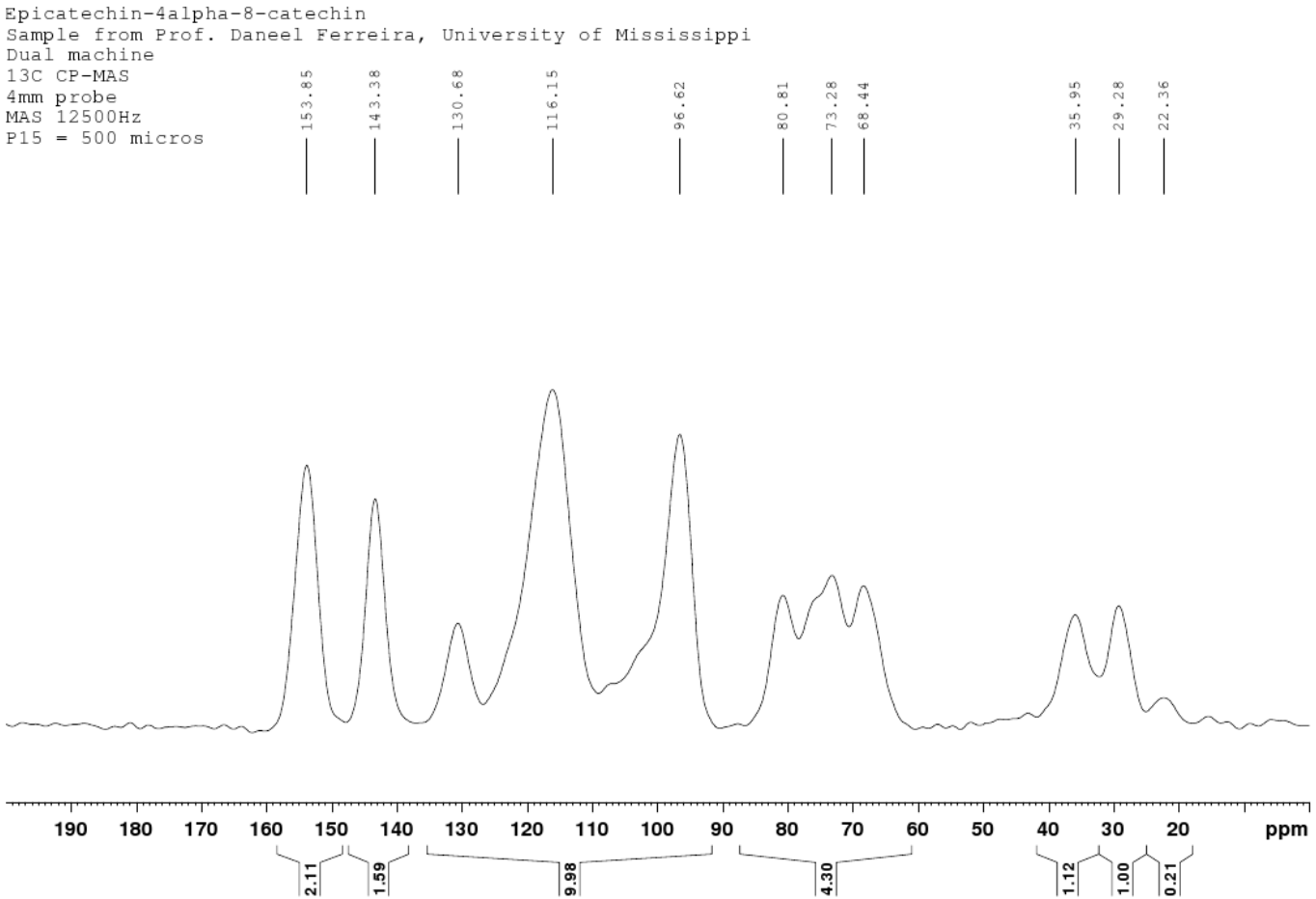

Figure 4-37: ^{13}C solid state NMR of the dimer B1

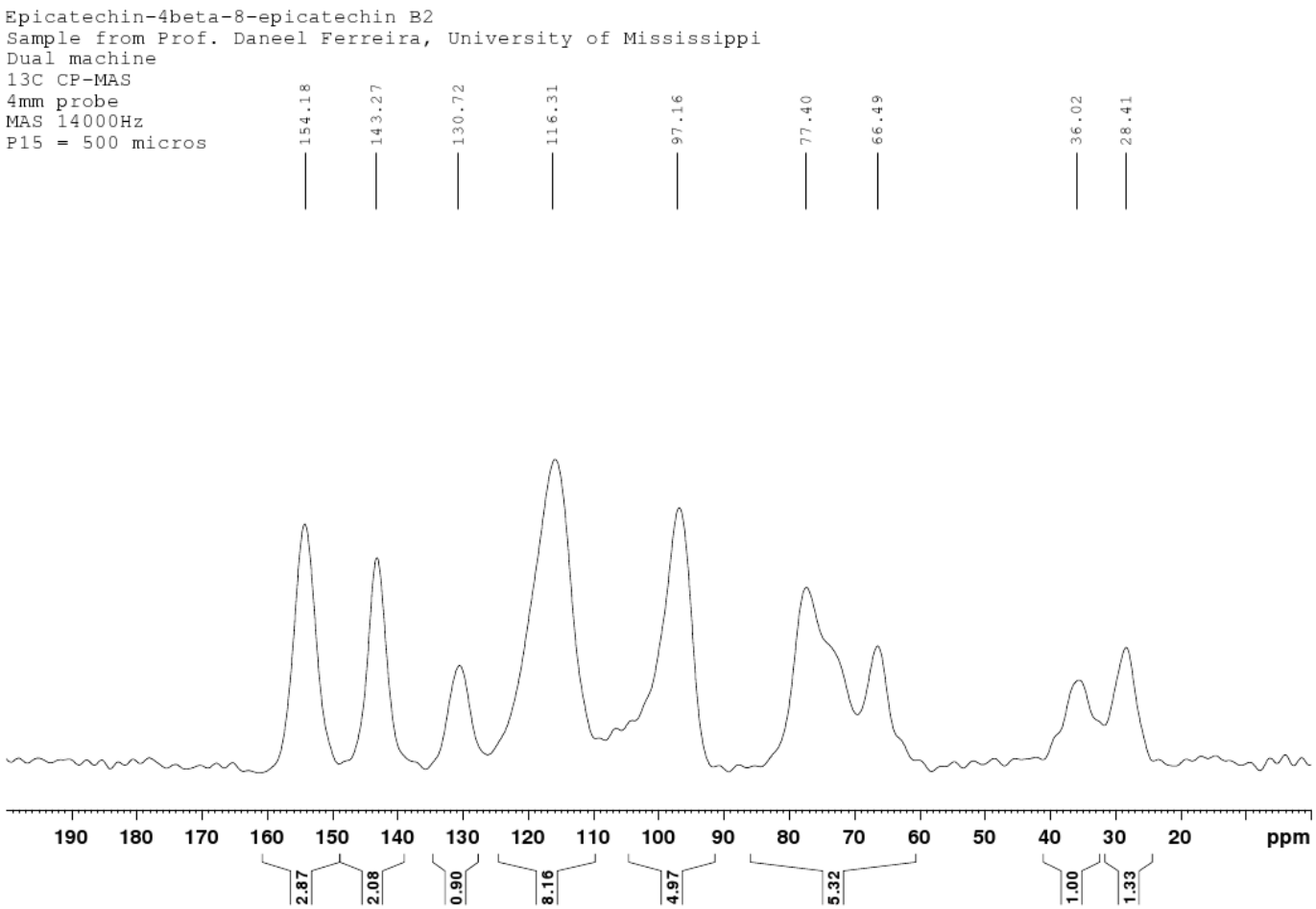

Figure 4-38: ^{13}Csolid state NMR of the dimer B2

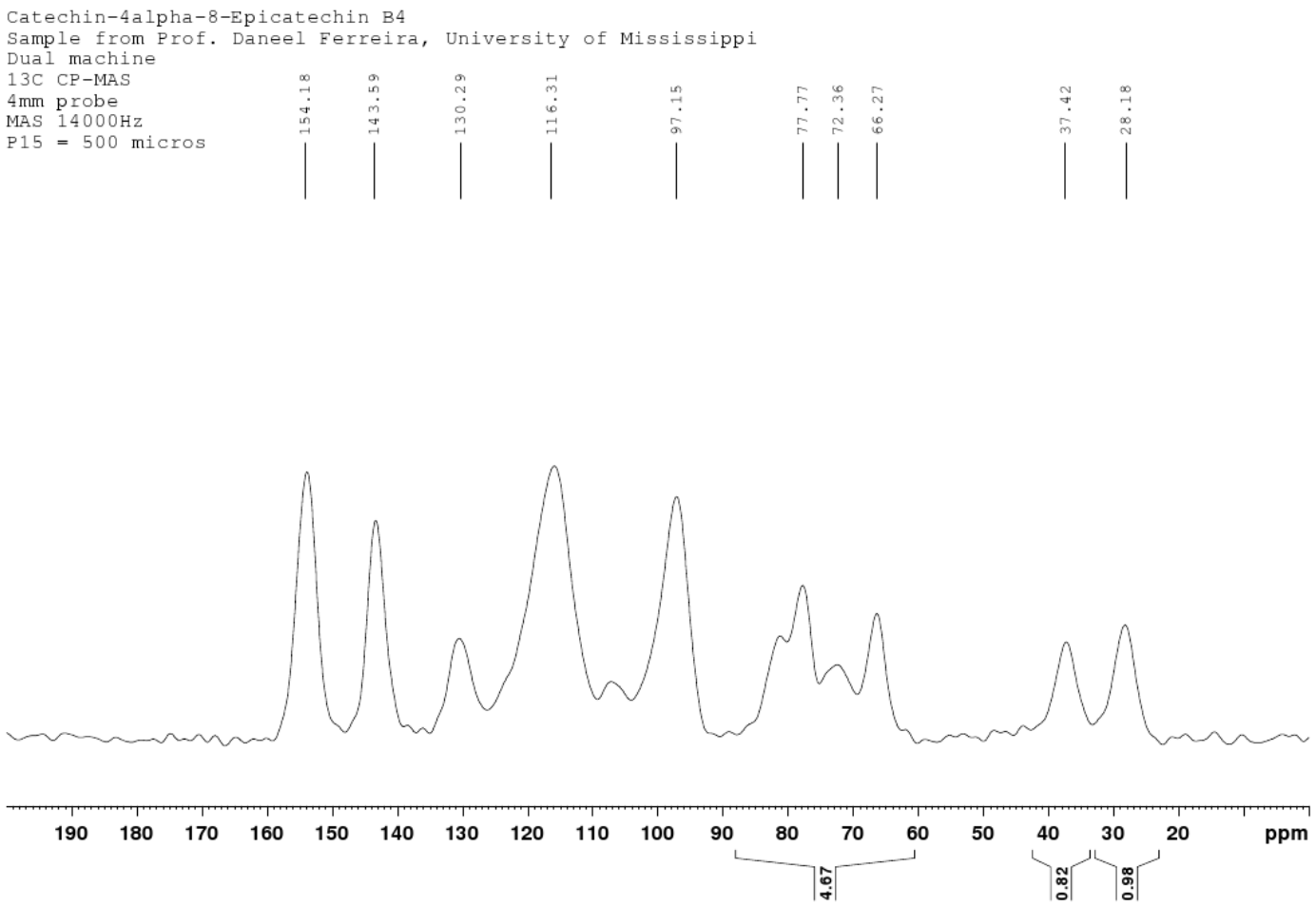

Figure 4-39: ^{13}C solid state NMR of the dimer B4

Table 4-7: ^{13}C CP-MAS chemical shifts of stereochemically different dimers			
Carbon number	B1/2,3-*cis*-2,3-*trans*	B2/2,3-*cis*-2,3-*cis*	B4/2,3-*trans*-2,3-*cis*
2 repeat	*cis*/76	*cis*/77	trans/81
2 terminal	trans/81	*cis*/77	*cis*/78
3 repeat	*cis*/73	*cis*/67	trans/66
3 terminal	trans/68	*cis*/73	*cis*/72
4 repeat (I)	36	37	37
4 terminal (II)	29	28	28
4a,6,8	116	116	116
5,7,8a	154	154	154
1',4'	131	131	130
2',6'	97	97	97
3',5'	143	143	143

4.11.3 Conclusion

^{13}C solid state NMR can be used to distinguish between dimers with 2,3-*cis* and 2,3-*trans* stereochemistry. When a bond is *trans*, the chemical shift is above 80 ppm and when it is *cis*, the chemical shift is below 80 ppm. The terminal C-4 can be distinguished from the repeat C-4, but 3,4-stereochemistry could not be determined with solid state NMR due to the overlap of resonances.

4.12 Experiment 9: Two dimensional solid state NMR

4.12.1 Introduction

As discussed above, the non-homogenous nature of solid state NMR samples leads to peak broadening and poor resolution. ^{13}C NMR has a 230 ppm range which compensates for poor resolution. The usefulness of solid state ^{1}H NMR is however severely limited by its 10 ppm range and the extreme broadening of proton signals, which can only be removed by spinning speeds higher than 50 kHz, due to residual proton-proton dipole-dipole interactions.

In this experiment a 2D solid state NMR was performed in an effort to obtain better ^{1}H chemical shift values. HETCOR experiments will also confirm our ^{13}C assignments.

4.12.2 Results and Discussion

A ^{1}H solid state NMR in general, shows strong overlapping of resonances and is not reliable to assign chemical shifts. The signals are broad and henceforth HETCOR experiments were done to attempt the assignment of the catechin.

The following experiments were performed:

4.12.2.1 Experiment 1: The HETCOR of catechin

The HETCOR of catechin is shown in Figure 4-40.

It is possible to use the 2D spectra of catechin to derive the proton spectrum thereof with the help of solution state NMR.

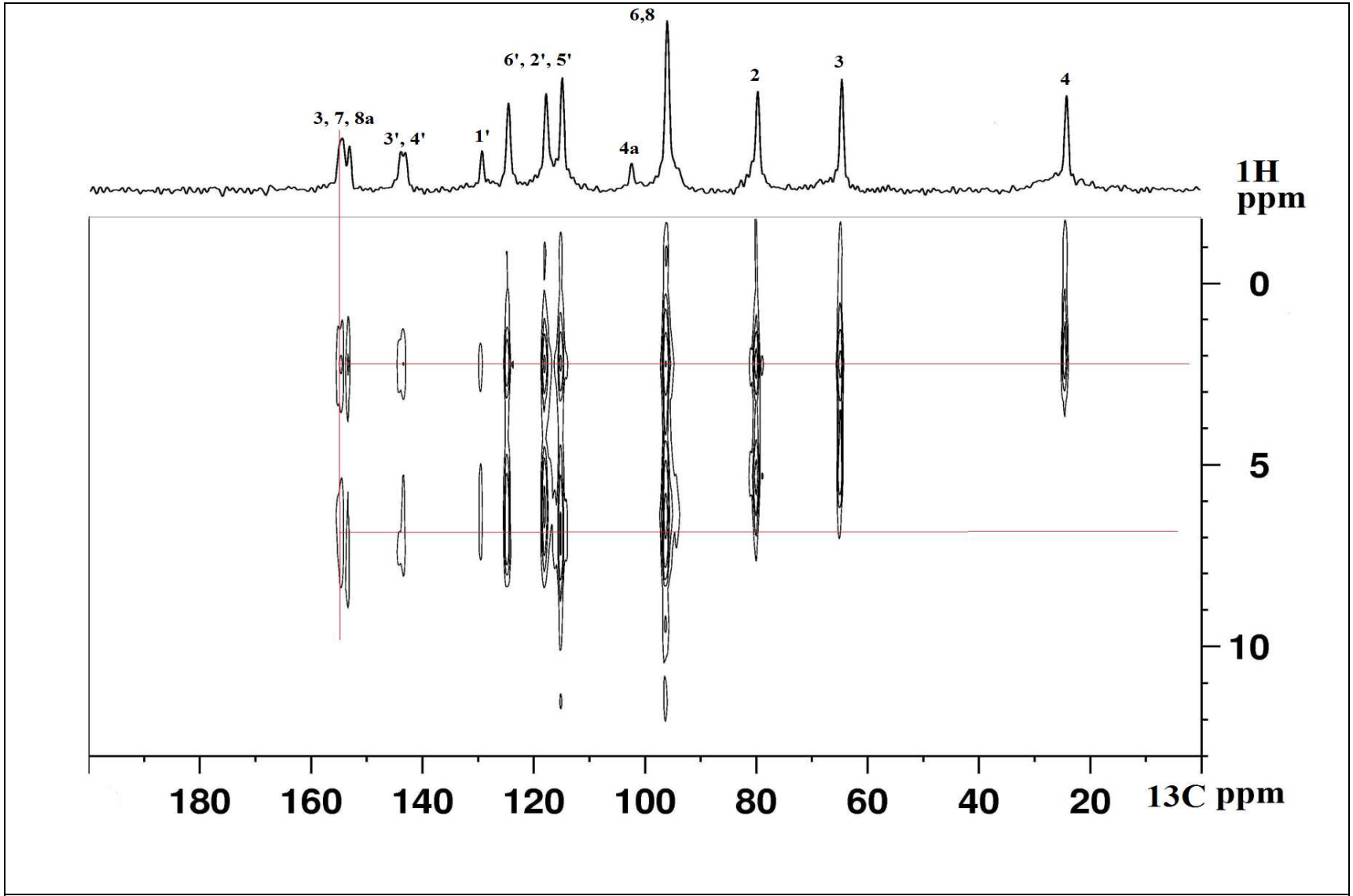

Figure 4-40: HETCOR of catechin

4.12.2.2 Experiment 2: The HETCOR of a dimer

Figure 4-41 and Figure 4-42 shows the HETCOR of the dimer B1 (epicatechin-4α-8-catechin) with contact times of 50 and 200 μs respectively.

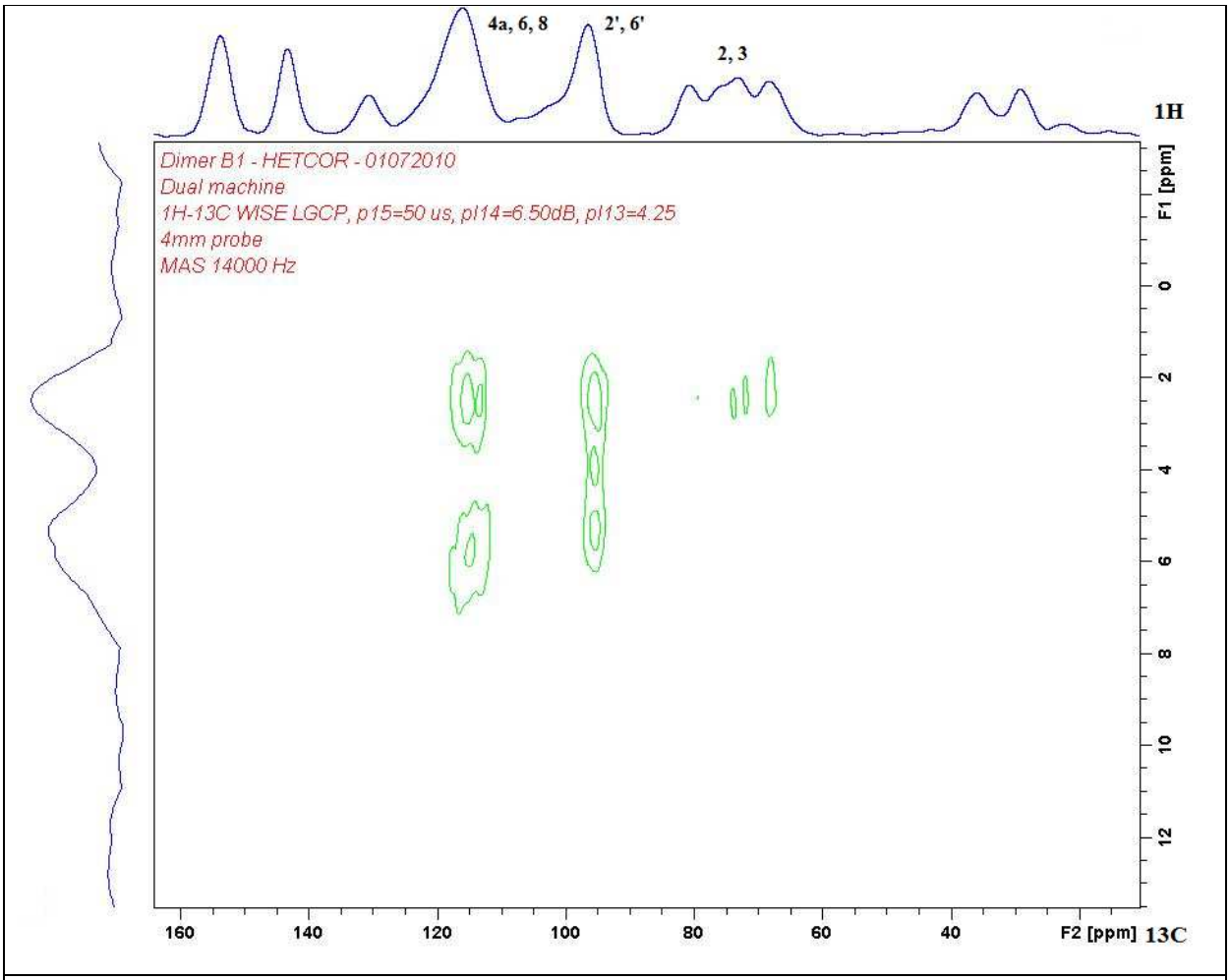

Figure 4-41: 2D NMR of the dimer epicatechin-4β-8-catechin, with a contact time of 50 μs

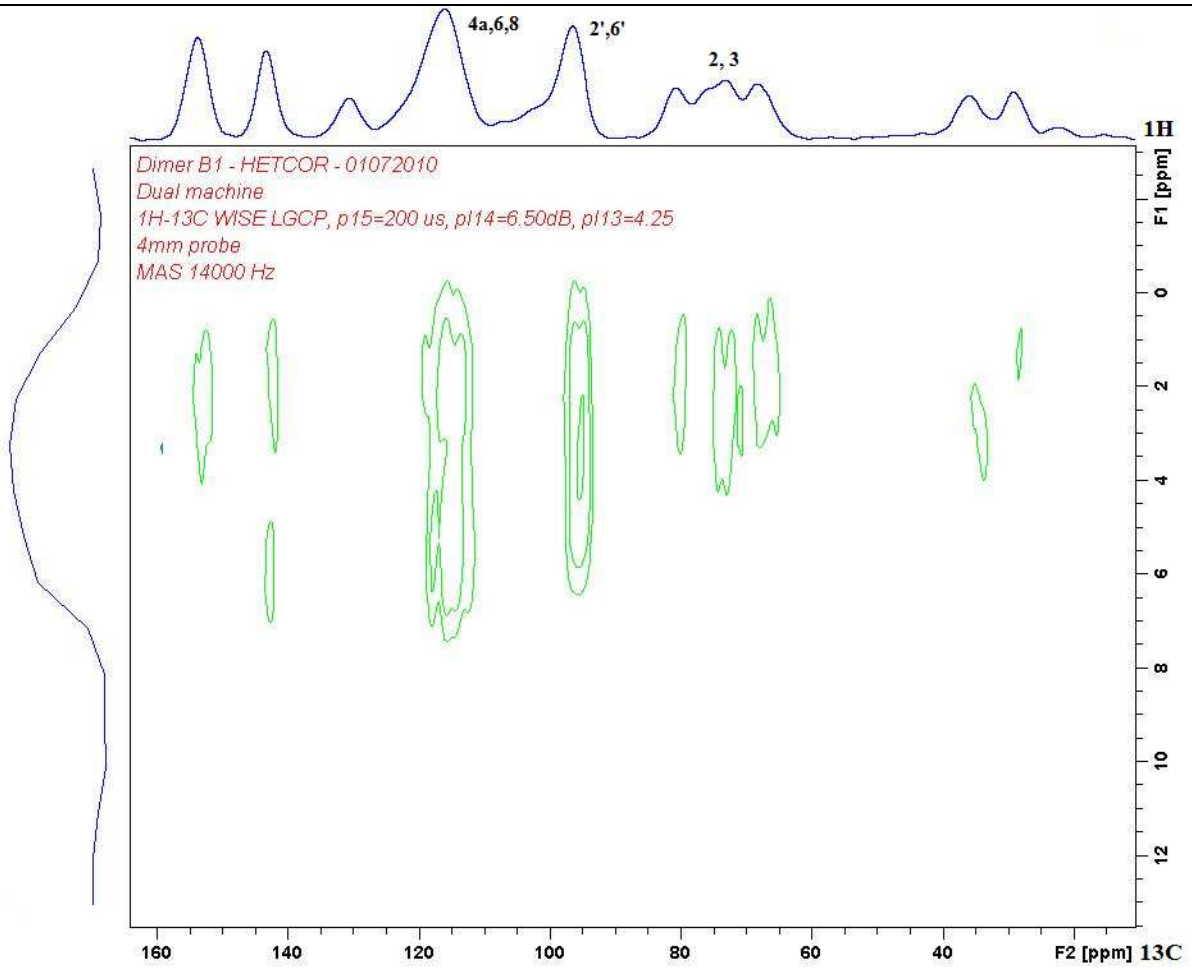

Figure 4-42: 2D NMR of the dimer epicatechin-4β-8-catechin , with a contact time of 200 µs

4.12.2.3 Experiment 3: The HETCOR of a deuterated dimer

Figure 4-43 and Figure 4-44 shows the HETCOR of B2 (epicatechin-4α-8-epicatechin) which was deuterated for six hours, with contact times of 50 and 200 μs respectively.

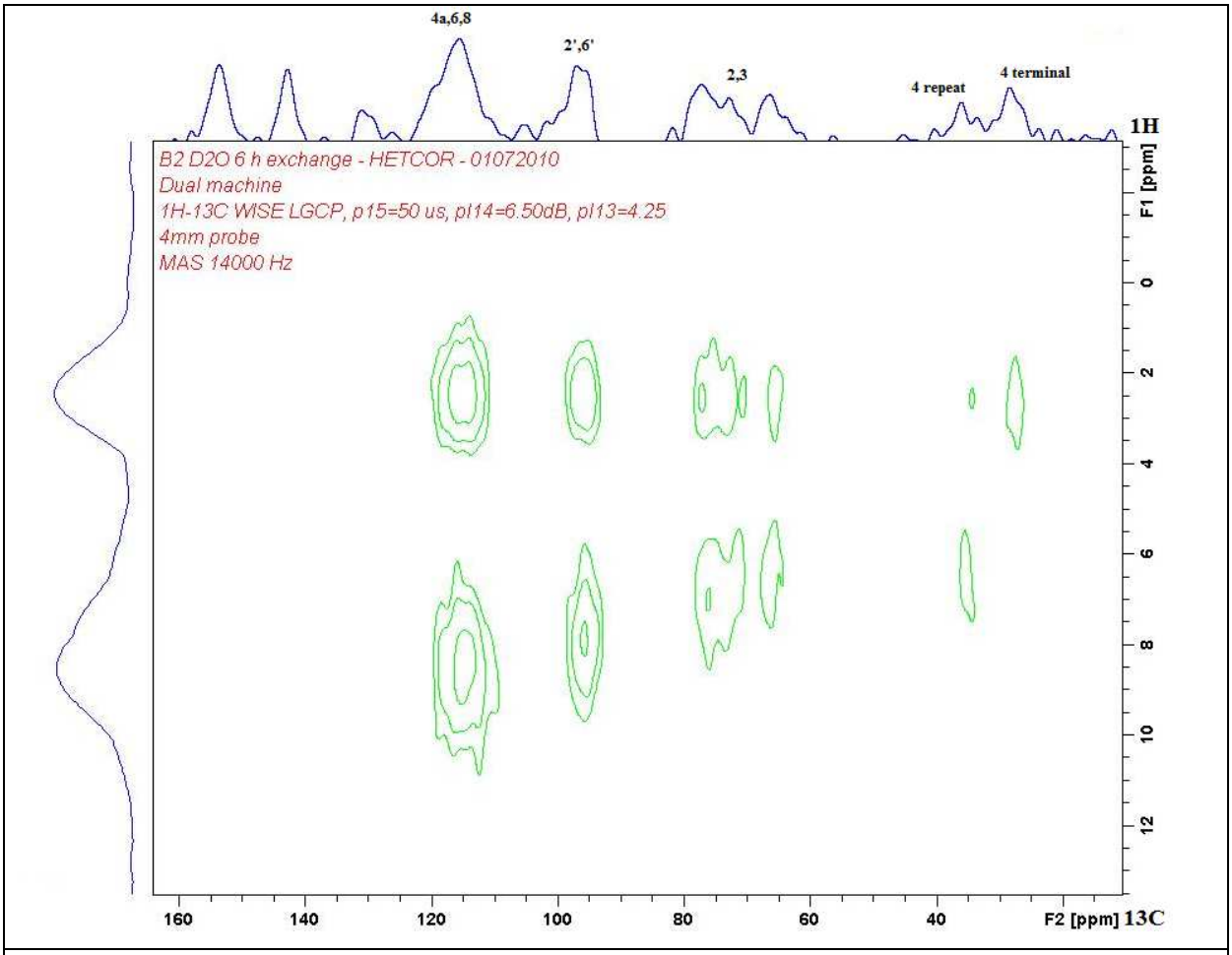

Figure 4-43: 2D NMR of the 6 hour deuterated dimer epicatechin-4β-8-epicatechin, with a contact time of 50 μs

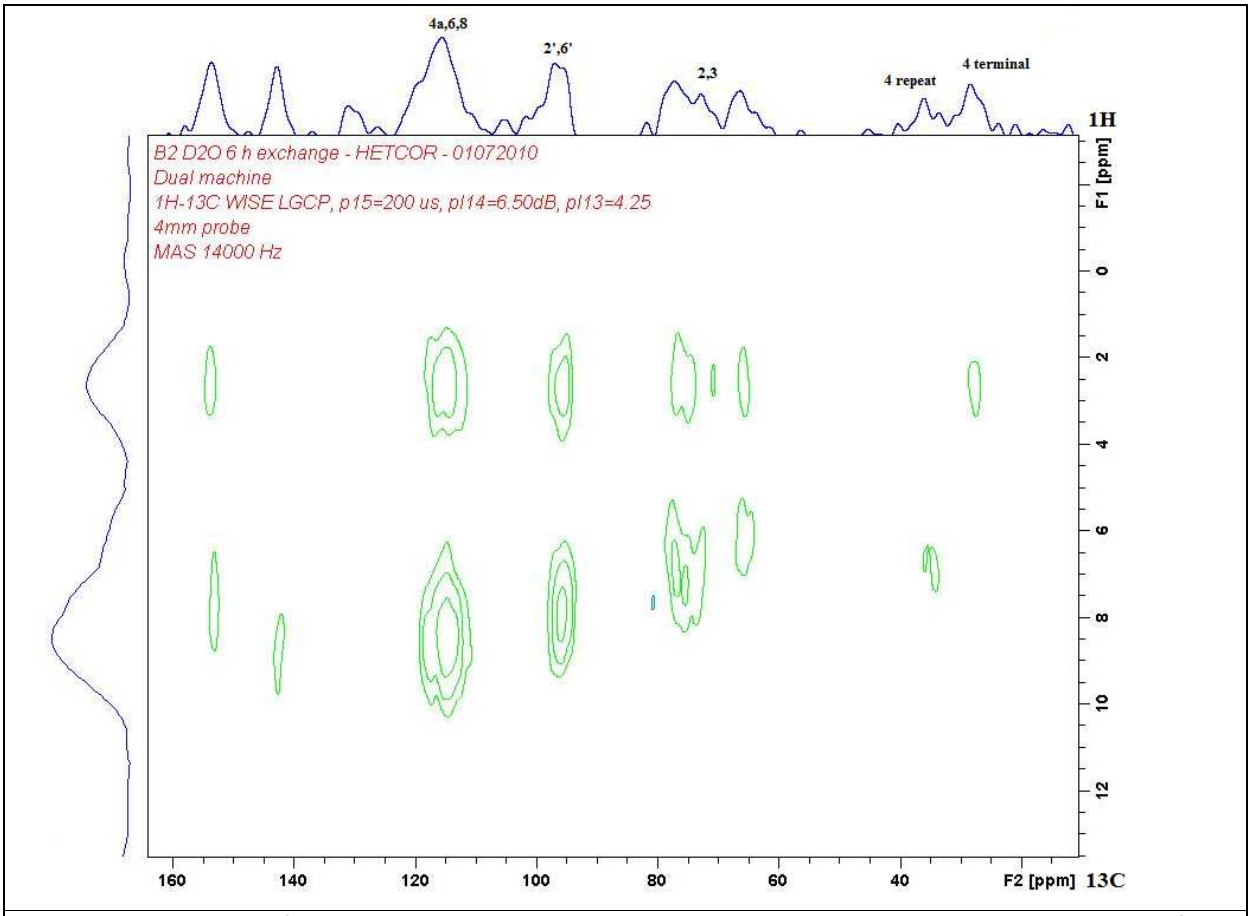

Figure 4-44: 2D NMR of the 6 hour deuterated dimer epicatechin-4β-8-epicatechin, with a contact time of 200 µs

4.12.2.4 Experiment 4: The HETCOR of a deuterated mimosa tannin extract

2D HETCOR experiments were performed on deuterated samples (dissolved in D_2O followed by freeze drying) of the methanol extract of fresh mimosa bark (N1, see paragraph 6.1.1). Experiments were done at two different contact times (Figure 4-45 and Figure 4-46 at 50 and 200 µs respectively)

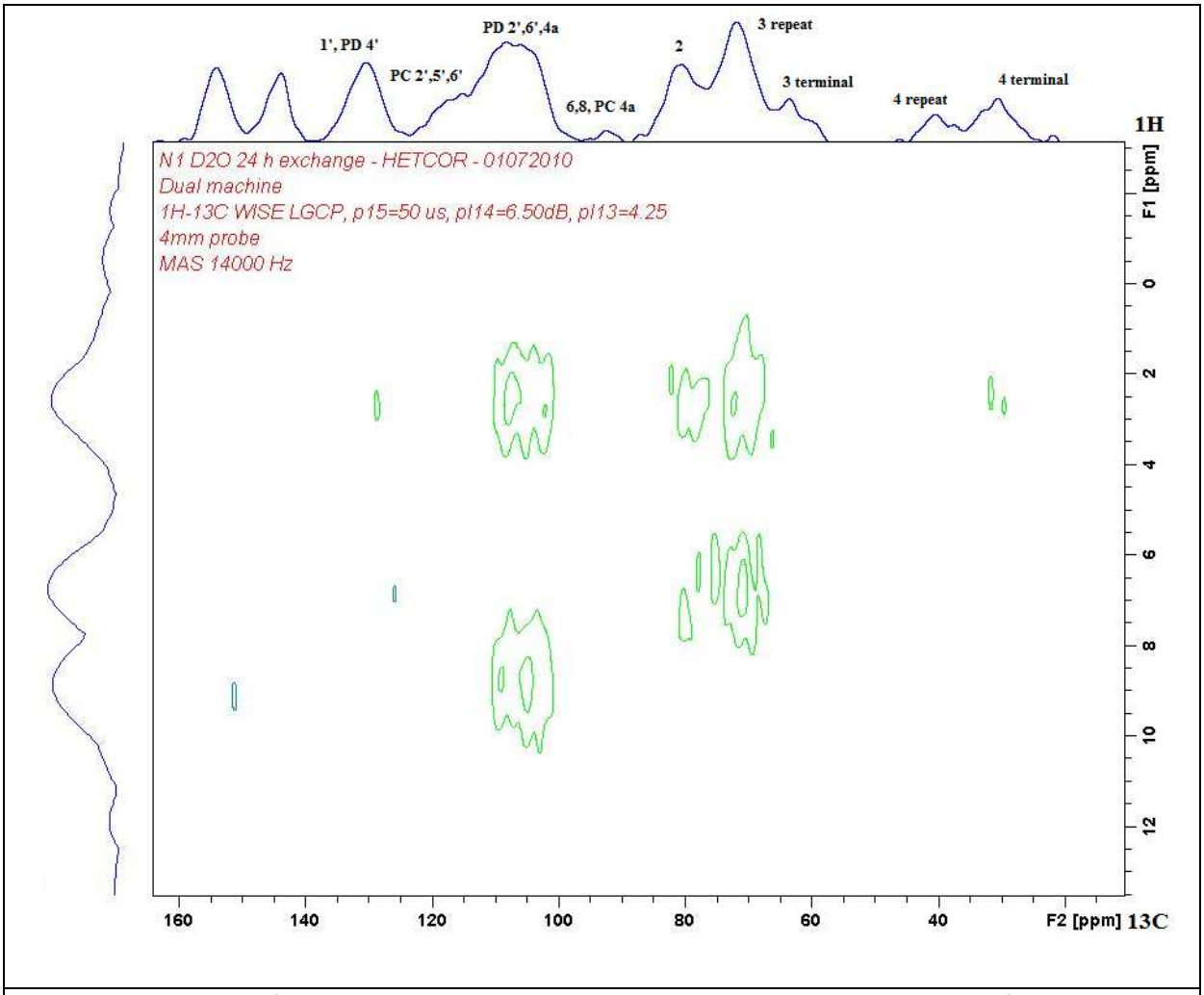

Figure 4-45: 2D NMR of the 24 hour deuterated mimosa tannin extract with a contact time of 50 µs

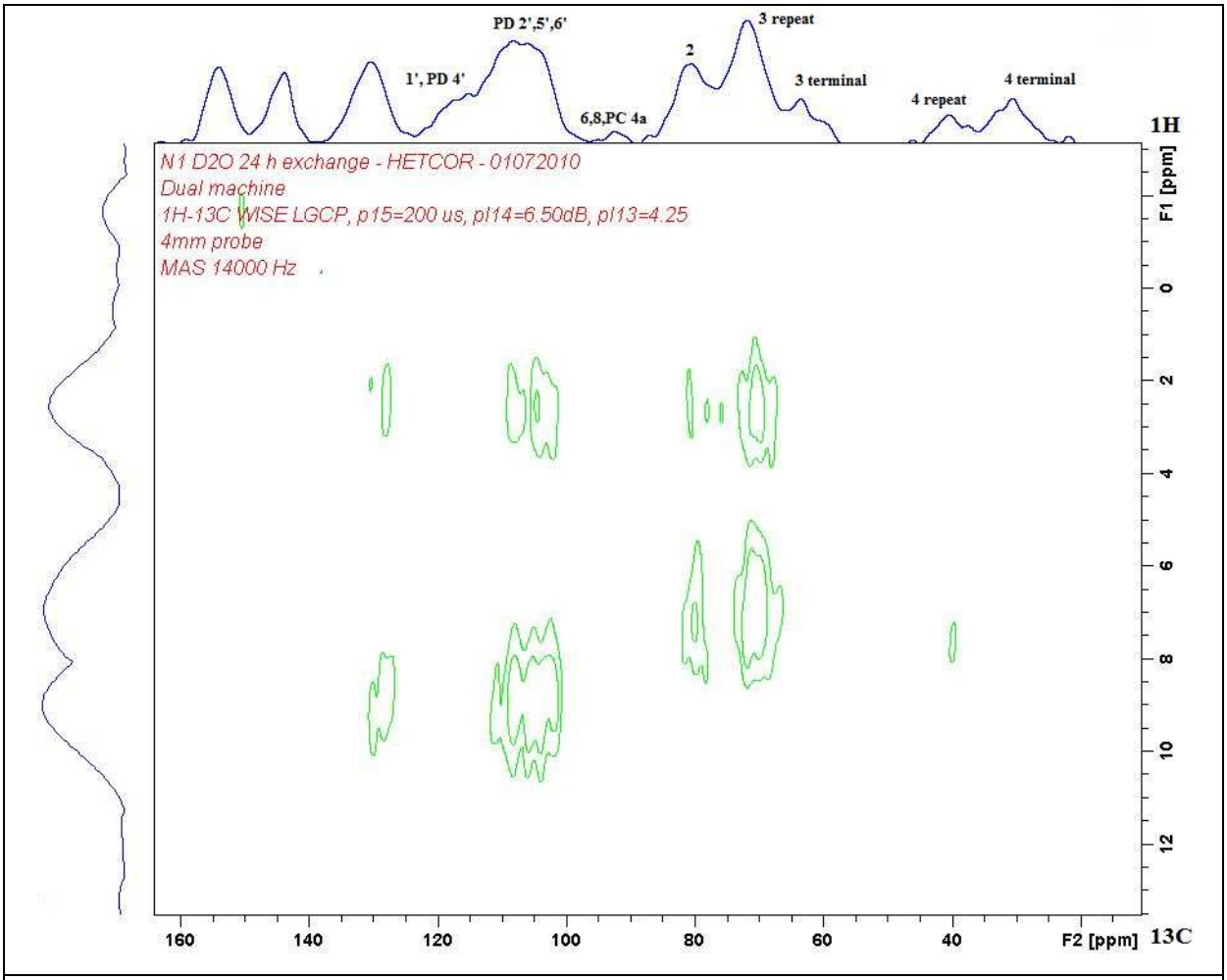

Figure 4-46: 2D NMR of the 24 hour deuterated mimosa tannin extract with a contact time of 200 µs

The cross peaks involving the OH carbons become much weaker after deuteration, most likely reflecting that they no longer show the through-space correlation to these OH protons. The remaining cross peaks at 2 to 4 ppm may be from the protons on the sp^3 carbons 2, 3 and 4.

4.12.2.5 Experiment 5: The HETCOR of quebracho tannin

The 2D HETCOR of quebracho tannin is shown in Figure 4-47. From this spectrum it was attempted to assign the aliphatic and aromatic regions of the protons but the spectrum still has broad peaks, all in the region of 0 – 10 ppm and the distinction could not be made.

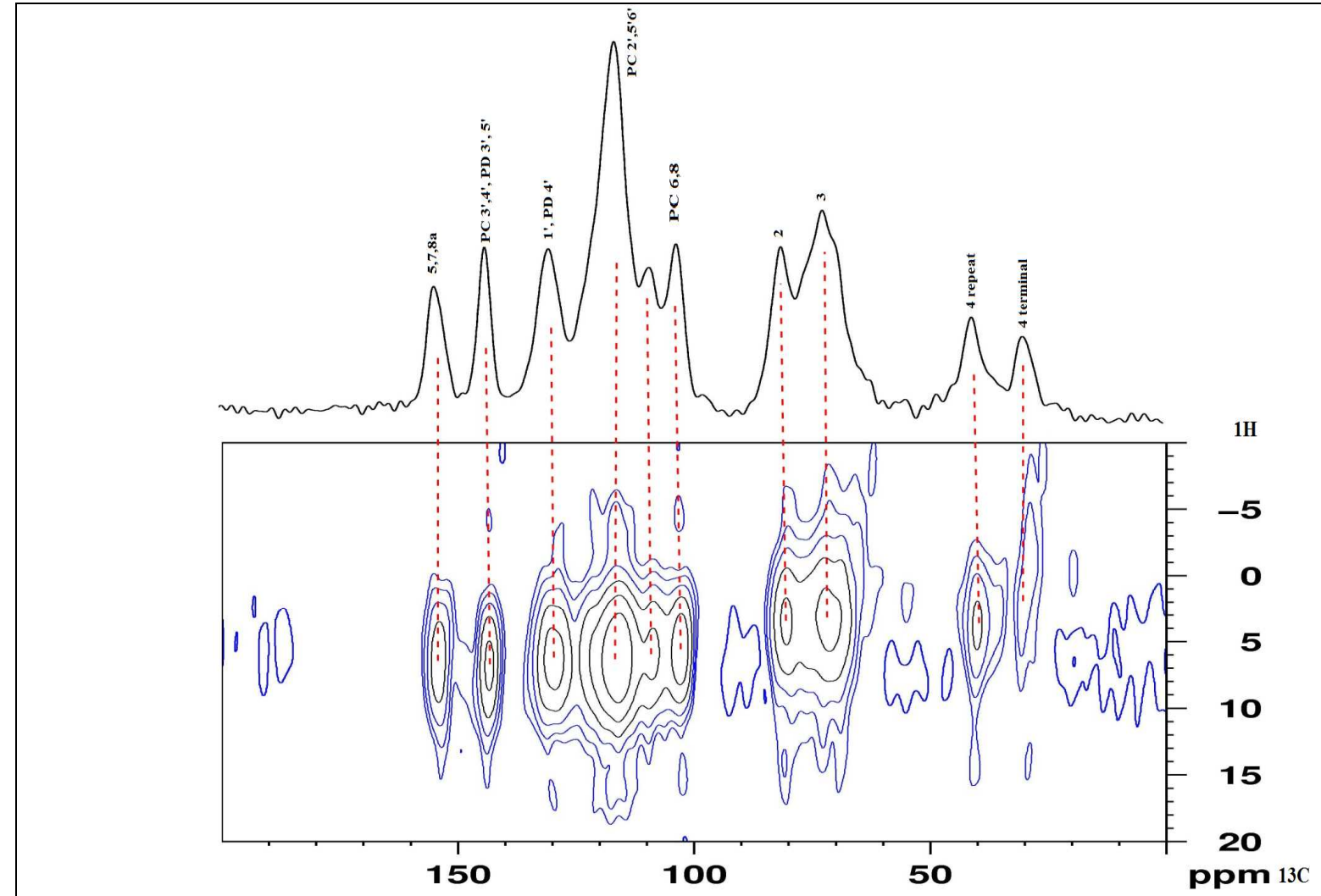

Figure 4-47: HETCOR of quebracho tannin

4.12.3 Conclusion

HETCOR experiments allowed us to measure ^{1}H chemical shifts of condensed tannin protons, although the broadness and overlap of the proton spectra precluded detailed assignments. It also confirmed our ^{13}C assignments.

We observed strong overlapping of resonances in the aromatic region associated with the A- and B-rings. Similar overlapping broad resonances in the aliphatic region are assigned to the heterocyclic C-ring protons.

HETCOR experiments do not give the ^{1}H chemical shift accurately, however, 2D NMR can possibly be used to develop a fingerprint method as all C-H's correlations are evident. More work is required on this subject.

The deuterated exchange of OH with OD removes or reduces the attached C resonance and corresponding peaks. This can be explained in terms of the magnetization transfer from the proton which does not occur with a deuterium atom. This may be useful in assigning a C-OH resonance where this is required.

4.13 Experiment 12: Solid state NMR investigation of leathers tanned with different tanning materials

4.13.1 Introduction

The word "tannin" comes from the use of plant extracts to manufacture leather from hides and skins. It is a very ancient process and records on the manufacturing of leather in the Mediterranean dates back to 1500 BC. Despite the age and the commercial importance of the process, the chemistry of the interaction between tannins and leather (protein) that transform skin into leather is still "shrouded in mystery".[31,p374] It is generally assumed that tannins diffuse into the spaces between collagen fibres and crosslink different fibres *via* hydrogen bonds between the tannin polyphenols and the collagen amino acids. This imparts stability towards water, bacteria, heat and abrasion.

Synthetic tannins and mineral tannins (mostly chromium salts) nowadays compete with vegetable tannins. Tannage is complete after absorption of about 3% of the inorganic salt compared to about 50% in the case of vegetable tannins. Disposal of waste chrome tanned leathers poses environmental concerns.

The leather tanning industry uses physical characteristics such as shrinkage, shrinkage temperature and thermal properties to monitor tanning and control quality. These techniques give no direct clue to the chemical changes involved in the process. It was envisaged that solid state NMR could give information that would assist in improving tanning methodology and authenticating high value leathers.

Liquid state NMR have been used to characterize leathers[33,34] and, in a single case, infer their tannin content.[35] These papers indicated the potentially useful spectral "window" between *ca.* 70 ppm and *ca.* 165 ppm which contains numerous tannin resonances but few leather collagen protein resonances. Solution state NMR was also used to study the molecular mechanisms of metal salt tanning.[36,37]

4.13.2 Results and Discussion

Samples of unprocessed hide tanned with chromium (III), aluminium (III), condensed tannins (mimosa and quebracho), hydrolysable tannins (tara and chestnut) and a synthetic tanning material (glutaric aldehyde) were obtained. The vegetable tanned samples (mimosa, quebracho, tara and chestnut) were specially prepared by the Mimosa Extract Company (Pty) Ltd without any other additives (Chapter 6: Experimental procedure). These samples were used as the commercially available samples may contain unknown additives.

A visible colour difference could be seen in the leather samples. Tara is cream coloured, chestnut more yellow-brown, quebracho is orange-brown and mimosa is a lighter shade of orange-brown than quebracho. The colour of the chrome-tanned leather is grey-silver and the texture of unprocessed raw hide is hairy, but the inside of the hide is white. See Figure 4-48.

Tara

Chestnut

Quebracho

Mimosa

Chrome-tanned leather

Unprocessed raw hide

Figure 4-48: Colour difference of tannin-treated leather samples

Solid state ^{13}C NMR spectra were obtained using standard cross polarization (CP) MAS techniques.

Figure 4-49 superimposes solid state ^{13}C CP-MAS spectra of unprocessed raw hide over that of chrome (III) tanned leather. The ^{13}C NMR spectrum of untanned powdered hide is similar to that of pure collagen[38], and assignments of some signals to specific amino acid residues or functional groups are shown in the figure.

Figure 4-50 superimposes solid state ^{13}C CP-MAS spectra of unprocessed raw hide over that of aluminium (III) and glutaraldehyde tanned leather.

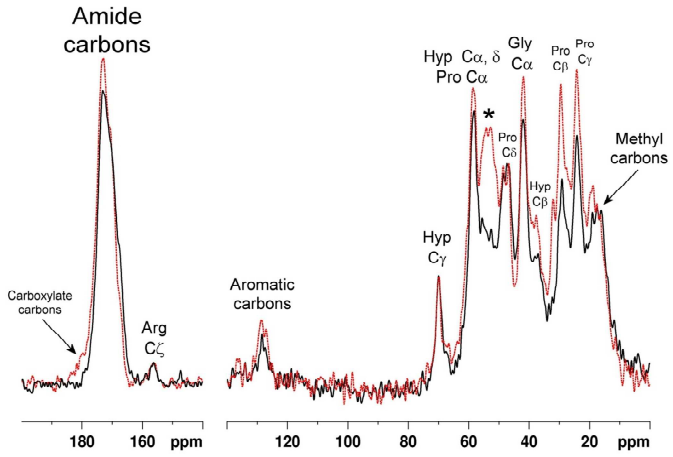

Figure 1: Untanned (red) vs Cr (III) tanned leather (black)

Figure 4-49: Untanned leather compared to chrome-tanned leather

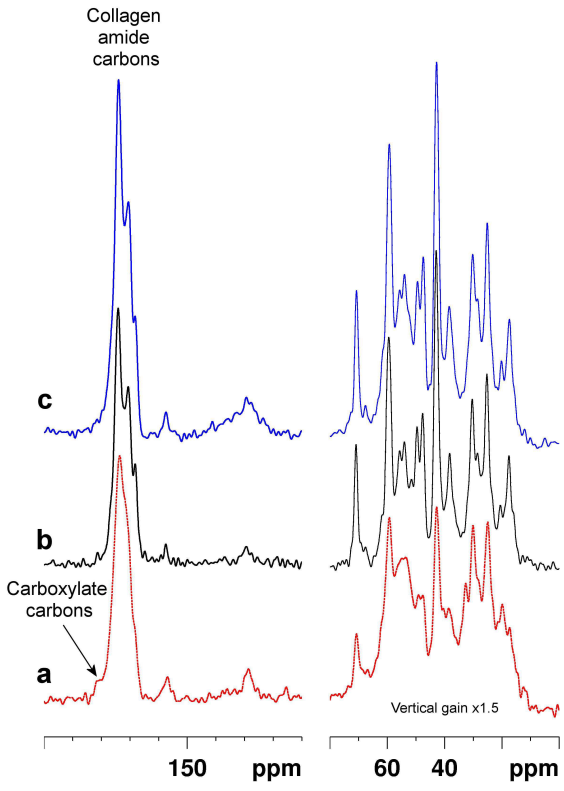

Figure 4-50: Untanned leather (a, red) compared to aluminium (III) (b, black)-and glutaraldehyde (c, blue) tanned leather

Figure 4-51 superimposes solid state ^{13}C CP-MAS spectra of leather (the black solid traces) tanned with tannins from mimosa (left) and quebracho (right) over identically acquired spectra from the respective pure tannins (the red dotted traces). The spectra of both pure tannins are consistent with their structures and with literature assignments of whole tannins and constituent monomers.[3,39,40,41]

Tannin signals which are well resolved from signals from the collagen in the leather are marked with a "T". Also shown is a generic structure of the repeating flavonoid units typical of condensed tannins, and some assignments in the case of the mimosa tannin; assignments of quebracho tannin signals are distinct from those of mimosa tannin and are not shown. "4 int" and "4 term" refer to signals from the flavonoid C-4 atom which are conjugated by condensation to another flavonoid unit, or terminal to the tannin oligomer and hence non-condensed, respectively. In the spectra of the tanned leather, tannin signals which are well resolved from collagen signals, and therefore valid "fingerprints" of the tannin type used in the tanning process, are marked "T". Asterisks highlight signals indicative of the use of condensed polyflavonoid tannins.

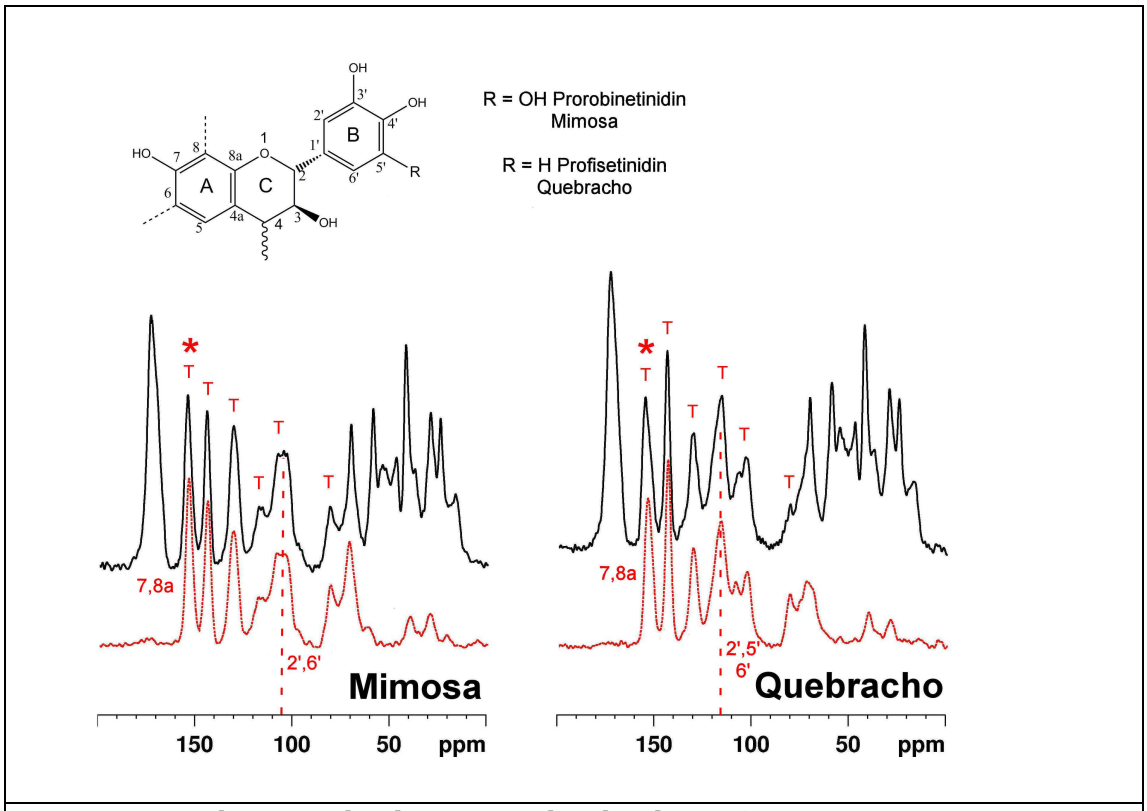

Figure 4-51: Leathers tanned with mimosa and quebracho tannins

Most importantly each tannin spectrum is faithfully reproduced in the spectra of the leathers tanned by them. Quebracho tannin is predominantly a profisetinidin (resorcinol type A- and catechol-type B-ring, see Figure 4-2) and mimosa predominantly a prorobinetinidin polymer (resorcinol type A-ring and pyrogallol type B-ring, see Figure 4-1). The B-ring C-H carbons of quebracho (2', 5', 6') resonates strongly at *ca.* 115 ppm and those of mimosa (2', 6' carbons) resonates strongly at 105 ppm. These resonances are therefore diagnostic.

Figure 4-52 superimposes solid state ^{13}C CP-MAS spectra of leather tanned with two hydrolysable tannins, chestnut (left) and tara (right) (black traces) superimposed over the pure tannin (red dotted line). Hydrolysable tannins are complex mixtures of sugar or quinic acid monomers esterified with polyphenols such as gallic acid and derivatives and closely related compounds.[42,43,44] Structural formulae of typical constituents of hydrolysable tannin are also shown. The asterisk (*) indicates a signal due to non-sugar sp^3 carbons in compounds such as the chebulic acid depicted here. As with condensed tannins, the spectra reflects the constitution of each pure tannin.[45-48]

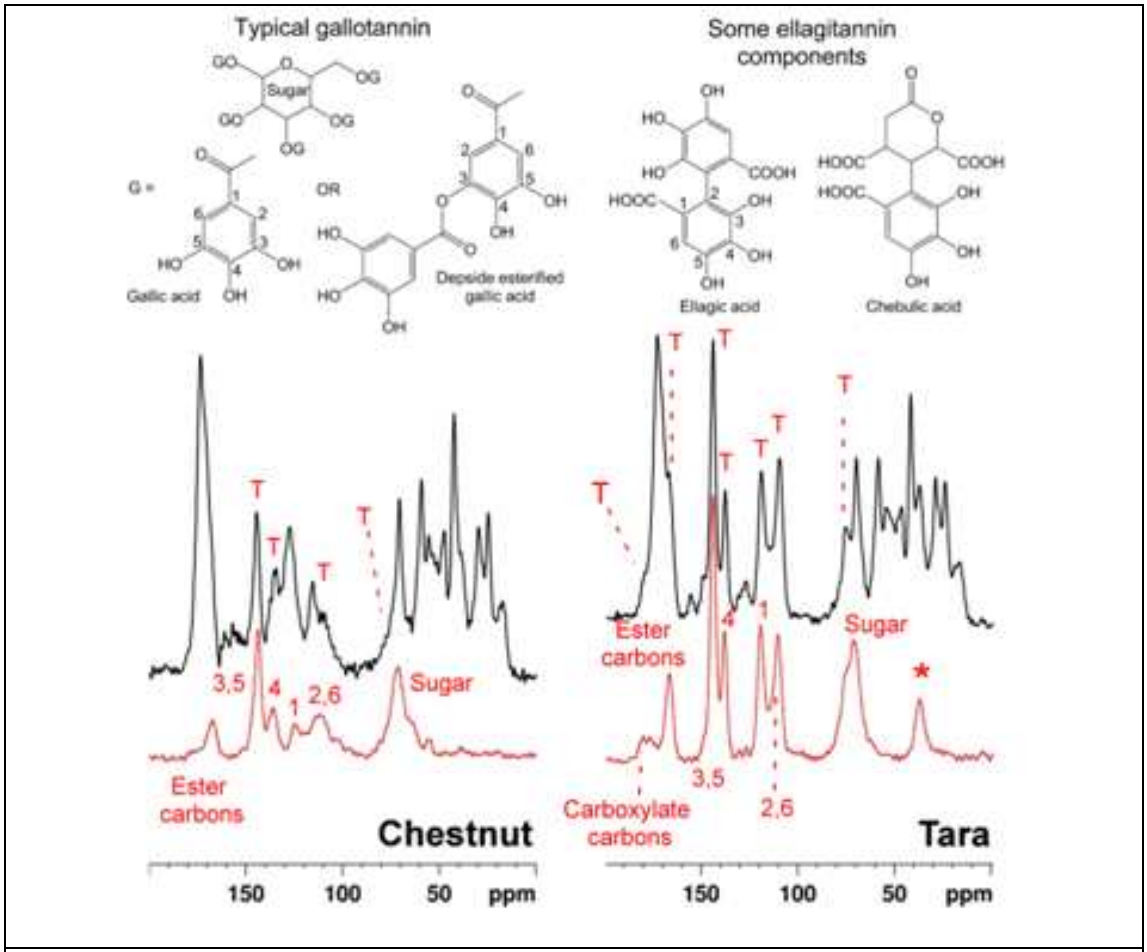

Figure 4-52: Leathers tanned with chestnut and tara tannins

4.13.3 Conclusion

Chromium (III) tanning caused widespread but selective spectral changes. Notable is the disappearance of a number of signals, some due to acidic aspartyl and glutamyl residues. These are likely directly legated to Cr (III). Cr (III), with three ground state unpaired 3d electrons in its outer valence shell, is strongly paramagnetic. The large electronic magnetic moment associated with paramagnetic chrome may shift the NMR frequencies of nuclei which are close in space to the paramagnetic centre. It may also increase the relaxation rate from excited nuclear spin state back to ground state causing resonances from atoms close to the paramagnetic centre to become broader. They can become so broad that they become unobservable.

Each signal in the collagen spectrum is due to overlap of numerous signals from chemically equivalent atoms in the large collagen (over 1,000 amino acid residues) molecule and so it is impossible to ascribe chromium induced signal broadening to the

binding to any particular portion of the collagen structure. The precise magnitude of chromium induced signal broadening (or shifting) is also a complex function of the geometric relationship of chromium ions and affected atoms, and of their sharing of unpaired paramagnetic electron density through direct bonding. It is therefore impossible to pinpoint interactions at specific amino acid residues or locations on the collagen triple helix.

However, it is of interest that marked broadening occurs on the envelope of signals centred at *ca.* 53 ppm containing, among others, signals from the α-carbons of acidic aspartate and glutamate residues, and of the shoulder to high frequency of the amide carbon signal, centred at *ca*. 180 ppm, comprising signals from the carboxylate carbons of the same acidic residues. These are the resonances associated with the acidic residues which are likely to be involved in the binding of Cr (III) to the collagen network.

The effects of Al (III) or glutaraldehyde, one a metal ion and the other a bifunctional organic reagent, are distinctly different from those of Cr (III), even when the paramagnetic signal broadening effects of the latter are taken into account. The linewidth of the well resolved signal of the collagen hydroxyproline γ-carbons at *ca*. 71 ppm remains unchanged after Cr (III) tanning (Figure 4-49) but is considerably sharper after tanning with either Al (III) or glutaraldehyde.

Neither the diamagnetic Al (III) ion nor the organic glutaraldehyde reagent introduces the large changes in peak intensity caused by the paramagnetic Cr (III) ion. This is most likely because their magnetic perturbations influencing the NMR properties of the leather are much weaker and less far reaching than those of paramagnetic Cr (III). The response of the spectral line widths of leather to tanning with either material is remarkable. Both tanned leathers exhibit signals which are generally much sharper than the parent untanned leather. In solid state NMR a significant cause of signal broadening is environmental heterogeneity resulting from partial or complete molecular disorder. Thus the signal sharpening seen with both processes is likely attributable to an increase in molecular order brought about by intermolecular interactions that occur between aluminium (III) and glutaraldehyde and the collagen

matrix. Two chemically different reagents produce similar changes indicating similar molecular ordering probably *via* different underlying chemical processes.

Collagen molecular ordering processes induced by Al (III) or glutaraldehyde are different from the effects exerted by Cr (III). It is likely that correlations exist between these ordering effects, or lack thereof, and the material properties of the final products but their molecular level details needs further investigation.

Comparison with the leather spectra in Figure 4-51 shows that NMR readily differentiates between leathers tanned with condensed and leathers tanned with hydrolysable tannins. The well resolved strong signal from the 5, 7 and 8a hydroxylated carbons of the flavonoid A-ring at *ca*. 160 ppm (asterisked in Figure 4-51) is particularly diagnostic of the condensed tannin structure. The strong ester resonance of hydrolysable tannins is partly obscured by the carbonyl amide resonance of the leather collagens. However, only a single aromatic resonance, associated with the galloyl residue is observed, compared with two strong resonances from the condensed tannin.

^{13}C solid state NMR provides easily recognisable spectral fingerprints of the materials used in important tanning processes. Because fingerprints are directly comparable with process molecular events, NMR is potentially a powerful tool in leather processing enhancement and quality or provenance assurance.

4.14 Overall Conclusion

From the experiments done with solid–state NMR, the following conclusions can be made:

- Hydrolysable tannins have NMR spectra that can be interpreted in terms of their chemical composition.
- Condensed tannins have characteristic solid state NMR spectra compatible with their chemical composition (oligomers of flavan-3-ols).
- Solid state NMR can reliably and routinely be used to distinguish between quebracho and mimosa tannins.
- Solid state NMR can reliably and routinely be used to distinguish between hydrolysable and condensed tannins.
- Unprocessed bark can be analysed directly to identify it as quebracho, mimosa or hydrolysable tannin types.
- Solid state NMR indicates that the heterocyclic ring is opened during sulfitation of mimosa and quebracho tannins.
- Solid state NMR can be used routinely to identify the tannin used to tan a specific leather (mimosa, quebracho, chestnut or tara) or whether a mineral tanning material was used.
- No higher oligomeric insoluble condensed tannins or hydrolysable tannins remain in spent mimosa bark.
- Spent mimosa bark consists predominantly of water insoluble gums, bigger than.
- Further work is required to develop the potential of solid state NMR in determinining the average chain length of mimosa and quebracho tannins.

4.15 References

1. Roux, D. G. *J.S.L.T.C.*, **1949**, *33*, 393.
2. Porter, L. J. **Tannins** In: **Methods in plant biochemistry**, Harbone, J. B. ed. London Academic Press, **1989**, *1*, 289 – 419.
3. Foo, L. Y.; Porter, L.J. *J. C. S. Perkin 1* **1978**, 1186-1190.
4. Czochanska Z.; Foo L. Y.; Newman R. H.; Porter L. J. *J.C.S. Perkin I.*, **1980**, *10*, 2278-2286.
5. Jones, W. T.; Broadhurst, R. B.; Lyttleton, J. W. *Phytochemistry*, **1976**, *15*, 1407 – 1409.
6. Tamir, M.; Nachtomi E.; Alumot, E. *Phytochemistry*, **1971**, *10*, 2769.
7. Strumeyer, D. H.; Malin, M. J. *J. Agric. Food Chem.*, **1975**, *23*, 909.
8. Meagher, L. P.; Lane, G.; Sivakumaran, S.; Tavendale, M.H.; Fraser, K. *Animal Feed Science and Technology*, **2004**, *117*, 151.
9. Covington, A. D.; Lilley, T. H.; Song, L.; Evans, C. S. *JALCA*, **2005**, *100*, 325.
10. Pasch, H.; Pizzi, A.; Rode, K. *Polymer*, **2001**, 42, 7531–7539.
11. Lorenz, K.; Preston, C. M.; Raspe, S.; Morrison, I. K.; Feger, K. H. *Soil Biology & Biochemistry*, **2000**, *32*, 779-792.
12. Gamble, G. R.; Akin, D. E.; Paul, H.; Makkar, S.; Becker, K. *Applied and Environmental Microbiology*, October **1996**, 3600–3604.
13. Conte, P.; Piccolo, A.; Van Lagen, B.; Buurman, P.; De Jager, P. A.; *Geoderma*, **1997**, *80 (3-4)*, 327.
14. Van der Westhuizen, J. H.; Reid, D. An Investigation into the potential of ^{13}CP MAS NMR spectrometry to characterise and investigate structural properties of commercial tannin extracts for Mimosa Extract Company (Pty) Ltd, October **2009**.
15. Hemingway, R. W.; Foo, L. Y.; and Porter, L. J. *J. Chem. Soc. Perkin I*, **1982,** 1209 – 1216.
16. Morgan, K. R.; Newman, R. H. *Appita*, **1987**, *40*, 450–454.
17. Hoong, Y. B.; Paridah, M. T.; Luqman, M. P.; Koh, M. P.; Loh, Y. F. *Industrial Crops and Products*, **2009**, *30*, 416–421.
18. Pizzi, A. *J. Appl. Polym. Sci.*, **1979**, *24*, 1247–1256.

19. Foo, L. Y.; McGraw, G. W.; Hemingway, R. W. *J. Chem. Soc., Chem. Commun.* **1983**, 672–673.
20. Fletcher, A. C.; Porter, L. J.; Haslam, E.; Gupta, R.K. *J. Chem. Soc. Pekin Trans. 1*, **1977**, 1628.
21. Roux, D. G.; Ferreira, D.; Hundt, K. L.; Malan, E. *Applied Polymer Symposium, No. 28*, John Wiley & Sons, **1975**, 335 – 353.
22. Evelyn, S. R. J. Soc. Leather Trades Chem. **1954**, 38, 142.
23. Thompson, D.; Pizzi, A. *Journal of Applied Polymer Science*, **1995**, *55*, 107.
24. Roux, D. G. *Journal Society of Leather Trades' Chemists*, **1952**, 36, 210.
25. Roux, D. G. *Journal Society of Leather Trades' Chemists*, **1953**, 37, 274.
26. Stephen, J. *J. Chem. Soc.*, **1951**, 646.
27. Robinson, R.; Robinson, G.M. *Biochem. J*., **1933**, *27*, 206-212.
28. Robinson, R.; Robinson, G.M. *J. Chem. Soc.* **1935**, 744-752.
29. Hillis, W. E.; Swain, T. *J. Sci. Food Agric.* **1959**, *10*:135-144.
30. Bate-Smith, E. C. *Phytochemistry*, **1975**, *14 (4)*, 1107-1113.
31. Haslam, E. *Practical Polyphenolics*, Cambridge University Press, Cambridge, **2005**, *24*, 34.
32. Schofield, P.; Mbugua, D. M.; Pell, A. N. ; *Animal Feed Science and Technology*, **2001**, *91*, 21-40.
33. Odlyha, M.; Cohen, N. S.; Foster, G. M.; Aliev, A.; Verdonck, E.; Grandy, D. *Journal of Thermal Analysis and Calorimetry*, **2003**, *71*, 939.
34. Simon, C.; Pizzi, A. *Journal of the American Leather Chemists Association*, **2003,** 98, 83.
35. Berdet, M.; Gerbaud, G.; Le Pape, L.; Hediger, S.; Tran, Q. K.; Boumlil, N. *Anal Chem*, **2009,** *81*, 1505.
36. Brown, E. M.; Dudley, R. L. *Journal of the American Leather Chemists Association*, **2005**, 100, 401.
37. Brown, E. M.; Dudley, R. L.; Elsetinow, A.R. *Journal of the American Leather Chemists Association*, **1997**, 92, 225.
38. Aliev, A. E. *Biopolymers*. **2005**, *77*, 230.
39. Ayres, M. P.; Clausen, T. P.; MacLean, S. F.; Redman, A. M.; Reichardt, P. B. *Ecology*. **1997,** *78*, 1996.

40. Tarascou, I.; Barathieu, K.; Simon, C.; Ducasse, M. A.; Andre, Y.; Fouquet, E.; Dufourc, E. J.; de Freitas, V.; Laguerre, M.; Pianet, I. *Magnetic Resonance in Chemistry*, **2006**, *44*, 868.
41. Davis, A. L.; Cai, Y.; Davies, A. P.; Lewis, J. R. *Magnetic Resonance in Chemistry*, **1996**, *34*, 887.
42. Covington, A. D., Vegetable tanning. *Tanning Chemistry; the Science of Leather*, RSC Publishing: Cambridge, **2009**, 281.
43. Galvez, J. M G.; Riedl, B.; Conner, A. H. *Holzforschung.***1997**, *51*, 235.
44. Pizzo, A.; Pasch, H.; Rode, K.; Giovando, S. *Journal of Applied Polymer Sciences.* **2009**, *113*, 3847.
45. Mueller-Harvey, I. *Animal Feed Science and Technology*, **2001**, 91, 3.
46. Tang, R. H.; Covington, A. D.; Hancock, R. A. *Journal of the Society of Leather technologists and Chemists*, **2003**, 87, 179.
47. Orabi, M. A. A.; Taniguchi, S.; Yoshimura, M.; Yoshida, T.; Kishino, K.; Sakagami, A.; Hatano, T. *Journal of Natural Products.* **2010**, *73*, 870.
48. Magid, A. A.; Voutquenne-Nazabadioko, L.; Harakat, D.; Moretti, C.; Lavaud, C. *Journal of Natural Products*, **2008**, *71*, 914.

CHAPTER 5

5. ANALYSIS and CHARACTERISATION of CONDENSED (MIMOSA and QUEBRACHO), and HYDROLYSABLE (TARA and CHESTNUT) TANNINS with MASS SPECTROMETRY

5.1 General Introduction

As discussed in Chapter 2 and Chapter 3, many questions about the composition and chemistry of tannins in general and the commercially important condensed tannins such as mimosa and quebracho in particular, remain unanswered.

No satisfactory method exists to fractionate mimosa and quebracho tannin extracts into its constituent molecules or even oligomer groups with the same degree of polymerisation. This includes normal and reverse phase silica gel based chromatography, size exclusion, countercurrent and paper chromatography. Monomers, dimers, trimers and tetramers can be obtained but bigger molecules do not subject themselves to being separated. The situation is similar with hydrolysable tannins.

The situation with mimosa and quebracho tannins is further complicated by the resorcinol type A-rings in these compounds. The absence of a 5-OH group imparts stability to the interflavanyl bond against acid hydrolysis. This renders the classical method to analyse proanthocyanins *via* acid hydrolysis of the interflavanyl bond, followed by trapping of intermediates with toluene-α-thiol or phloroglucinol and analysis of the trapped intermediates with HPLC, unreliable. The high temperatures thus required to hydrolyse the interflavanyl bond in mimosa and quebracho tannins leads to decomposition.[1]

Be that as it may, the acid hydrolysis method gives average values if applied to a mixture of oligomers. We can thus obtain average values such as the average chain

length (*via* the terminal / repeat unit ratio) of all the oligomers present, but no information on the individual polymer molecules such as the fraction of each oligomer present.[2]

Mass spectrometry of mixtures is essentially a fractionation technique. The mixture is fractionated into different molecular mass fractions and the molecular mass of each fraction is obtainable. It thus provides important information on the monomer, oligomer and polymer molecules present in a tannin extract.

Mass spectrometry detects and measures only evaporated charged molecules. Unfortunately we cannot assume that all the molecules in a tannin extract evaporate at the same temperature and vacuum, nor accepts charge with the same ease. In the absence of suitable internal standards, mass spectrometry data should be interpreted with caution.

Pasch and co-workers[3] investigated commercial mimosa and sulfited quebraco (*Schinopsis balansae*) extracts with MALDI-TOF. They concluded the following:

a) Mimosa tannin is constructed predominantly from robinetinidol (A) (major component), fisetinidol (B) and gallocatechin (C) monomers whereas quebracho is predominantly composed of fisetinidol (B) (major component) and robinetinidol (A) monomers.
b) Mimosa tannin is profoundly branched as it consists of a high proportion of angular units whilst quebracho is a mostly a linear tannin.
c) The interflavanyl link in quebracho is easily hydrolysable but in mimosa it is stable to hydrolysis.
d) The changes brought about by sulfitation are more pronounced in tannins with a catechol B-ring (quebracho) than with a pyrogallol-type B-ring (mimosa).
e) The number average degree of polymerisation of quebracho and mimosa tannin determined with MALDI-TOF mass spectrometry compares well with results obtained with other techniques.

Some of the above conclusions (particularly b, but also c and d) were, in our opinion, not substantiated by the evidence and arguments provided in the publication and do not necessarily correspond with what is accepted in the tannin industry. Some of the fragments were also assigned wrong structures based on faulty arithmetic. Despite this, the work made an important contribution to our knowledge of tannin chemistry, particularly in terms of conclusions 'a' and 'e' above.

Vivas and co-workers[4] studied the unsulfited acetone-water extract of quebracho (*Schinopsis balansae*) and obtained similar results. A MALDI-TOF spectrum of unsulfited *Schinopsis lorentzii* extract, obtained from Unitan S.A.I.C.A. (Figure 5-1) is similar to the Vivas[4] and Pasch[3] spectra, probably explaining the indiscriminate use of the term quebracho extract for the tannin extract from both trees.

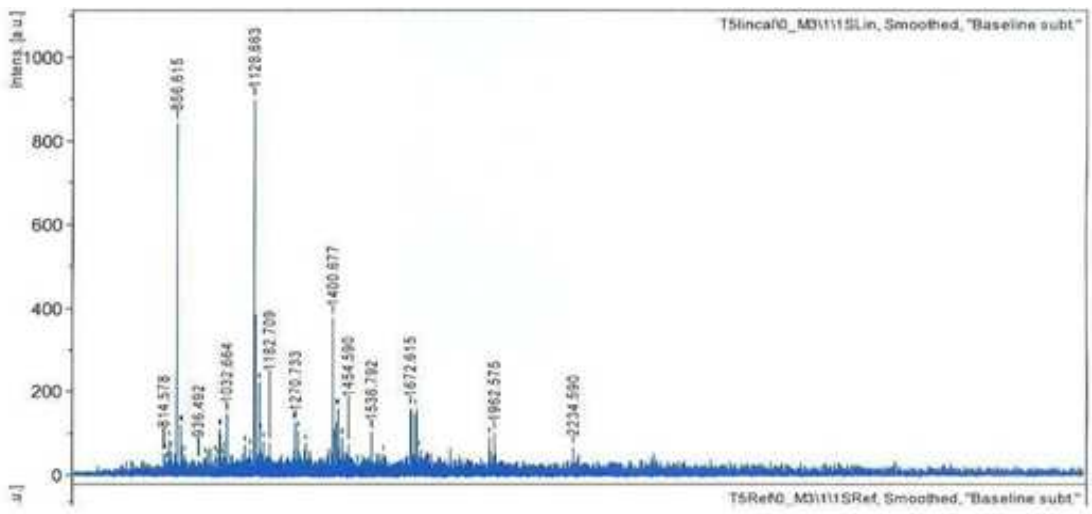

Figure 5-1: MALDI-TOF spectrum of unsulfited *Schinopsis lorentzii* extract (Unitan S.A.I.C.A)

We argued that electrospray mass spectrometry may give additional information to the MALDI-TOF data. Combining the three techniques of MALDI, electrospray and solid state NMR, helped to overcome limitations when using only one technique.

5.2 Problem Statement

In this chapter we aim to answer the following questions that can be rephrased as hypotheses:

a) Can ESI MS give additional information (compared to MALDI-TOF) on the chemical composition of tannin extracts?
b) Can ESI MS distinguish between hydrolysable and condensed tannin extracts?
c) Can ESI MS distinguish between quebracho and mimosa tannins?
d) Can we obtain information about the chemical changes that take place during sulfitation of mimosa and quebracho tannins (treatment with bisulphite) by analysis with ESI MS?

5.3 Experiment 1: An electrospray MS investigation into the composition of mimosa, quebracho and chinese mimosa tannin extracts

5.3.1 Introduction

According to *Covington et al*.[5] mimosa (black wattle) tannins from *Acacia mearnsii* consists mostly of prorobinetinidin (70%) and profisetinidin (25%) with a small amount of prodelphinidin (5%) whereas quebracho consists of 100% profisetinidin. The MALDI-TOF work by Pasch and co-workers[3] supported his conclusion on mimosa but detected a prorobinetinidin fraction in addition to the major profisetinidin fraction in quebracho extract.

MALDI-TOF mass spectrometry has shown that mimosa extract consists of a range of oligomeric flavan-3-ol units up to the octamer level (n = 8) (Figure 5-2 and Table 5-1). From the table it is evident that mimosa condensed tannin oligomers are permutations and combinations of mainly fisetinidol (A) and robinetinidol (B) monomers but with a relatively important fraction of gallocatechin monomers (C). (Mimosa tannins are thus profisetinidins, prorobinetinidins or prodelphinidins). The data indicated, according to Pasch[3], a high frequency of angular trimers and tetramers. It is not clear to us how Pasch came to this conclusion, as linear condensed tannins would give the same mass values. The resistance of mimosa tannins to acid hydrolysis was attributed to these angular condensed tannins. It is not clear to us how Pasch came to this conclusion either.

Table 5-1: MALDI peaks for industrial mimosa tannin extract (Pasch et.al).[3]						
M+Na+ Experimental	M+Na+ Calculated	Relative Intensity %		Unit Type		
				A	B	C
Dimers						
602	601.6	29		-	2	-
Trimers						
858	857.9	10		2	1	-
874	873.9	34		1	2	-
			or	2	-	1
890[a]	889.9	78		1	1	1
				-	3	-
906[a]	905.9	72		-	2	1
			or	1	-	2
922	921.9	18		-	1	2
Tetramers						
1147	1146.2	10.5		2	2	-
			or	3	-	1
1163	1162.2	29		1	3	-
			or	2	1	1
1179	1178.2	45		-	4	-
			or	1	2	1
			or	2	-	2
1195	1194.2	36		-	3	1
			or	1	1	2
1211	1210.2	11		-	2	2
			or	1	-	3
Pentamers						
1467	1466.5	28				
Hexamers						
1765	1754.8	13				
Heptamers						
2045	2043.1	5				
Octamers						
2333	2331.4	3				
[a] Dominant oligomer						

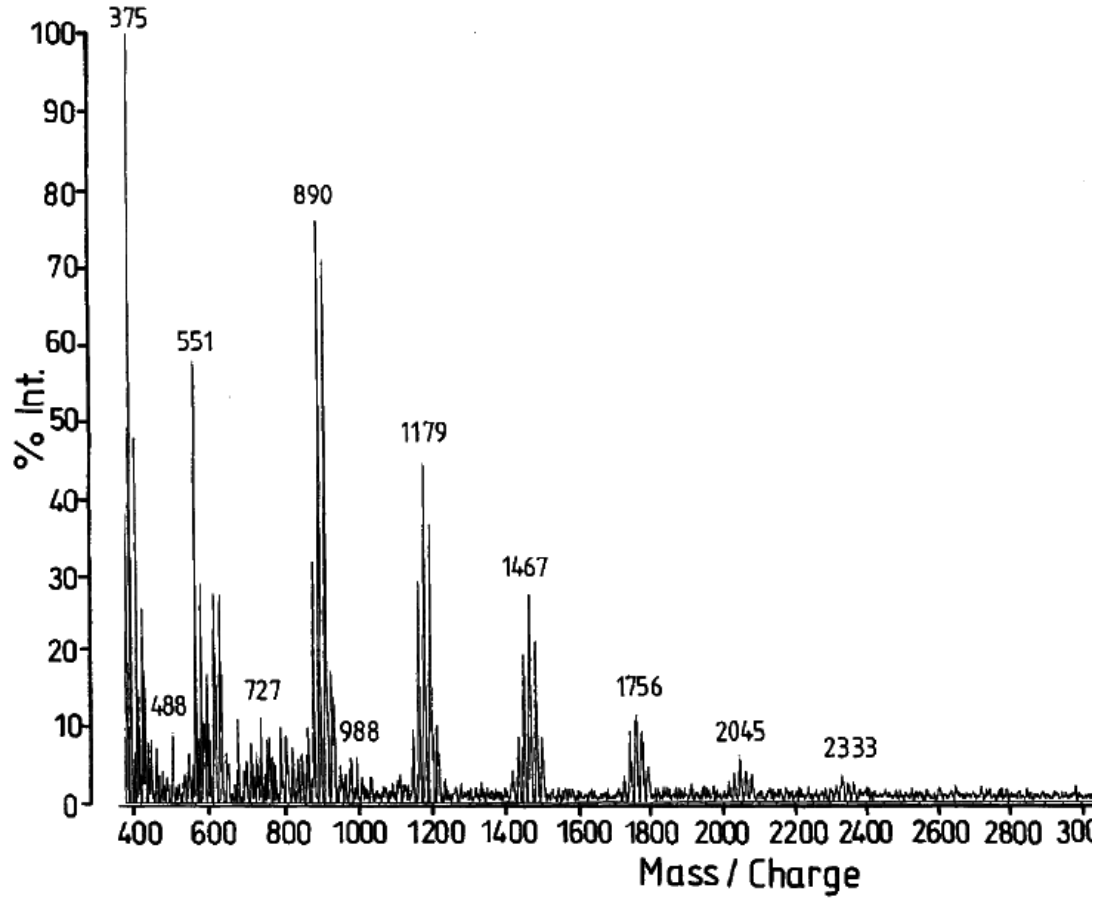

Figure 5-2: MALDI-TOF spectrum of mimosa oligomeric units (Pasch et. al.).

Turning to the sulfited quebracho (*Schinopsis balansae*) spectrum given in Figure 5-3 and the corresponding Table 5-2 which summarizes the data, we note peaks at 1965, 2237, 2510 and 2800 amu corresponding to the sodium adducts of respectively heptamers, octamers, nonamers and decamers. This provides definite proof of the existence of high oligomers in commercial quebracho extract. The number average degree of the sample was found by ^{13}C NMR to be 6.74 which agrees with the existence of high molecular mass oligomers.

Analysis of relative peak intensities indicates that quebracho consists of between 70- and 80% of A-type units (fisetinidol) and between 20- and 30% B-type units (robinetinidol) and has a number average degree of polymerisation of 6.25 (c.f. 6.74 determined by ^{13}C above). Mass discrimination for higher molecular mass oligomers may explain the lower value obtained with MS compared to NMR. Mass

discrimination means higher molecular mass intensities are too low or not observed at all compared to lower molecular mass oligomers.

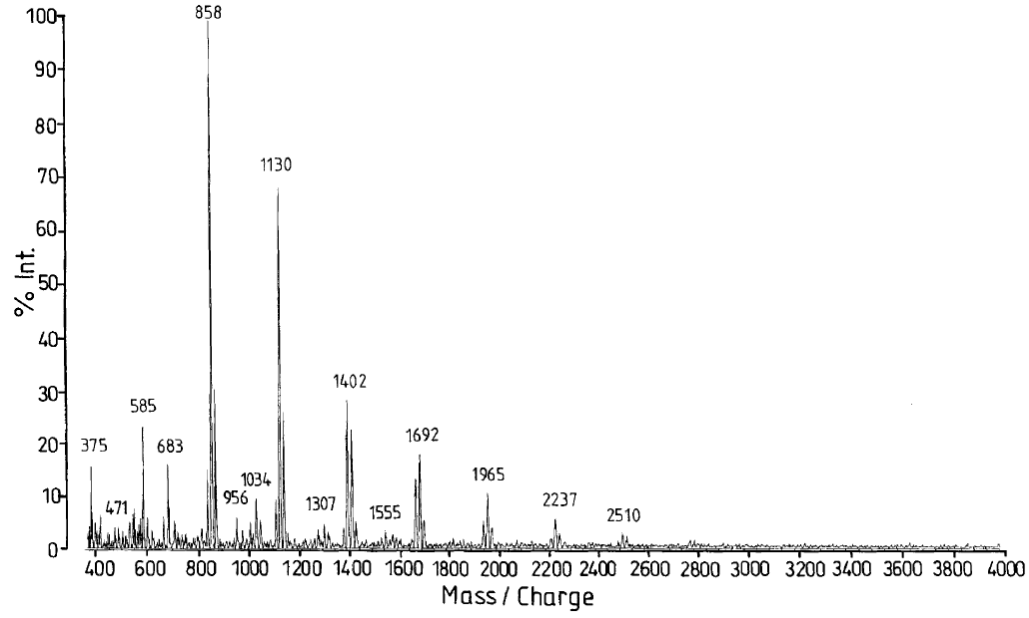

Figure 5-3: MALDI-TOF spectrum of commercial quebracho extract (the commercial quebracho extract is sulfited).[1]

Table 5-2: Observed and calculated mass of commercial quebracho (*Schinopsis balansae*) proanthocyanidins by MALDI-TOF (sulfited boiling water extract) (Pasch et. Al.).[3]

Polymer	$M+N^{a+}$ Calculated	$M+Na^{+}$ Observed	Fisetinidol unit A	Robinetinidol unit B
Dimers	585.6	585	1	1
	601,6	601		2
Trimer	841.9	842	3	0
	857.9	857a	2	1
	873.9	874	1	2
Tetramer	114.2	1114	4	0
	1130.2	1130a	3	1
	1146.2	1146	2	2
Pentamer	1386.5	1387	5	0
	1402.5	1402a	4	1
	1418.5	1420	3	2
	1434.5	1435	2	3
Hexamer	1658.8	1658	6	0
	1674.8	1675	5	1
	1690.8	1692a	4	2
	1706.8	1708	3	3
Heptamer	1947.1	1948	6	1
	1963.1	1965a	5	2
	1979.1	1982	4	3
Octamer	2235.4	2237a	6	2
Nonamer	2507.7	2510	7	2
Decamer	2780.0	2782a	8	2
	2796.0	2796	7	3

[a] Dominant oligomer

5.3.2 Results and Discussion

Plate 5-1, Plate 5-2, Plate 5-3 and Plate 5-4 give the negative mode electrospray mass spectra of commercial mimosa (ME) (*Acacia mearnsii*) and quebracho (ATN) (*Schinopsis lorentzii* unsulfited) tannin extracts with some detail. Table 5-3 and Table 5-4 summarise the data. These results were obtained in negative mode. This is due to the polyphenol nature of these compounds and the fact that the ionisation of the aromatic group to a negatively charged hydroxyl group under negative mode MS conditions can be relatively facile, compared to protonation of the hydroxyl group (positive mode).

A cursory inspection of the two spectra indicates the following:

a) The spectrum of mimosa is far more complex than that of quebracho. Quebracho is predominantly an oligomer of fisetinidin (M^+ = 288amu) and the peaks corresponds to multiples of 288 amu. The biggest singly charged oligomer that we observe in the quebracho spectrum is a tetramer at 1146. Also notable is a large quantity of robinetinidol at 301. This suggests that quebracho makes robinetinidol but does no incorporate it into condensed tannins.

b) The peaks corresponding to dimers, trimers and tetramers in mimosa are not single peaks as is the case with quebracho, but clusters of peaks 16 amu apart. This corresponds with a different number of hydroxyl groups and is explained by the fact that mimosa oligomers are permutations and combinations of fisetinidin (M^+ = 272), robinetinidin (M^+ = 288amu) and gallocatechin (M^+ = 304). There is a well-defined cluster at 1154 corresponding with a tetramer. We also observe a small cluster at 1442 corresponding with a pentamer.

c) However, the peak group at 1595 in the mimosa spectrum is 8 amu apart and not 16 amu as would be expected from varying number of OH groups. This indicates doubly charged ions corresponding to oligomers with a mass of about 3190. By looking at the doubly charged ions, we

can detect larger peaks with electrospray than we can with MALDI-TOF.

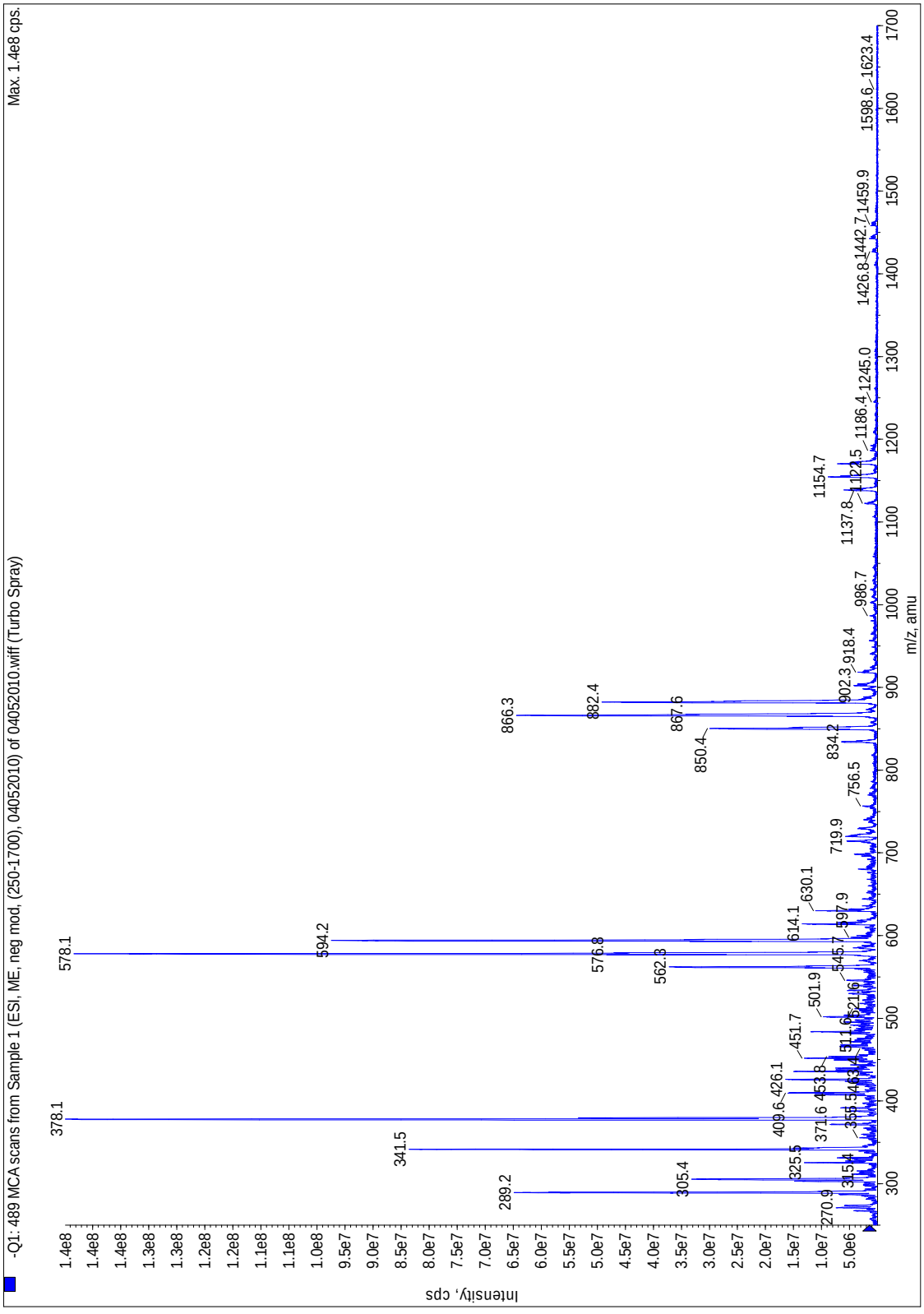

Plate 5-1: Electrospray Ionisation of normal industrial mimosa tannin extract (ME)

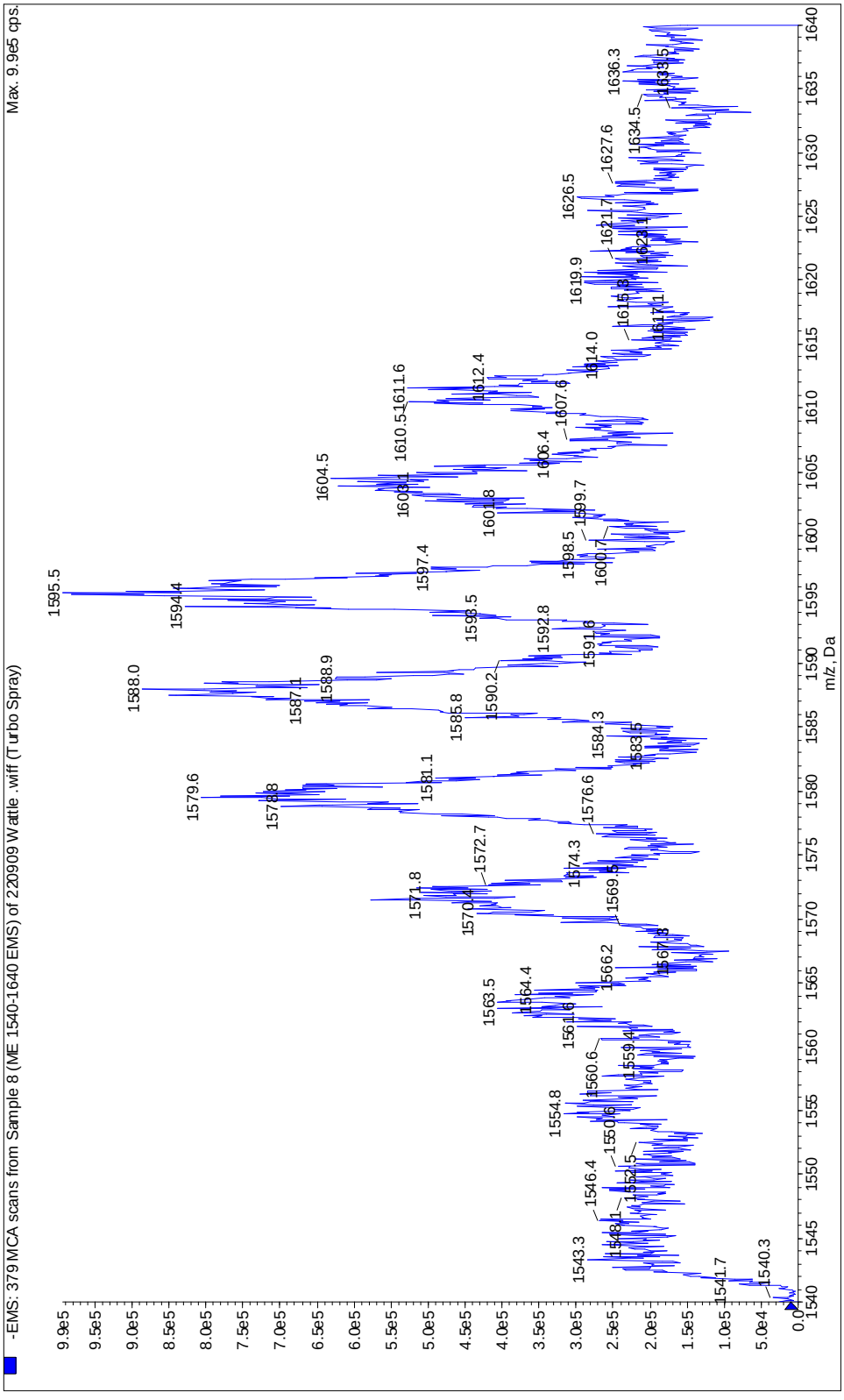

Plate 5-2: Detail of total ion scan for mimosa, showing the doubly charged ions, separated by 8 Da.

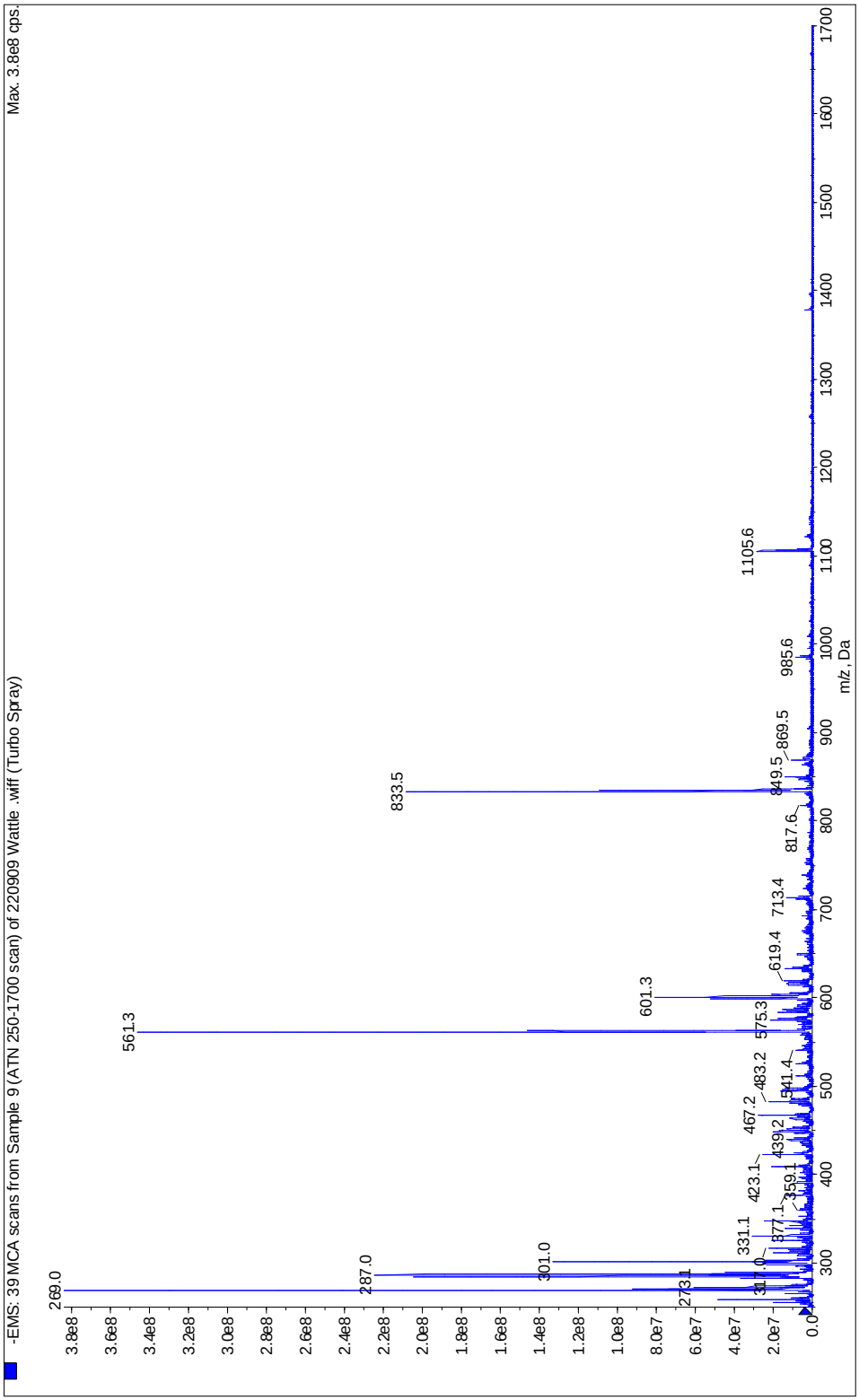

Plate 5-3: Electrospray Ionisation of normal industrial quebracho tannin extract (ATN)

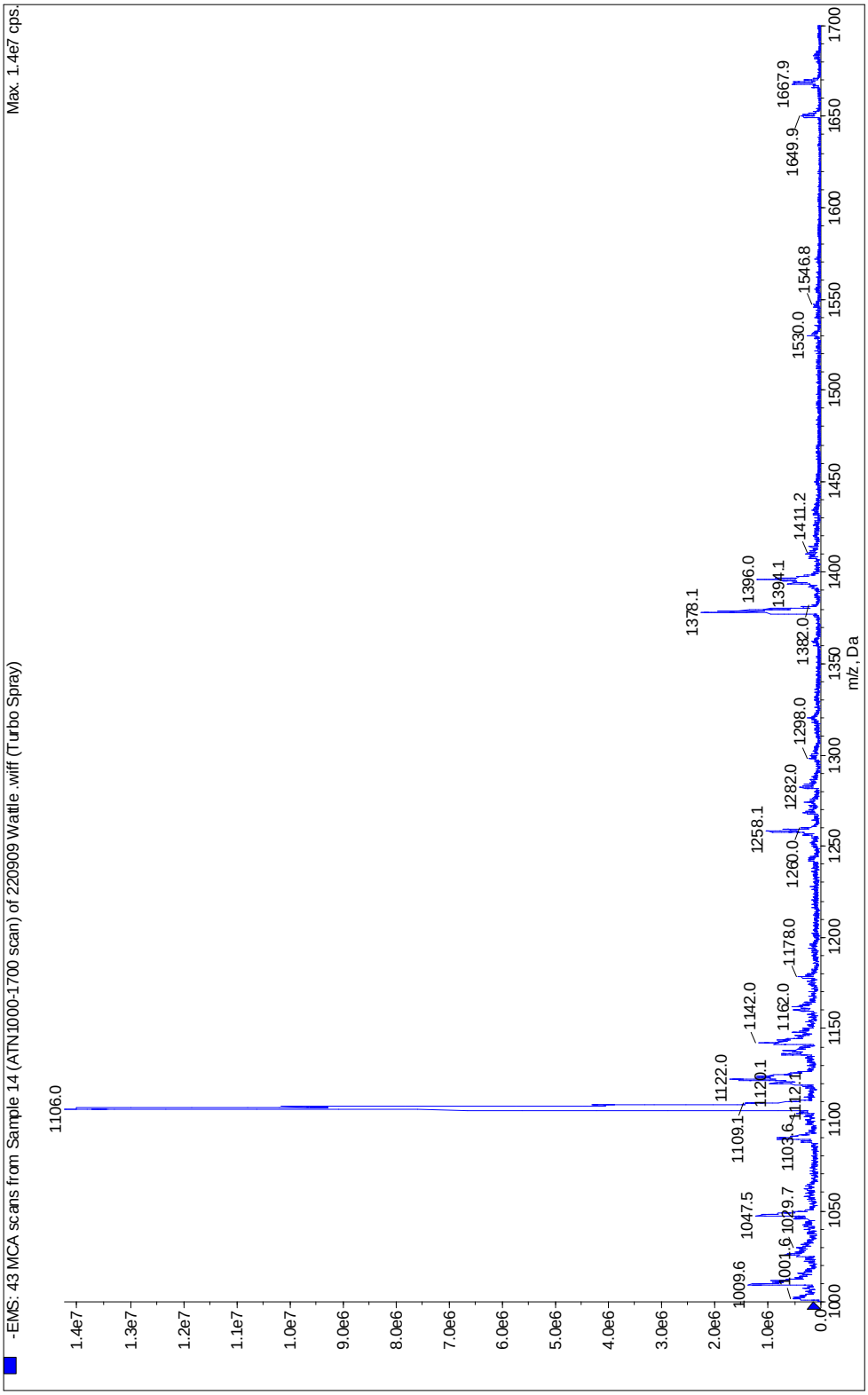

Plate 5-4: Detail of total scan of quebracho from 1000 to 1700

Table 5-3: ESI main peaks for industrial mimosa tannin extract (ME) and possible combinations of monomers (main peaks are in italics)						
Observed Mass	Theoretical Mass	Peak Intensity		Unit Type		
				PF(272.3)	PR(288.3)	PD(304.3)
Monomers						
270.9	272.3	16.88		1	0	0
289.2	*288.3*	*76.36*		*0*	*1*	*0*
305.2	304.3	32.74		0	0	1
Dimers						
562.3	560.6	27.00		1	1	0
594.2	592.6	67.29		0	1	1
578.1	*576.6*	*100.00*		*0*	*2*	*0*
Trimers						
834.2	832.9	5.34		2	1	0
850.4	848.9	19.67		1	2	0
866.3	*864.9*	*43.28*		*1*	*1*	*1*
			or	0	3	0
882.4	880.9	28.25		0	2	1
Tetramers						
1122.5	1121.2	1.05		2	2	0
1137.8	1137.2	2.72		2	1	1
			or	1	3	0
1154.7	*1153.2*	*4.19*		*1*	*2*	*1*
			or	0	4	0
1169.3	1169.2	3.67		1	1	2
			or	0	3	1
1186.4	1185.2	0.16		0	2	2
Pentamers						
1426.8	1425.5	0.51		2	2	1
			or	1	4	0
1459.9	*1457.5*	*0.62*		*1*	*2*	*2*
			or	0	4	1
1442.7	1441.5	0.45		1	3	1
			or	2	1	2
			or	0	5	0

Table 5-4: ESI peaks for industrial quebracho tannin extract (ATN) and possible combinations of monomers						
Observed Mass	Theoretical Mass	Intensity		Unit Type		
				PF	PR	PD
				272.3	288.3	304.3
Monomers						
271.2	272.3	27.26		1	0	0
287.0	*288.3*	*97.27*		*0*	*1*	*0*
301.1	304.3	11.30		0	0	1
Dimers						
561.3	*560.6*	*100.00*		*1*	*1*	*0*
575.3	576.6	4.32		1	0	1
			or	0	2	0
Trimers						
833.5	*832.9*	*79.25*		*2*	*1*	*0*
849.5	848.9	5.19		2	0	1
			or	1	2	0
Tetramers						
1089.4	1089.2	1.06		4	0	0
1106.6	*1105.2*	*11.90*		*3*	*1*	*0*
1121.4	1121.2	1.53		3	0	1
			or	2	2	0
Pentamers						
1378.7	*1377.5*	*1.58*		*4*	*1*	*0*
1408.1	1409.5	0.25		3	1	1
			or	2	3	0

5.3.3 Conclusion

Elecrospray ionisation MS allows unambiguous distinction between mimosa and quebracho tannin extracts. It indicates that quebracho consists mainly of fisetinidin monomers and that mimosa consists of fisetinidin, robinetinidin and gallocatechin

monomers in various permutations and combinations. Quebracho, showing mainly one peak in every series, is argued to consist of fisetinidin monomers with only one robinetinidin monomer attached to the oligomer. This means the oligomers consist of a minimum of one robinetinidin monomer plus further fisetinidin monomers that make up the polymer chain. Pasch *et. al*[3] however observed, from *Schinopsis balansae*, two robinitinidol monomers in oligomers bigger than pentamers. The largest oligomer that we could observe was a decamer with mimosa and a tetramer with quebracho.

MALDI-TOF is more reliable in showing the higher molecular mass ranges than electrospray, but electrospray is more reliable for the lower ranges than MALDI. However, by using doubly charged ions in electrospray we could detect decamers in the mimosa spectrum.

5.4 Experiment 2: An elecrospray investigation into the composition of sulfited quebracho (*Scinopsis lorentzii*) and mimosa (*Acacia mearnsii*) tannins

5.4.1 Introduction

Mimosa and quebracho are treated with different levels of bisulphate to enhance certain properties, for example increasing their solubility in water.[6] The nature of the chemical transformations and products that form is uncertain. It is also difficult to determine the level of sulphur introduction in tannin molecules *via* conventional analysis as unreacted bisulfite cannot be removed from the tannin.

In this experiment an investigate-and-interpret the effect of sulfitation on the electrospray MS of the corresponding tannin extracts.

5.4.2 Results and Discussion

Low resolution (one decimal point) elecrospray MS (done in negative mode) of the following spray dried commercial tannin extracts were obtained (all our quebracho extracts was from *Schinopsis lorentzii*):

- Normal unsulfited mimosa tannin extract (ME) Plate 5-1
- Medium sulfited mimosa tannin extract (FS) Plate 5-5
- Heavily sulfited mimosa tannin exract (WS) Plate 5-6
- Normal unsulfited quebracho tannin extract (ATN) Plate 5-3
- Medium sulfited quebracho tannin extract (ATO) Plate 5-7
- Heavily sulfited quebracho tannin extract (ATD) Plate 5-8

The results are summarised in Table 5-5 (mimosa tannins) and Table 5-6 (quebracho tannins). In all the sulfited samples we see +82 Dalton fragments corresponding with a single sulfonic acid group attached to the corresponding unsulfited M+ fragments. The +82 Dalton fragments correspond with C-ring opened products (D in Figure 5-4). The alternative structures with sulfitation without ring opening would have a +80

Dalton peak (E in Figure 5-4). Introduction of the SO_3H group creates peaks of the same intervals as in the flavonoid combinations (16 amu), but shifted from the normal oligomer peaks with a value of 82 amu. In Plate 5-5 and Plate 5-7, sulfitation of oligomers for mimosa and quebracho up to tetramers can be observed. During sulfitation we did not observe double sulfitation of any higher oligomers.

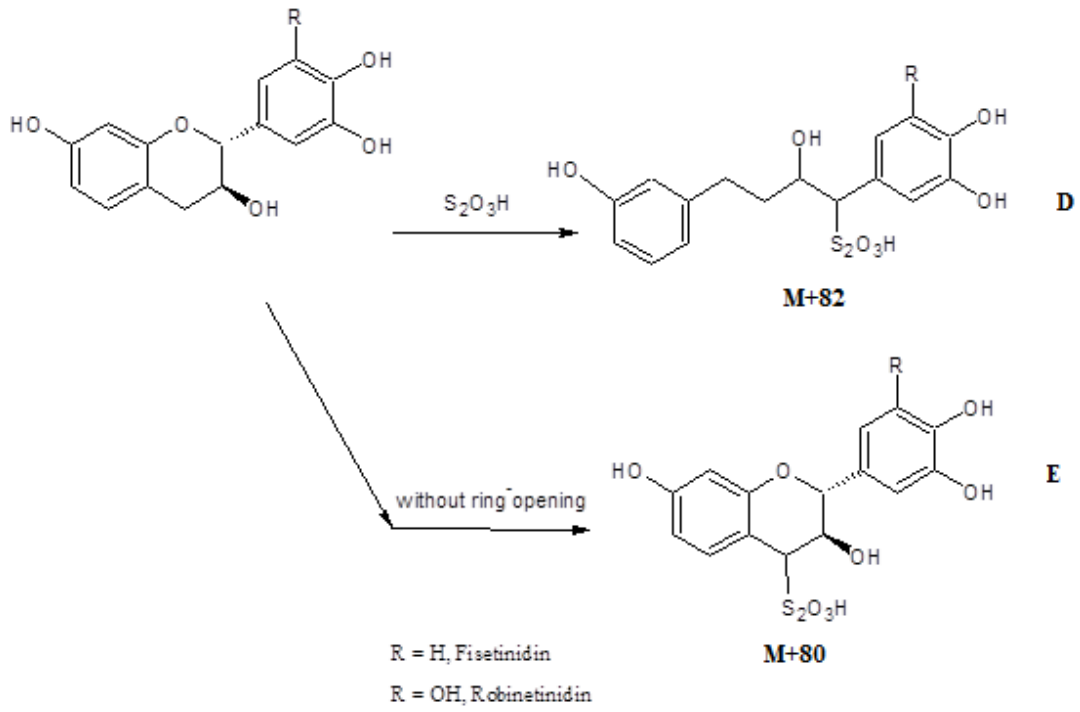

Figure 5-4: The effect of sulfitation on robinetinidin / fisetinidin showing ring-opened and unopened ring products

The difference between the sulfited (FS) and heavily sulfited (WS) spectra is that in the heavily sulfited spectra the peaks of the sulfited combinations are much higher in relative intensity than in the FS sample. The ratio between M / M+82 in the sulfited extract (FS) (Plate 5-5) and the heavily sulfited extract (WS) (Plate 5-6) is about 2:1 and 1:1 respectively, indicating roughly 30 and 50% incorporation of sulphate, assuming that the sulfited species evaporate and ionise similarly to the unsulfited species. A more accurate estimate of sulfitation levels would require hitherto unavailable internal standards.

Another difference is that in the heavily sulfited spectra the peaks of the sulfited combinations are much higher in absolute intensity than in the FS sample. The intensity of the unsulfited peaks is lower in the heavily sulfited sample (WS) than in the medium sulfited sample (FS). Thus, in WS, sulfitation occurs at such a high level that the occurance of unsulfited oligomers decreases. Of note in WS is that the intenisty at the sulfited tetramers is lower than that at FS. This could show that the sulfitation of higher oligomers, from tetramers upwards, does not take place so succesfully when a heavy amount of sulfitation is applied. A pattern can be observed by looking at normal mimosa, then medium sulfited and lastly at heavily sulfited mimosa: the intensity of unsulfited oligomers decrease from the one to the next and the intensity of sulfited peaks increase. The sulfitation can only be observed up to sulfited tetramers. Table 5-5 shows all observed values for industrial and modified mimosa, with intensities higher than 1 and matching expected combinations

The ESI spectrum for sulfited Quebracho (ATO) shows that the same peaks as in the normal quebracho spectrum can be observed as well as their individually sulfited counterparts. These can be seen at intervals of 82 amu from the unsulfited peaks as sulfition occurred in the form of sulfate, as in mimosa.

Pasch and co-workers[3] did not detect any M + 80 or M + 82 peaks in their MALDI-TOF spectrum of sulfited commercial mimosa extract (Figure 5-2). It is uncertain whether this is due to a sample with very low levels of sulfitation or whether the MALDI-TOF matrix does not ionise the sulfited molecules.

In contrast to the mimosa spectra of FS and WS, where the level of sulfitation could be detected from the intensity of the peaks, in quebracho this does not seem to be the case. The ratio of M + 82 / M peaks in the ESI spectrum for heavily sulfited quebracho (ATD) is similar to that of that of medium sulfited quebracho (ATO). This could mean that medium sulfitation, as in ATO, allows sufficient sulfitation of the flavonoid oligomers and any further sulfitation is rendered useless as the positions available on the oligomer molecules are satiated at the medium level of bisulfate addition.

For the first time, the existence of sulfited molecules has been observed here. In quebracho, diferent than in mimosa, the effect of sulfitation from medium to heavily sulfited shows an increase only in the monomer and dimer combinations. In the trimer and tetramer, the effect of sulfitation decreases from ATO to ATD. This could mean that sulfitation saturation has taken place with the medium level addition of bisulfite and adding more bisulfite, may break interflavanyl bonds.

High resolution spectra (Plate 5-9, Plate 5-10, Plate 5-11, Plate 5-12 and Plate 5-13) of the commercial samples give similar results. These high resolution spectra allow unambiguous molecular formula assignments and prove that the M + 82 peaks contain sulphur in the SO_4 form.

MALDI-TOF spectra are commonly assumed to represent milder conditions than electrospray ionisation and more suitable for polymer analysis.[7] However, MALDI-TOF requires a matrix that transfers the ionisation to the analyte mixture. The risk of selective ionisation is in our opinion bigger than with electrospray ionisation, where the whole sample is injected into the ionisation chamber. The matrix itself may also be ionised and interferes with the smaller analytes in the mixture.

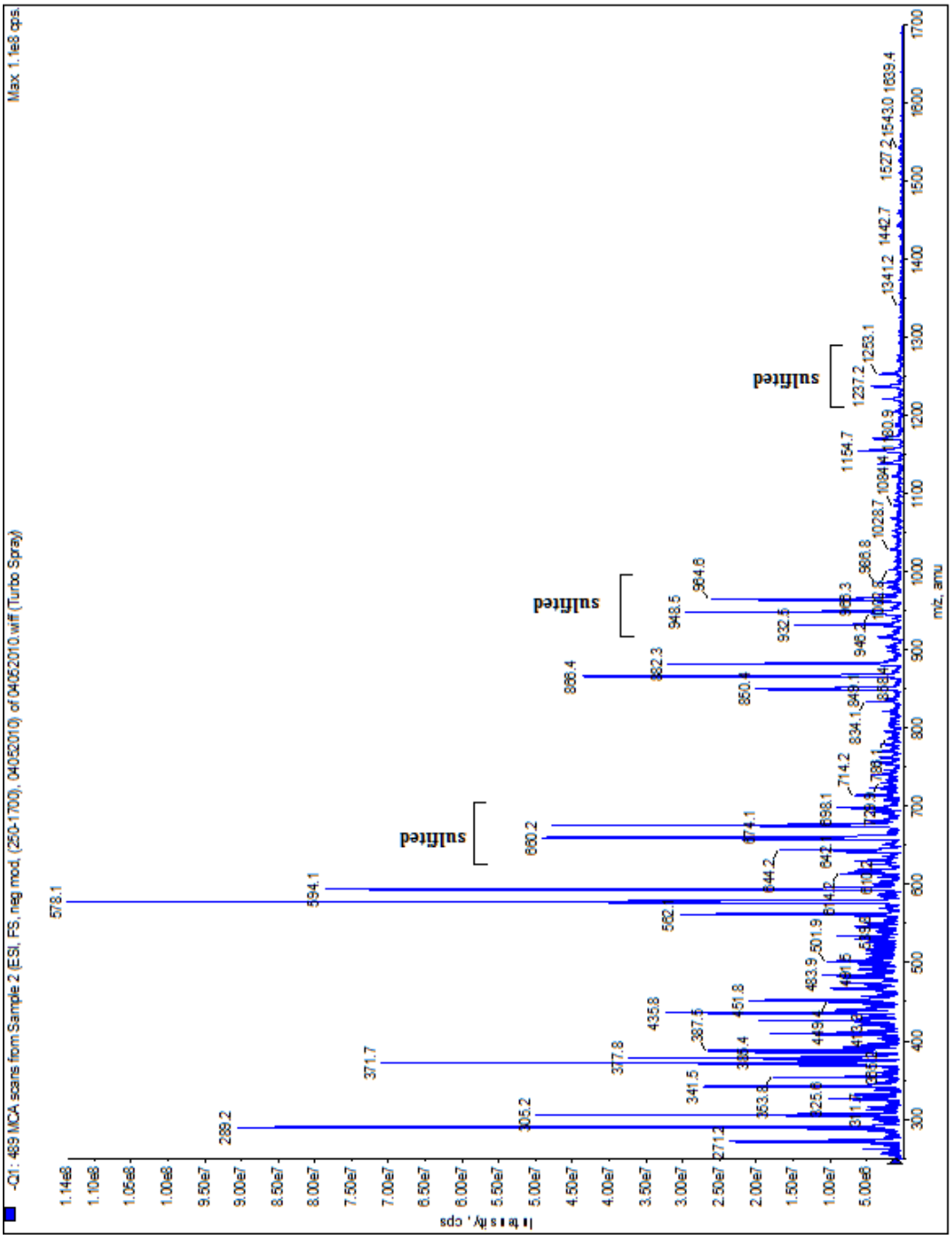

Plate 5-5: Electrospray Ionisation of sulfited industrial mimosa tannin extract (FS)

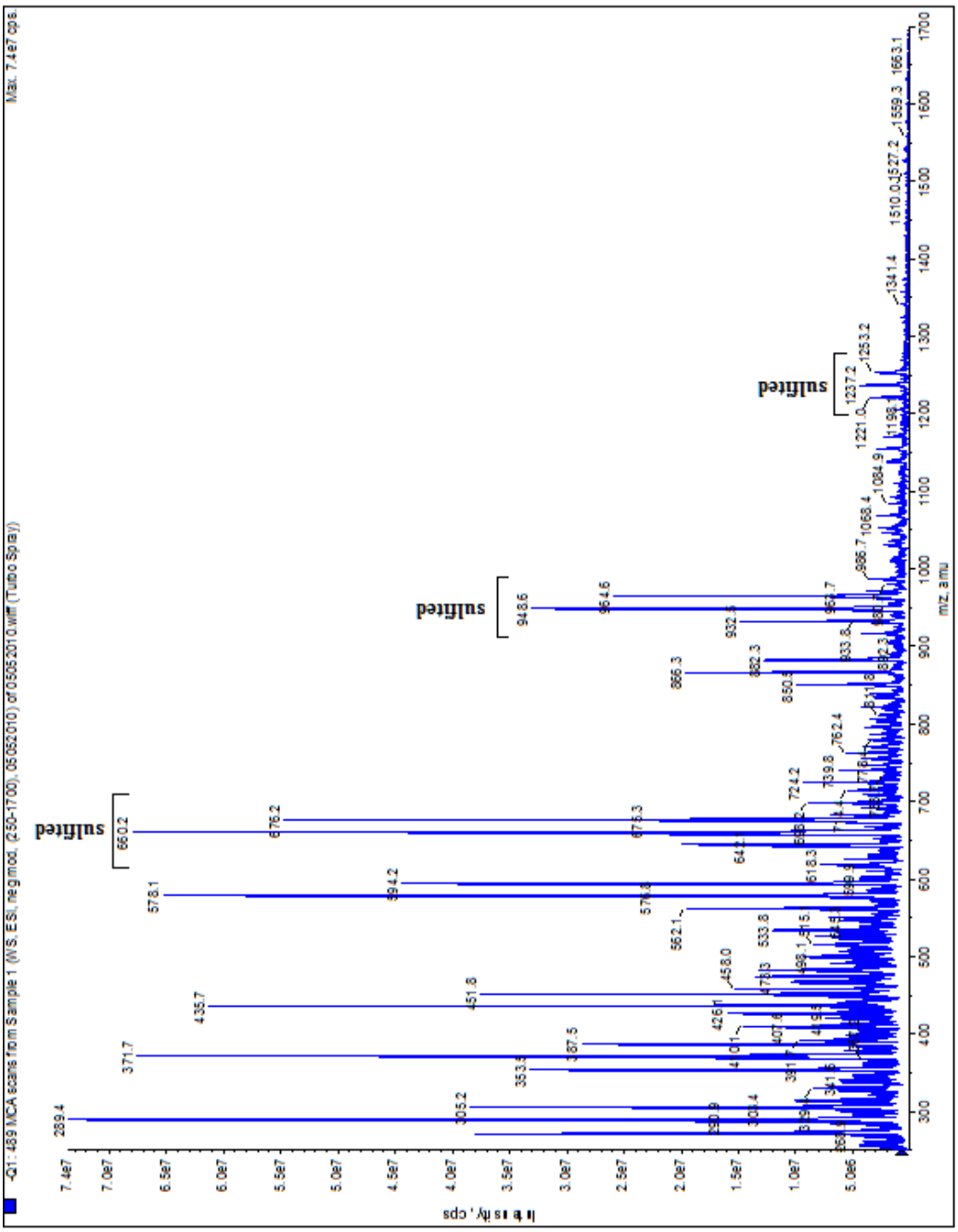

Plate 5-6: Electrospray Ionisation of heavily sulfited industrial mimosa tannin extract (WS)

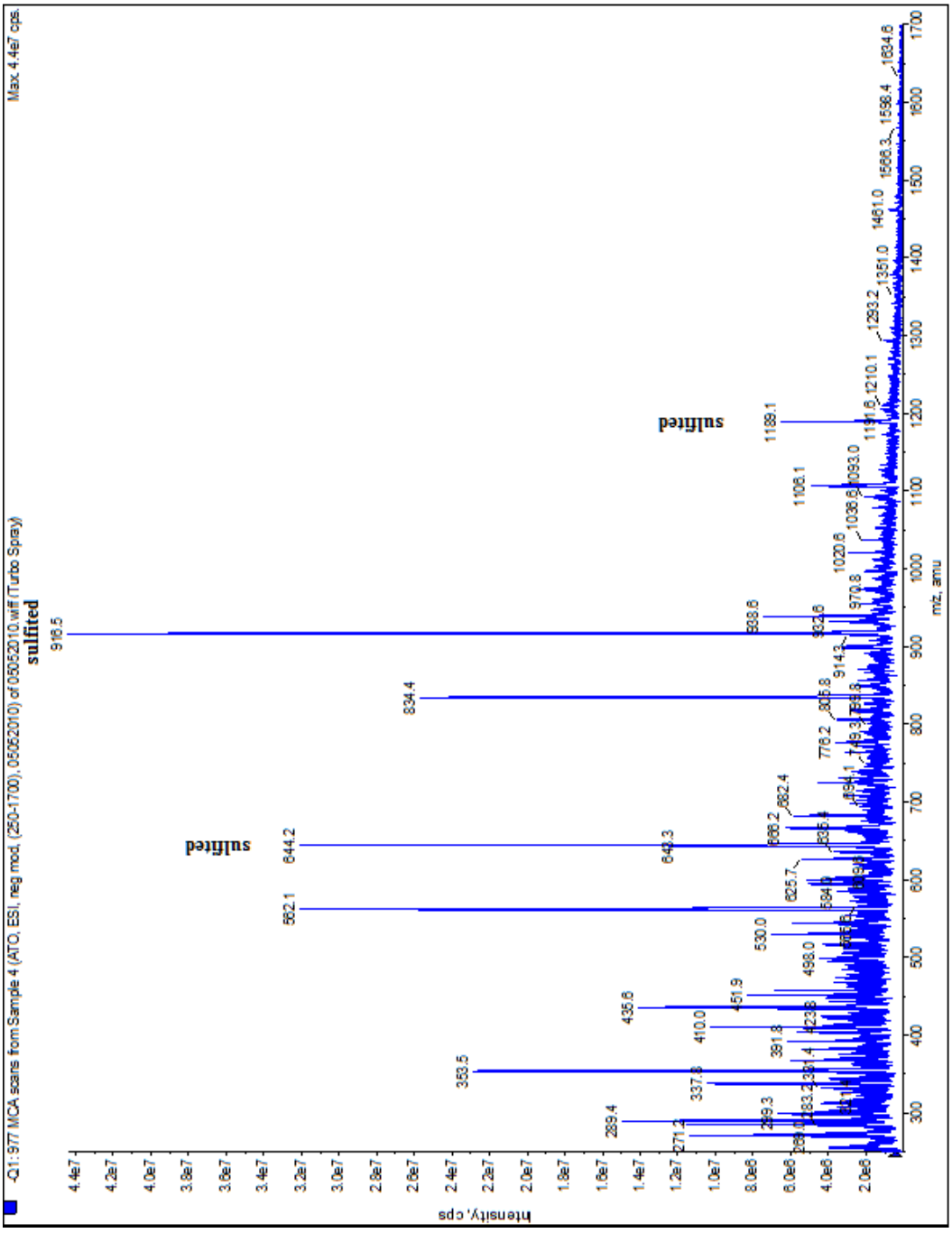

Plate 5-7: Electrospray Ionisation of sulfited industrial quebracho tannin extract (ATO)

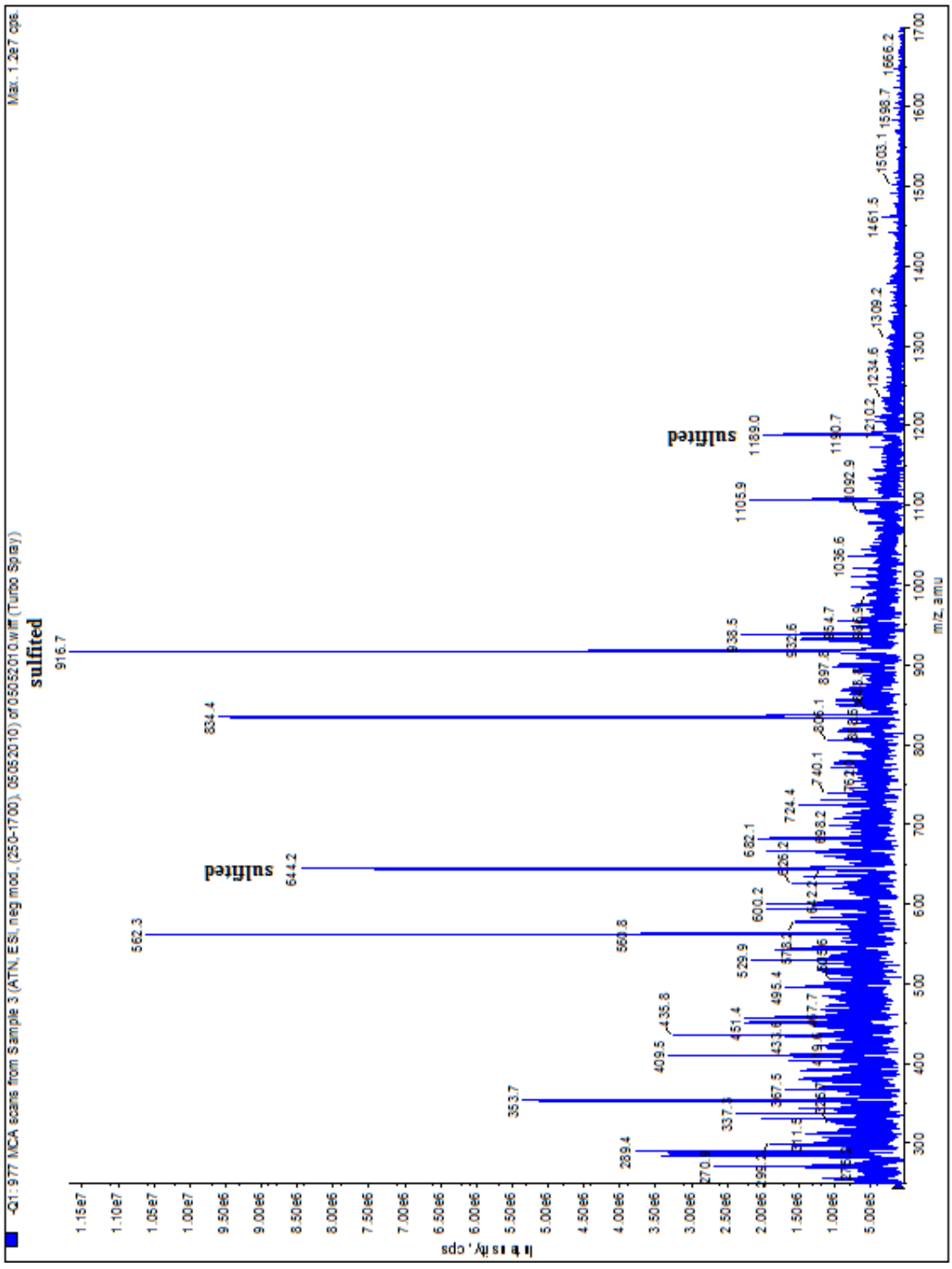

Plate 5-8: Electrospray Ionisation of heavily sulfited industrial quebracho tannin extract (ATD)

Table 5-5: ESI Peak values comparing normal, sulfited and heavily sulfited mimosa										
Calculated Mass		**PF**	**PR**	**PD**	**Observed Mass**		**Observed Mass**		**Observed Mass**	
		272.3	**288.3**	**304.3**	**Normal Mimosa**	**Intensity (%)**	**Sulfited mimosa**	**Intensity (%)**	**Heavily sulfited mimosa**	**Intensity (%)**
*Monomers**										
272.3		1	0	0	271.2	16.88	271.2	35.94	271.2	68.57
288.3		0	1	0	289.2	76.36	289.3	100.00	289.3	100.00
304.3		0	0	1	305.2	32.74	305.3	51.36	305.3	48.52
Sulfited Monomers										
354.3		1	0	0			353.3	11.99	353.3	27.70
370.3		0	1	0			371.2	41.97	371.2	46.82
386.3		0	0	1			387.2	16.47	387.2	19.14
Dimers										
560.6		1	1	0	561.3	27.00	561.4	21.49	561.3	16.54
592.6		0	1	1	593.2	67.29	593.3	53.38	593.3	42.60
576.6		0	2	0	578.3	100.0	577.3	78.68	577.3	60.49
Sulfited Dimers										
642.6		1	1	0			643.2	8.52	643.2	13.38
674.6		0	1	1			675.5	23.48	675.3	33.53
658.6		0	2	0			659.3	32.09	659.2	47.11
Trimers										
832.9		2	1	0	833.3	5.34	833.4	4.17	833.2	2.74
848.9		1	2	0	849.3	19.67	849.4	15.51	849.2	8.36
864.9		1	1	1	865.3	43.28	865.2	30.75	865.2	17.34
	or	0	3	0						

880.9		0	2	1	881.2	28.25	881.3	19.73	881.5	10.22
Sulfited Trimers										
914.9		2	1	0			915.5	2.27	915.4	3.19
930.9		1	2	0			931.4	6.58	931.4	9.38
946.9		1	1	1			947.5	14.54	947.5	17.74
	or	0	3	0						
962.9		0	2	1			963.5	10.00	963.5	12.48
Tetramers										
1137.2		2	1	1	1137.2	2.72	1137.3	2.32	1137.3	1.28
1137.2	or	1	3	0	1137.2	2.72	1137.3	2.32	1137.3	1.28
1153.2		1	2	1	1153.4	4.19	1153.4	3.33	1153.3	1.50
	or	0	4	0						
1169.2		1	1	2	1169.3	3.67	1169.3	1.99	1169.4	1.42
	or	0	3	1						
1169.2					1169.3	3.67	1169.3	1.99	1169.4	1.42
Sulfited Tetramers										
1219.2		2	1	1			1219.4	1.35	1219.6	1.25
	or	1	3	0						
1235.2		1	2	1			1235.4	2.02	1235.5	1.81
	or	0	4	0						
1251.2		1	1	2			1251.3	1.56	1251.5	1.33
	or	0	3	1						

* Number combination of monomers observed

Table 5-6: ESI Peak values comparing normal, sulfited and heavily sulfited quebracho										
Calculated Mass		**PF**	**PR**	**PD**	**Observed Mass**	**Intensity (%)**	**Observed Mass**	**Intensity (%)**	**Observed Mass**	**Intensity (%)**
		272.3	**288.3**	**304.3**	**ATN**		**ATO**		**ATD**	
Monomers										
272.3		1	0	0	271.2	27.26	271.2	25.66	271.2	88.26
288.3		0	1	0	289.2	97.27	289.4	33.58	289.3	83.77
		0	0	1						
Sulfited Monomers										
354.3		1	0	0			353.5	51.53	353.3	100.00
370.3		0	1	0			372.8	6.9	371.3	10.13
386.3		0	0	1					387.3	5.95
Dimers										
560.6		1	1	0	561.4	100.00	562.1	72.2014	561.4	76.41
576.6		1	0	1	577.2	4.32	577.3	5.4633	577.2	5.69
	or	0	2	0						
592.6		0	1	1	593.2	1.06	593.5	9.7483	593.2	12.11
Sulfited dimers										
626.6		2	0	0			625.7	12.2121	625.3	14.82
642.6		1	1	0			644.3	72.0943	643.4	64.75
658.6		1	0	1			657.5	4.9813	657.4	3.82

674.6		0	1	1			674.3	4.0171	675.3	2.47
658.6		0	2	0					659.5	4.72
Trimers										
832.9		2	1	0	833.3	79.25	834.4	57.8468	833.3	30.95
848.9		2	0	1	849.3	5.19	848	4.4456	849.3	2.55
	or	1	2	0						
864.9		1	1	1	865.4	1.60	864.6	2.4638	865.2	2.02
	or	0	3	0						
896.9		0	1	2			897.6	7.3915	897.2	5.32
Sulfited Trimers										
914.9		2	1	0			916.5	100	915.4	59.80
930.9		2	0	1			932.6	8.9448		
	or	1	2	0						
Tetramers										
1105.2		3	1	0	1105.4	11.90	1106.1	11.0873	1105.4	4.50
1121.2		3	0	1	1121.4	1.53	1121.7	2.3032	1121.5	1.12
	or	2	2	0						
Sulfited Tetramers										
1187.2		3	1	0			1189.1	14.676	1187.6	7.12

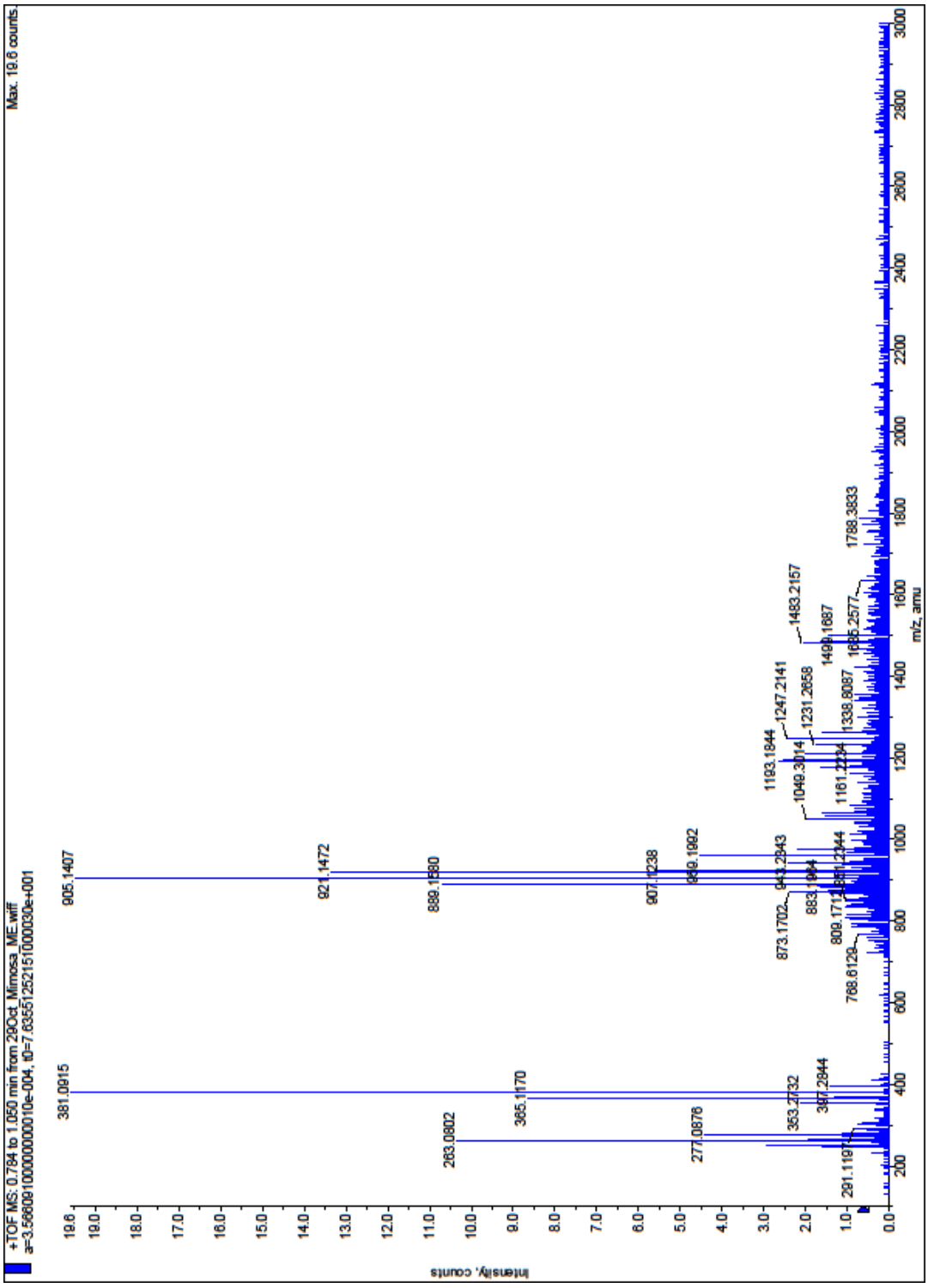

Plate 5-9: High resolution ESI of normal mimosa

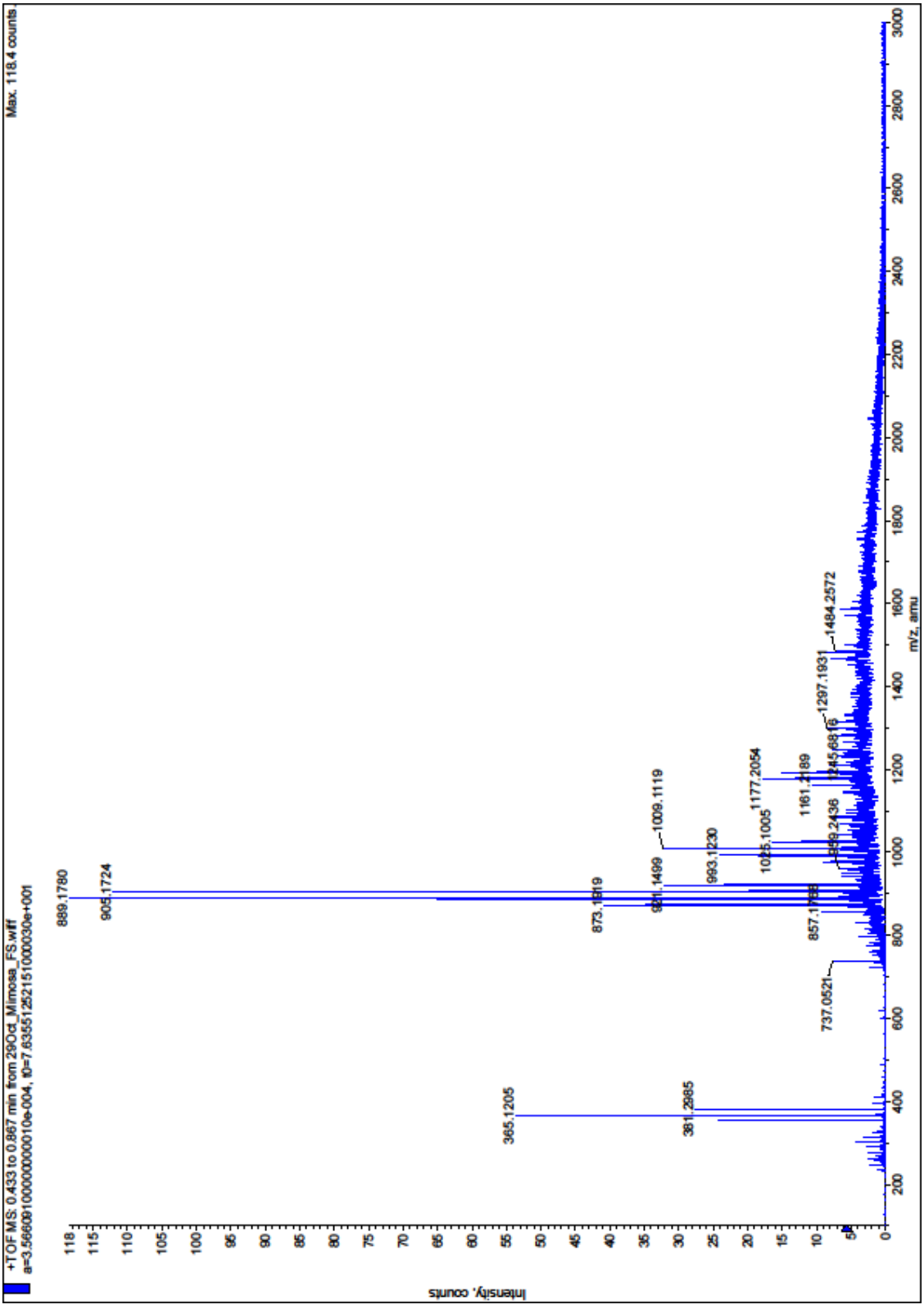

Plate 5-10: High resolution ESI spectrum of sulfited mimosa (FS)

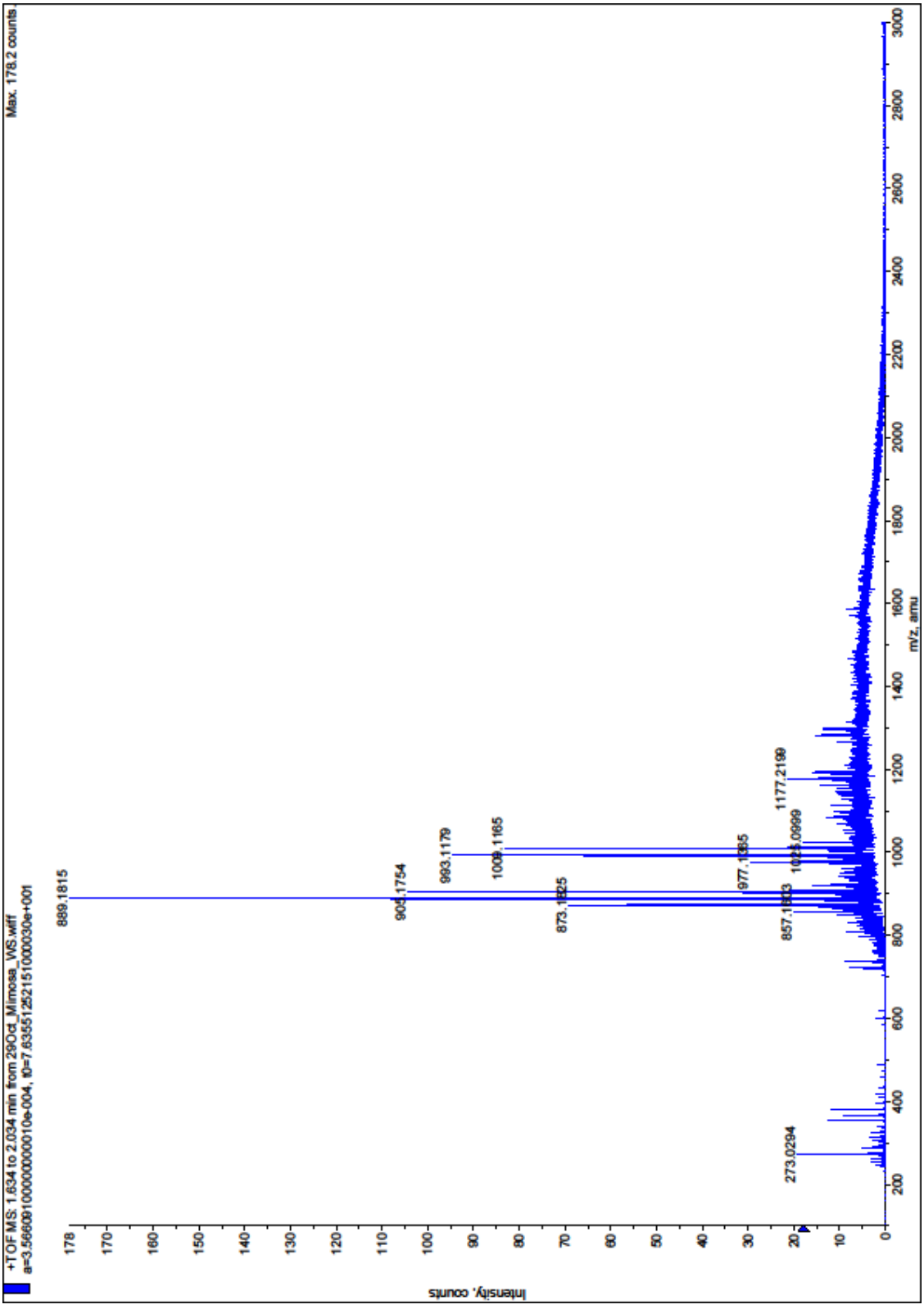

Plate 5-11: High resolution ESI spectrum of heavily sulfited mimosa (WS)

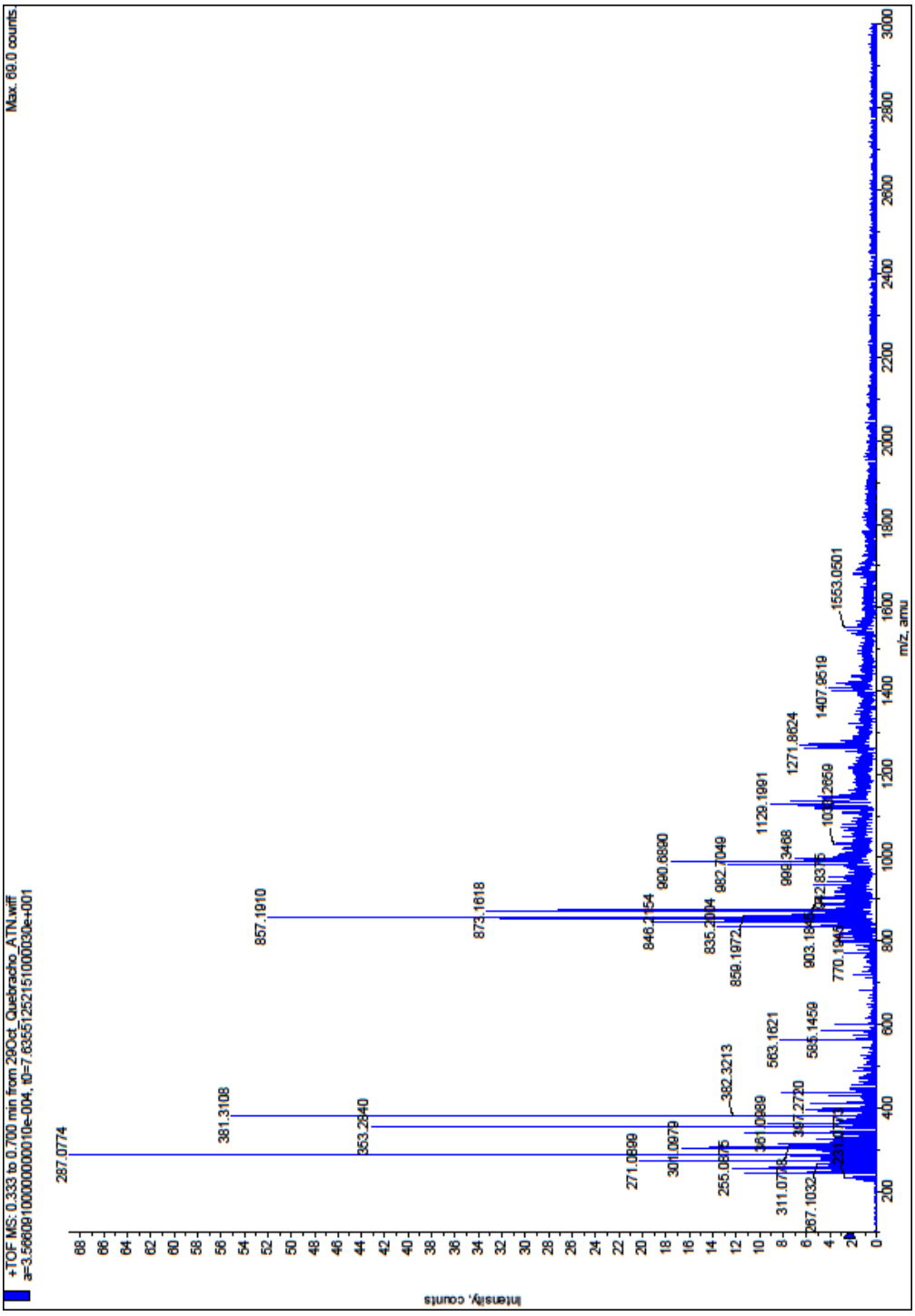

Plate 5-12: High resolution ESI of normal quebracho (ATN)

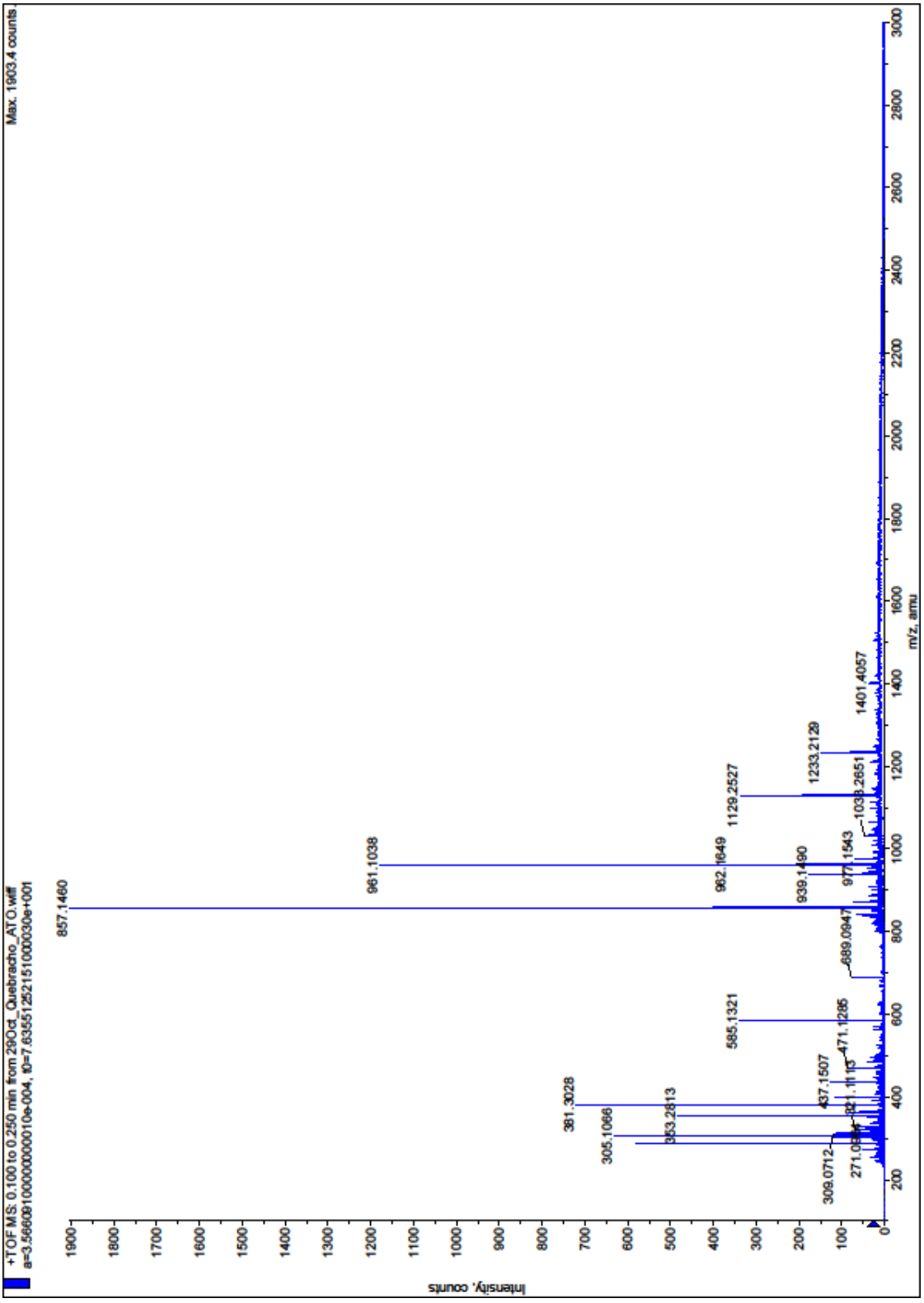

Plate 5-13: High resolution ESI spectrum of sulfited quebracho (ATO)

Chinese Mimosa (Plate 5-14) has a mass spectrum similar to sulfited South African mimosa tannin (ME). It is thus not an untreated natural extract and has been treated with bisulfite. The presence of a resonance at about 82 ppm in the solid state NMR however suggests that 2,3-*trans* stereochemistry is still present. Chinese mimosa is thus probably a lightly sulfited product which some C-rings unopened.

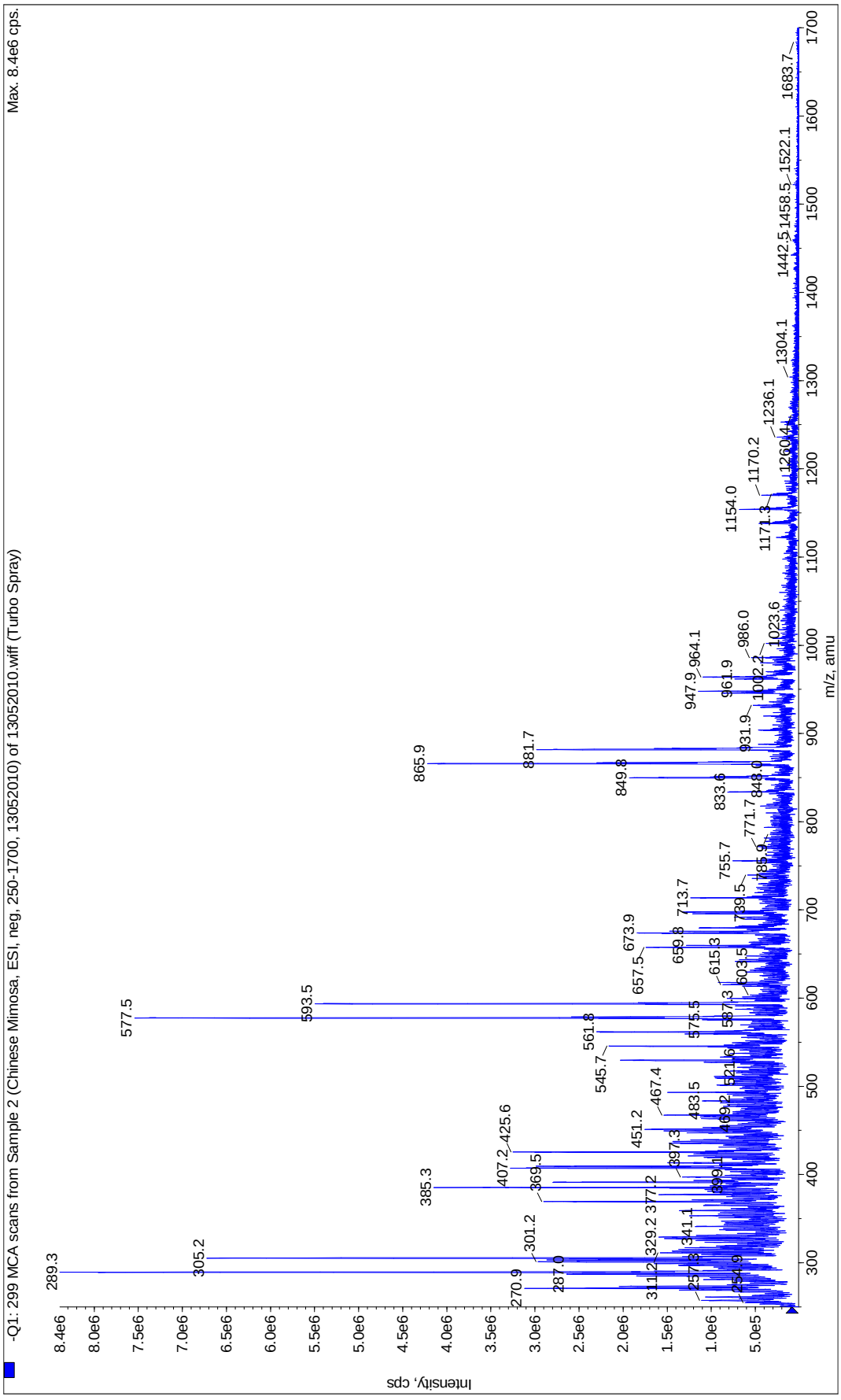

Plate 5-14: Electrospray Ionisation of Chinese mimosa tannin extract

5.4.3 Conclusion

Herein we report for the first time clear evidence of sulfited oligomer molecules, containing a sulfonic acid group. The mass of these species indicate sulfitation on the C-2 position and associated opening of the heterocyclic C-ring. The observation and identification of these sulfited species allow us to use electrospray ionisation MS (but not MALDI-TOF MS) to distinguish unequivocally between sulfited and nonsulfited mimosa and quebracho tannin extracts. It also allows a rough estimate of the level of sulphur incorporation into the tannin molecules. Electrospray ionisation MS allowed us, *via* identification of the sulfited molecules, to classify commercial chinese mimosa as a lightly sulfited mimosa extract.

5.5 Experiment 3. The use of MS to distinguish between condensed and hydrolysable tannins

5.5.1 Introduction

Hydrolisable tannins are galloyl (1) and hexahydroxydiphenoyl (2) esters (see Figure 5-5), most often with D-glucose and derivatives. Chestnut and tara are examples of hydrolysable tannins.

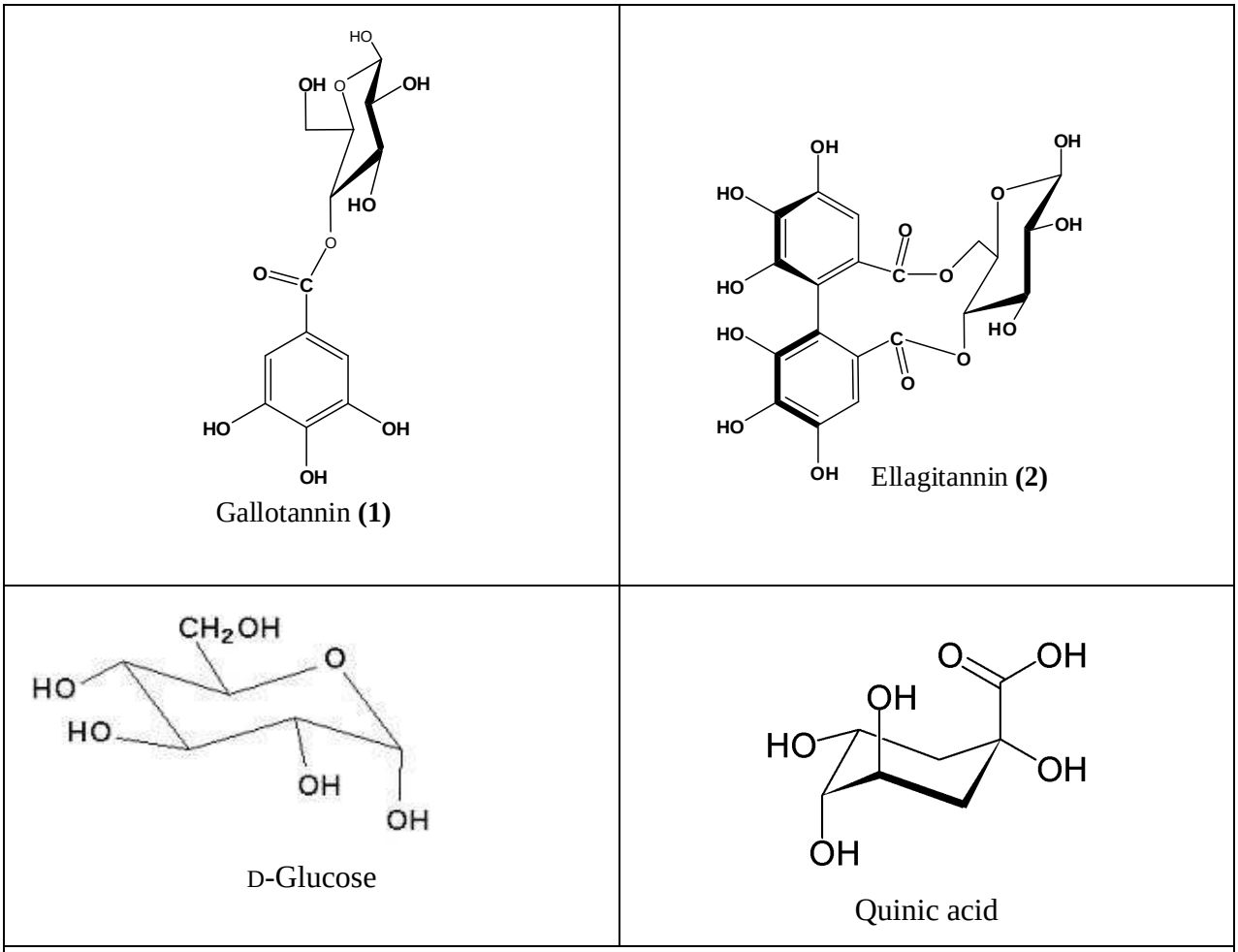

Figure 5-5: Hydrolysable tannins building blocks

5.5.2 Results and Discussion

In this experiment we compared tara, italian chestnut and chinese yugan. Tara (ESI Plate 5-15) shows a beautiful and well defined series of peaks in the negative mode $(M-1)^-$ at 343.3, 495.2, 647.7, 799.5 and 952.0 corresponding to the sodium adduct (+22) of a glucopyranose quinic acid attached to one, two, three, four and five gallic acid units respectively. The peak at 321 corresponds to a monogaloylated quinic acid without sodium. Sodium adducts contributes

towards stabilisation of mass spectrometry fragments and we assume that only the monogaloylated quinic acid is sufficiently stable to be observed without sodium.

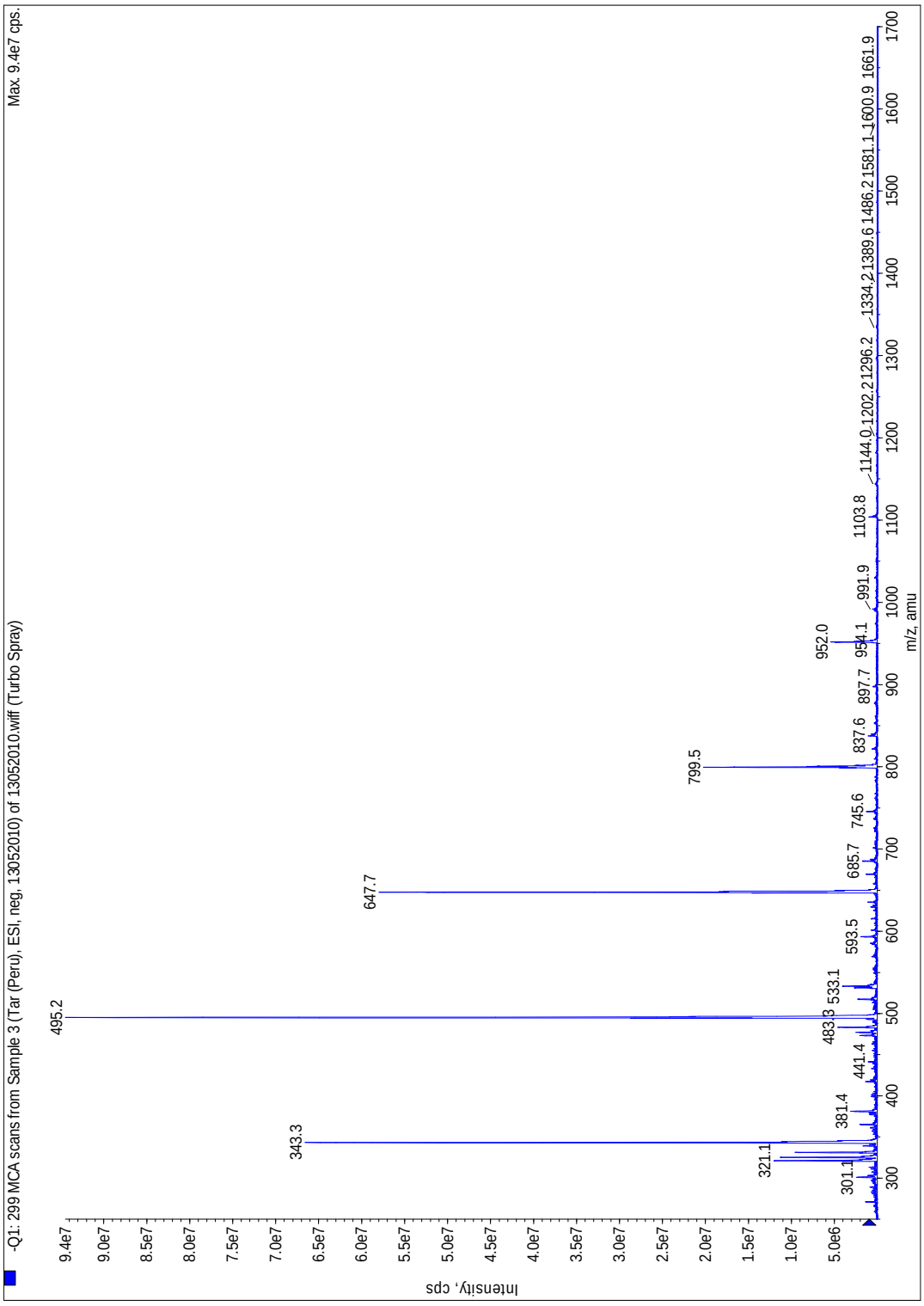

Plate 5-15: Electrospray Ionisation of Tara from Peru tannin extract

The molecular structure for tara tannin is shown in Figure 5-6. It shows that tara tannin is a mixture of gallic acid polymers with a quinic acid unit at its core. Quinic acid is acetylated by a changing number of gallic acid units.

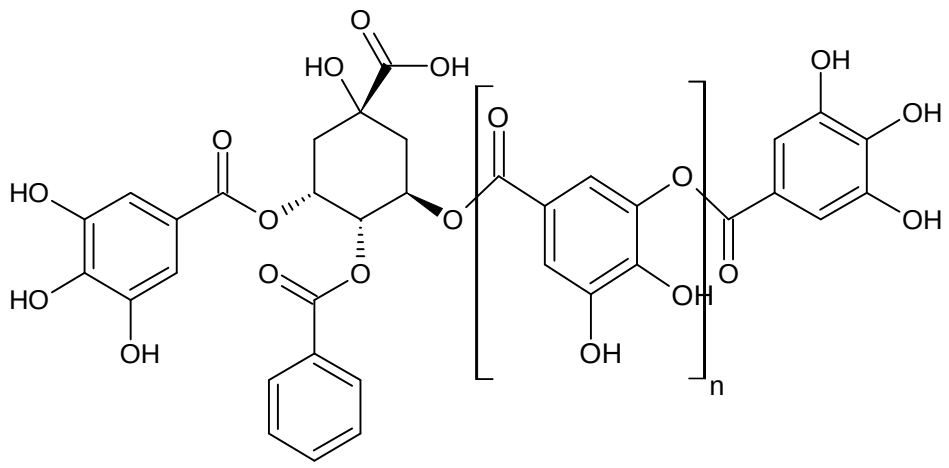

Figure 5-6: The tannin structure of tara, showing galloylated quinic acid

Table 5-7, taken from the Mané[8] MALDI-TOF (Figure 5-7) and our own electrospray results (Plate 5-15), shows the estimated composition of tara tannin.

Table 5-7: Estimated composition of tara tannin from MALDI-TOF and electrospray[8]

Number of gallic ester units attached to the quinic acid core	MW	MALDI $[M+Na]^+$ calculated	$[M+Na]^+$ *m/z* detected	Intensity %	ESI $[M+Na]^+$ calculated	$[M+Na]^+$ *m/z* detected	Intensity %
1G	344.07	367.06			343.07	343.3	71
2G	496.08	519.08	519.06	42	468.08	495.	100
3G	648.10	671.09	671.14	83	647.10	647.7	62
4G	800.11	823.10	823.18	100	799.11	799.5	21
5G	952.12	975.11	975.19	99	951.12	952.0	5
6G	1104.13	1127.12	1127.2	70	1103.13	103.8	-

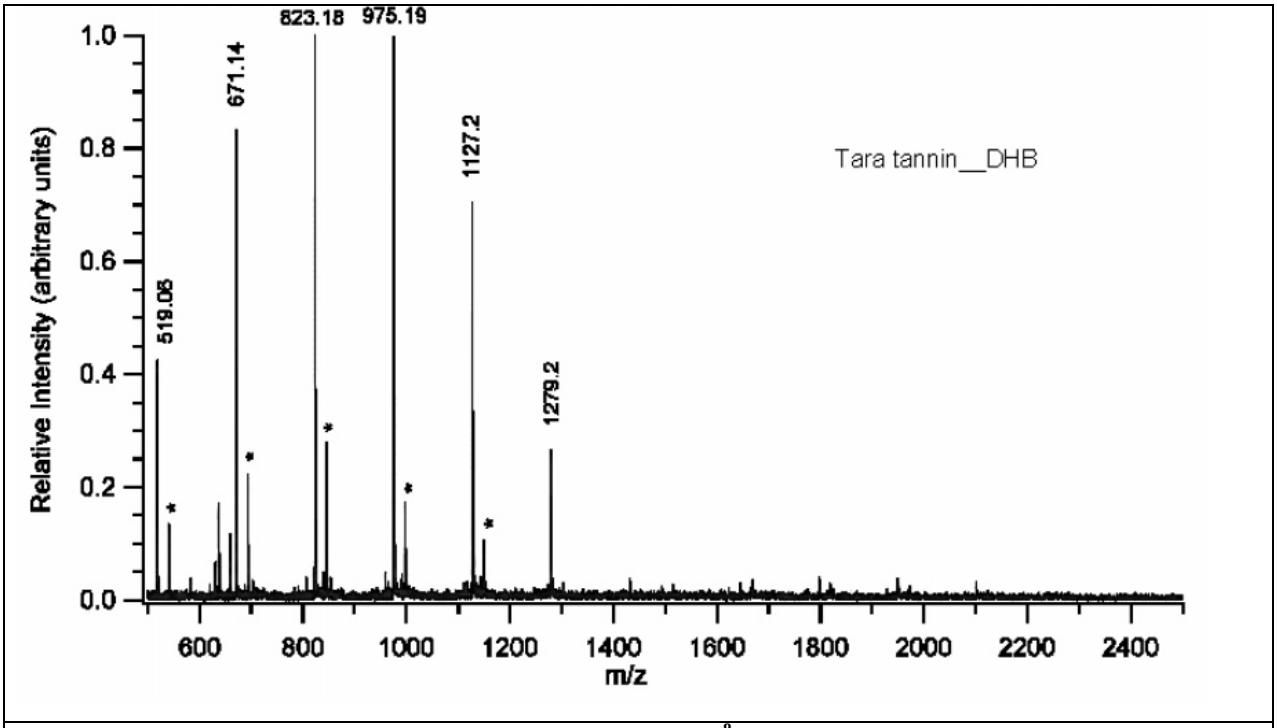

Figure 5-7: MALDI-TOF spectra of tara as obtained by Mané[8]

The electrospray ionization MS of italian chestnut (Plate 5-16) is similar to the MALDI-TOF MS published by Pasch and Pizzi[9] (Figure 5-8). As expected, the smaller oligomers are emphasized in the ESI spectrum relative to the larger oligomers in the MALDI-TOF. It differs from the electrospray spectrum of chestnut extracted by Zywicki *et al.*[10] from tannin wastewater. We detected two overlapping series of oligomers. The first series consists of mono-, di- and tri-galloylated glucose, also called gallotannins (M^+: m/e = 331.2, 483.7 and 635.6 respectively). Gallic acid is not detected. The second series consists of ellagic acid esters of glucose, also called ellagitannins (M^+: m/e = 301 [ellagic acid], 631, 933.9 and 1085.9 respectively). Peaks at 283.4, 613.3 and 915.8 correspond to a loss of water (M – 18) from the ellagitannin peaks. An example of the structure of the 635.6 gallotannin and the 933.9 ellagitannin (castaglagin / vescalin) are given in Figure 5-9.

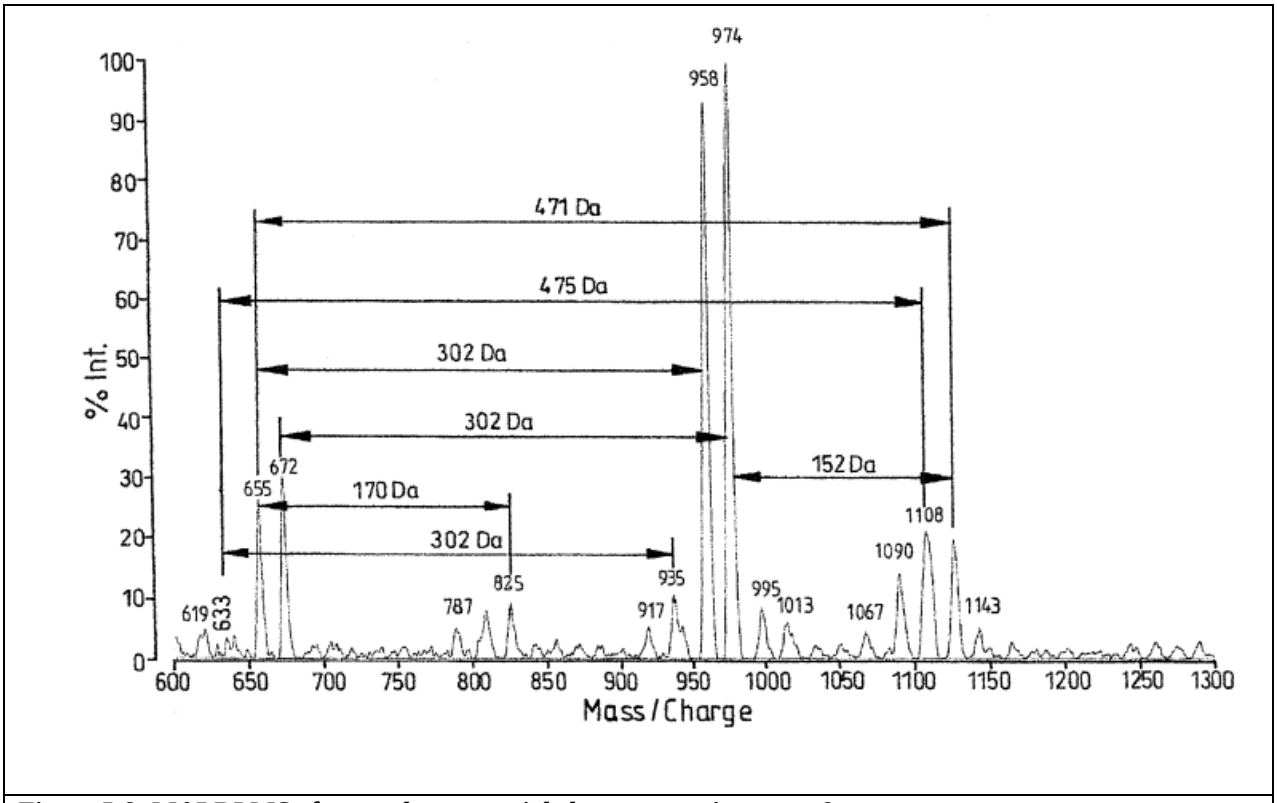

Figure 5-8: MALDI MS of natural commercial chestnut tannin extract9

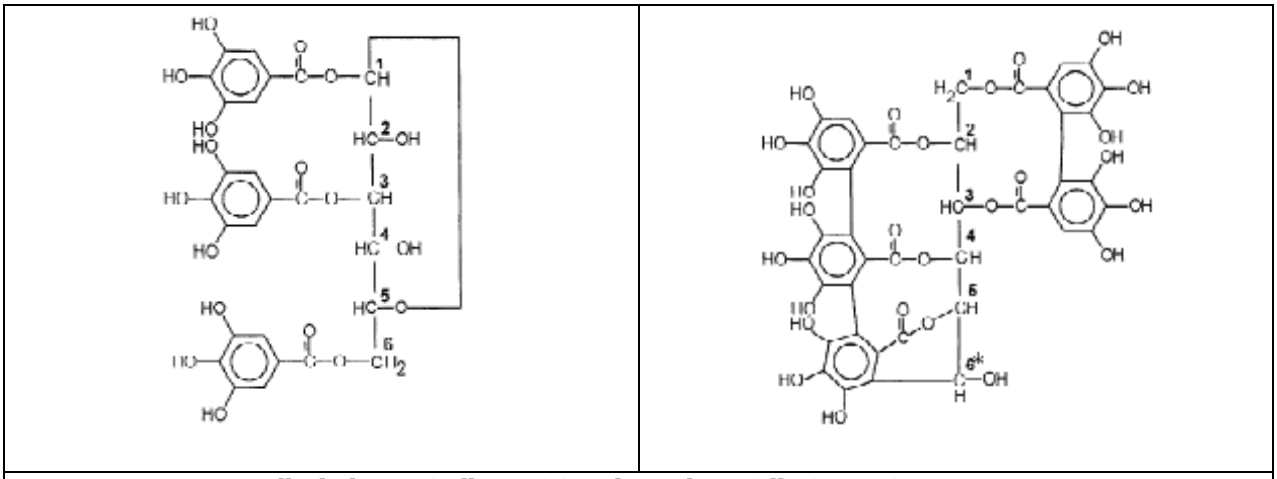

Figure 5-9: 1,3,6-Trigalloyl-glucose (gallotannin) and castalagin (ellagitannin)

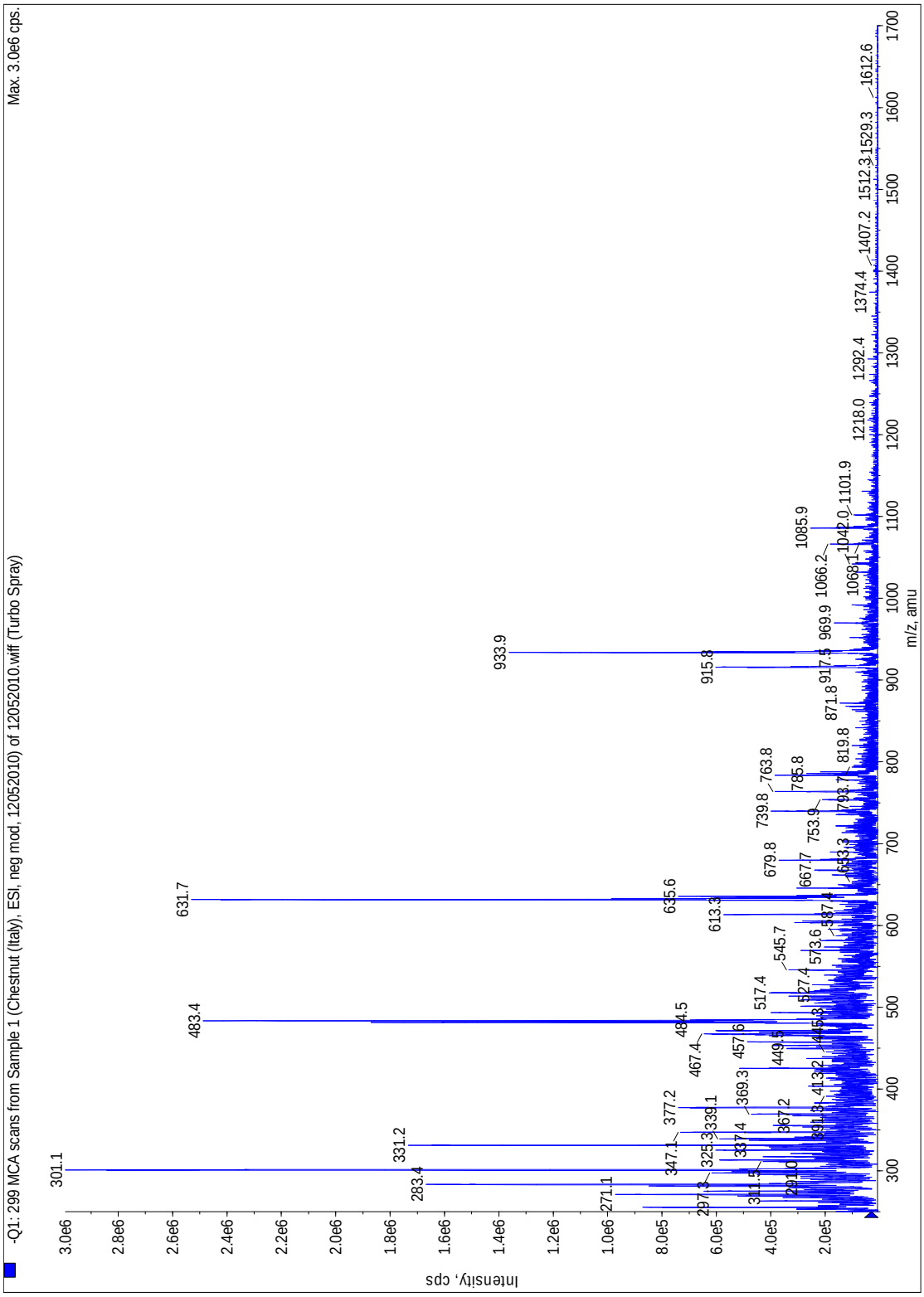

Plate 5-16: Electrospray Ionisation of chestnut Italy tannin extract

Chinese yugan has a spectrum (Plate 5-17) similar to that of tara. Salient is the absence of clusters of peaks 16 amu apart. Instead it is clearly a gallic acid oligomer with peaks 152 amu apart at 343.3, 495.3, 647.7, 799.5 and 951.9 Da. 951.9 Da. The basic 343.3 peak corresponds with quinic acid esterified with one molecule of gallic acid (the corresponding glucose gallic acid dimer would have a mass of 350). The peaks also do not correspond with those of quebracho.

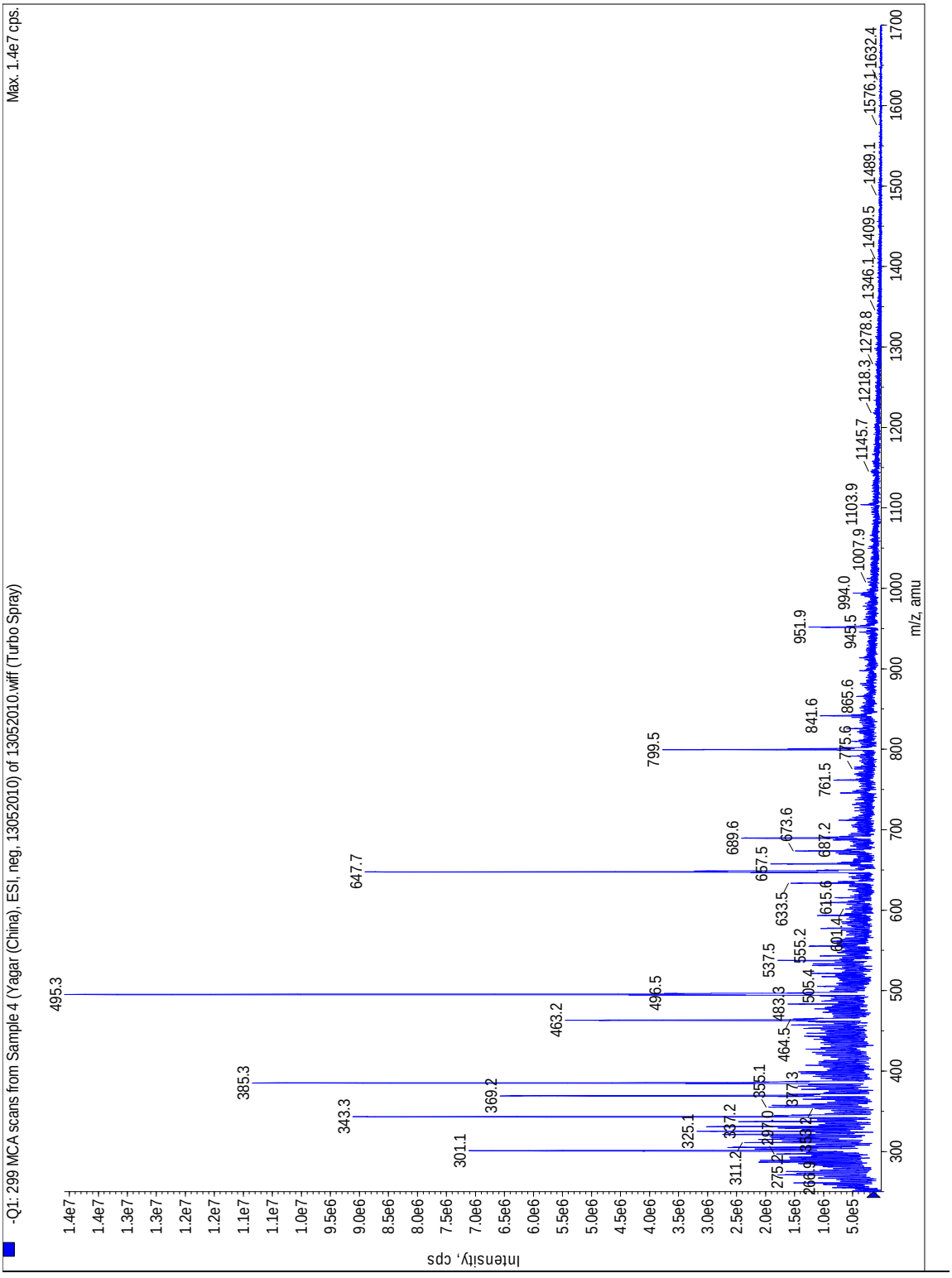

Plate 5-17: Electrospray Ionisation of yugan tannin extract

5.5.3 Conclusion

MALDI-TOF and electrospray ionization mass spectrometry are excellent techniques in analysing and distinguishing hydrolysable and condensed tannins once the fragmentation has been worked out. It can differentiate between tara (a hydrolysable tannin based on a quinic acid core) and italian chestnut (a hydrolysable tannin based on a glucose core). It can be used to calculate a rough estimate of the ratio of mono-, di- and trimmers in a polymer chain. MALDI-TOF emphasizes the bigger molecules better than ESI, although ESI shows doubly ionized molecules. ESI also emphasizes the smaller molecules much clearer than MALDI does.

5.6 Experiment 4: Calculation of the fraction of each oligomer in mimosa tannin

5.6.1 Introduction

As discussed in Chapter 2 (Literature), the average chain length of mimosa and quebracho tannin has been established by a variety of techniques, including ebulliomery and ^{13}C mass spectrometry. None of these techniques can be considered totally reliable as each requires certain assumptions. Mass spectrometry can also be used, using the assumption that mass discrimination does not take place. We assume that the surface area below each peak is an accurate estimate of the corresponding molecules concentration in the mixture. A further assumption is that if mass discrimination does take place, the larger oligomers will be underestimated and that the average chain length will in fact be bigger than the estimate and that the estimate is a minimum value.

5.6.2 Results and Discussion

We used both the modified Pasch[1] MALDI-TOF data and our own electrospray results to approximate the composition of the condensed tannin (polyphenolic) fraction of both mimosa and quebracho extracts. The ESI spectra were used to extrapolate the relative intensity of the monomer and dimer fraction (via the intensity of peaks that occur both in MALDI-TOF and electrospray) for the MALDI spectra, as the MALDI spectra do not show the lower molecular mass molecules. The results are summarised in Table 5-8 and Table 5-9. The higher oligomers in the tables are most likely underestimated since bigger molecules do not ionize or evaporate under mass spectrometry conditions as effectively as small molecules do.[13,14]

Table 5-8: Approximate composition by weight of the condensed tannin (polyphenolic) fraction of commercial mimosa extract (ME).		
n	**% Oligomer**	**Pasch**
1	Monomers	1.2
2	Dimers	5.1
3	Trimers	27.1
4	Tetramers	24.5
5	Pentamers	21.1
6	Hexamers	11.3
7	Septamers	5.8
8	Octamers	3.9
Sum		100

Table 5-9: The approximate composition of quebracho extract by weight based on MALDI-TOF data		
n	**Oligomer**	**Percentage**
1	Monomer	13
2	Dimer	18
3	Trimer	18
4	Tetramer	23
5	Pentamer	14
6	Hexamer	7
7	Septamer	5
8	Octamer	3

5.6.3 Conclusion

According to the tables above, mimosa consists mainly of trimers, tetramers and pentamers, and quebracho mainly of dimers, trimmers and tetramers. The average chain length (DPn) (by mass), according to Table 5-8 and Table 5-9, is 4.36 for mimosa and 3.67 for quebracho. It must be reiterated that the higher oligomers in the tables are most likely underestimated and hence a thorough image of the polyphenolic composition cannot be made with certainty.

5.7 References

1. Schofield, P.; Mbugua, D. M.; Pell, A. N. *Animal Feed Science and Technology*, 2001, 91, 21-40.
2. Monegar, *Journal of Pharmaceutical and Biomedical Analysis*, 338-372H.
3. Pasch, A. Pizzi, K. Rode, *Polymer*, **2001**, *42*, 7531–7539.
4. Vivas, N.; Nonier, M.; de Gaulejac, N. V.; Absalon, C.; Bertrand, A; Mirabel, M. *Analytica Chimica Acta*, **2004**, *513*, 247 – 256.
5. Covington, A. D.; Lilley, T. H; Song, L. *JALCA*, **2005**, *100*, 325–335.
6. Tambi, L.; Frediani, P.; Frediani, M.; Rosi, L.; Camaiti, M. *Wiley InterScience*, **2008**.
7. McMaster, M. C. *LC/MS A Practical user's Guide*, **2005**, John Wiley & Sons, Inc, Hoboken, New Jersey, 64, 109.
8. Mané, C.; Sommerer, N.; Yalcin, S.; Cheynier, V.; Cole, R.B.; Fulcrand, H. *Anal. Chem.*, **2007**, *79*, 2239 – 2248.
9. Pasch, H.; Pizzi, A. *J. Applied Pol. Science*, **2002**, *85*, 429-437.
10. Zywicki, B.; Reemtsma, T.; Jekel, M. *Journal of Chromatography A*, **2002**, *970*, 191 – 200.
11. Thompson, D.; Pizzi, D. *J. Appl. Polym. Sc.* **1995**, *55*, 107.
12. Fetchal, M.; Riedl, B. *Holzfoschung*, **1993**, *47*, 349.
13. Roux, D. G.; Evelyn, S. R. *Biochem J.* **1958**, *69*, 530.
14. Roux, D. G.; Evelyn, S. R. *Biochem J.*, **1960**, *76*, 17.

CHAPTER 6

6. EXPERIMENTAL CONDITIONS

6.1 SPECTROSCOPIC METHODS

6.1.1 Purification and Methylation of Extracts

6.1.1.1 Purification of extracts

Samples of the methanol extract of fresh bark and the methanol extract of stick bark were prepared by the Mimosa Extract Company.

N3: Ethanol extract from mimosa stick bark

Crude mimosa stick bark (10 g) was extracted in a soxhlet with ethanol (100 mL). The solvent was removed on a rotary evaporator to yield an extract of tannins and sugars (6.5 g).

N4: Lead acetate precipitate of the ethanol extract from mimosa stick bark

The tannins from mimosa stick bark were precipitated with lead acetate according to the method of Roux et al.[1] The ethanol extracted tannin (N3, 6.5 g) was dissolved in water (approx. 100 ml). While stirring the tannin solution, a strong solution of neutral lead acetate (1.5 g, 10%) was added in slight excess. A white precipitate of lead tannate formed immediately. The lead tannate was centrifuged at 10 000 G and 25 000 revolutions per minute, to remove the gums. The tannate was washed with H_2O (3 x 5 ml) to remove all non-tannins and excess lead acetate. The solvent was evaporated by rotary evaporation, the product air-dried and grounded into a powder.

N5: Ethanol precipitated gums from an aqueous solution of spray dried mimosa

Mimosa (ME) (1 g) was dissolved in water (10 ml). Ethanol (190 ml, 95%, v / v) was added and the mixture allowed to stand at room temperature for approximately 12 hours. The solution was

centrifuged at 25 000 revolutions per minute. The gum fraction was separated from the supernatant by decantation, air-dried and grounded into a powder.

N6: Supernatant from an ethanol extracted aqueous solution of spray dried mimosa

The solvent of the supernatant from N5 was removed by rotary evaporation to yield a fraction containing tannins and sugars. The product was grounded into a powder.

N7: Lead acetate precipitate from an ethanol extracted aqueous solution of spray dried mimosa

The supernatant from an ethanol extracted aqueous solution of spray dried mimosa (ME) was made up as in the method followed for N6. The supernatant (0.87 g) was dissolved in water (aprox. 50 ml). While stirring the tannin-sugar solution, a strong solution of neutral lead acetate (3 g, 10 %) was added in slight excess. A white precipitate of lead tannate formed immediately. The lead tannate was centrifuged at 25 000 revolutions per minute. The tannate was washed with H_2O (3 x 5 ml) to remove all non-tannins and excess lead acetate. The solvent was evaporated by rotary evaporation and the product air-dried. The product was grounded into a powder.

6.2 Solid State Nuclear Magnetic Resonance

Solid state NMR experiments were performed on a Bruker 9.4 Tesla Avance-400 wide bore spectrometer using a dual tuneable broad band probe at frequencies of 400.1 MHz (^{1}H) and 100.5 MHz (^{13}C). Samples were packed into 4 mm zirconia rotors (Bruker, Karlsruhe, Germany) and rotated at a magic angle spinning (MAS) rate of 14 kHz and at the magic angle of 54.7º. All samples were characterized using standard cross polarization (CP) MAS techniques; relevant parameters were: ^{1}H $\pi/2$ pulse length 2.5 μs, ^{1}H cross polarization field 70 kHz, ^{1}H-^{13}C cross-polarization contact time typically 0.5 μs but this was varied in some experiments to study cross polarization dynamics, broadband TPPM decoupling during signal acquisition at a ^{1}H field strength of 100 kHz, and repetition time of 2 s. For quantitative ^{13}C spectra, direct polarization (DP) was used with a $\pi/4$ excitation pulse of 2 μs, broadband TPPM decoupling during signal acquisition at a ^{1}H field strength of 100 kHz, and repetition time of 20 s to ensure complete relaxation between signal acquisitions. Chemical shifts were expressed as parts per million (ppm) on the delta (δ) scale.

The conditions for each experiment were as follows:

6.2.1 ^{13}C CP-MAS

6.2.1.1 Synthesized samples

Prof. D Ferreira (Department of Pharmacognosy, University of Mississippi, USA) provided us with the following synthetic oligomers based on epicatechin and catechin:

B1 - Epicatechin-4α-8-catechin
B2 - Epicatechin-4β-8-epicatechin
B3 – Catechin-4β-8-catechin
B4 – Catechin-4α-8-epicatechin
Trimer 1 – Epicatechin-4α-8-epicatechin-4α-8-epicatechin
Trimer 2 – Catechin-4β-8-catechin-4β-8-epicatechin

Tetramer – Epicatechin-4α-8-epicatechin-4α-8-epicatechin- 4α-8-epicatechin
Pentamer – Epicatechin-4β-8-epicatechin-4β-8-epicatechin-4β-8-epicatechin-4β-8-epicatechin

The optimal values for the cross-polarization contact time P15 were determined by varying P15 between 50 and 1000 µs in six consecutive ^{13}C CP MAS experiments performed on B1 (Experiment 1: Determination of optimum cross polarisation (CP) contact time). P15 times of 500 and 1000 µs were used in all the subsequent ^{13}C CP MAS solid state NMR experiments performed on the other synthetic oligomers.

6.2.1.2 Purified extracts

All ^{13}C CP MAS solid state NMR experiments were performed with P15 set at 500 µs. The following samples were prepared as described in paragraph 6.1.1.1:

N1: Methanol extract of fresh bark, prepared by the Mimosa Extract Company.
N2: Methanol extract of stick bark, prepared by the Mimosa Extract Company.
N3: Ethanol extract of stick bark, consisting of gums, tannins and sugars prepared as described in paragraph 6.1.1.1.
N4: Lead acetate precipitate of N3, consisting of tannins only as described in paragraph 6.1.1.1.
N5: Gums precipitated with ethanol from an aqueous solution of the spray dried commercial mimosa as described in paragraph 6.1.1.1.
N6: Supernatant from N5, consisting of tannins and sugars from the ethanol extract of spray dried commercial mimosa as described in paragraph 6.1.1.1.
N7: Lead acetate precipitate from N6, consisting of tannins only from the spray dried commercial mimosa as described in paragraph 6.1.1.1.

6.2.1.3 Crude extracts

All ^{13}C CP MAS solid state NMR experiments were performed with P15 set at 500 µs:

N9: Powdered fresh mimosa bark, received from the Mimosa Extract Company.
N10: Powdered mimosa stick bark, received from the Mimosa Extract Company.

6.2.1.4 Deuterated samples

N1, the methanol extract of fresh bark, was dissolved in D_2O and left to exchange for 10 minutes and a ^{13}C CP MAS solid state NMR was recorded. The same sample was left to exchange for 24 hours in D_2O and a ^{13}C CP MAS solid state NMR was recorded. Both experiments were done at P15 = 500 µs.

The dimer B2 was deuterated with D_2O for approximately 6 hours. A ^{13}C CP MAS solid state NMR was recorded at P15 = 500 µs.

6.2.2 2D HETCOR Experiments

The 2D HETCOR experiments on the dimer B1, the dimer B2 D_2O exchanged for 6 hours and N1 D_2O exchanged 24 hours were done with P15 set at both 50 µs and 200 µs.

6.2.3 Solid State NMR of Leather

The leather samples were cut into 1 to 2 mm pieces, frozen in liquid nitrogen and ball milled to a fine powder using a Sartorius Mikrodismembrator at 3 000 r.p.m. The ^{13}C signal intensity was enhanced using standard cross polarization (CP) MAS techniques (^1H $\pi/2$ pulse length 2.5 µs, ^1H cross polarization field 70 kHz, ^1H-^{13}C cross polarization contact time 2.5 ms, broadband TPPM15 decoupling during signal acquisition at a ^1H field strength of 100 kHz, recycle time 2 s, typical number of scans accumulated per spectrum ca. 3 000). Chemical shifts were referenced to the methylene signal from glycine at 43.1 ppm relative to tetramethylsilane at 0 ppm.

6.3 Electrospray Ionisation Mass Spectrometry

Experiments were done on two machines. One, an Applied Biosystems API QStar Pulsar I, with Nanospray ESI, the other a Applied Biosystems API 2000 LC/MS/MS System mass spectrometer.

Stock solutions:

Crude sample powder (10 mg) was dissolved in a mixture of methanol: water [50 %, 0.1% formic acid] (1 ml). A 5 µl sample of the stock solution was further diluted by making up a volume of 1 ml in the same solvent mixture (methanol: water, 50 %, 0.1% formic acid). This solution was injected *via* a Harvard 1000 µl syringe at a flow rate of 20 µl / minute by a Harvard-syringe micro pump. The sample was thus delivered into the electrospray ionization source of an Applied Biosystems API 2000 LC/MS/MS System mass spectrometer, operated in the negative mode. The capillary voltage was -4.5 kV, the source temperature 250 °C. The cone voltage was at -4500 V. The declustering potential and focusing potential was set individually for each experiment on both machines to obtain optimal spectral data by adjusting their values and looking at the spectral results after every experimental run. Data was acquired by scanning the mass range from mz = 100 or 250 to m/z = 1700 at a scan rate of 2 seconds/scan. A representative mass spectrum of the sample was produced by addition of the spectra across the injection peak and subtraction of the background.

6.4 References

1. Roux, D. G. *J.S.L.T.C.*, **1949**, *33*, 393 – 407.
2. Furniss, B. S.; Hannaford, A. J.; Smith, P. W. G.; Tatchell, A. R. *Vogel's Textbook of Practical Organic Chemistry*, Pearson Prentice Hall London, **1989**, p. 430 – 431.

7. CONCLUSION

From the experiments done with solidstate NMR, the following conclusions were made:

Hydrolysable and condensed tannins (oligomers of flavan-3-ols) respectively have solid state NMR spectra compatable with their chemical composion. Solid state NMR can therefore be used successfully and reliably to distinguish between these two types of tannins.

Solid state NMR can reliably and routinely be used to also distinguish between quebracho and mimosa tannins. During sulfitation of these two tannins, solid state NMR indicates that the heterocyclic ring is opened

Unprocessed bark as well as tanned leather can be analysed directly to identify the tannin it contains and which tannin was used to tan the leather or whether a mineral tanning material was used.

Spent mimosa bark consists predominantly of water insoluble gums. No higher oligomeric insoluble condensed tannins or hydrolysable tannins remain in spent mimosa bark.

Further work is required to develop the potential of solid state NMR in determinining the average chain length of mimosa and quebracho tannins.

From the experiments doen with mass spectrometry, the following conclusions were made:

Elecrospray ionisation MS allows unambiguous distinction between mimosa and quebracho tannin extracts. It indicates the composition of oligomers for both tannins. Quebracho was argued to consist of a minimum of one robinetinidin monomer plus further fisetinidin monomers that make up the polymer chain.

We reported for the first time clear evidence of sulfited oligomer molecules, containing a sulfonic acid group. The mass of these species indicate sulfitation on the C-2 position and associated opening of the heterocyclic C-ring. The observation and identification of these sulfited species allowed the unequivocal distinction between sulfited and nonsulfited mimosa and quebracho tannin extracts. A rough estimate of the level of sulphur incorporation into the tannin molecules was possible. Electrospray ionisation MS allowed us, *via* identification of the sulfited molecules, to classify commercial chinese mimosa as a lightly sulfited mimosa extract.

The average chain length (DPn) (by mass) is **4.36** for mimosa and **3.67** for quebracho. However, the higher oligomers in the tables are most likely underestimated and hence a thorough image of the polyphenolic composition cannot be made with certainty.

MALDI-TOF is more reliable in showing the higher molecular mass ranges than electrospray, but electrospray is more reliable for the lower ranges than MALDI. However, by using doubly charged ions in electrospray we could detect decamers in the mimosa spectrum.

MALDI-TOF and electrospray ionization mass spectrometry are excellent techniques in analysing and distinguishing hydrolysable and condensed tannins once the fragmentation has been worked out. It can be used to calculate a rough estimate of the ratio of mono-, di- and trimers and high polymers in a polymer chain.

ANNEX A

SOLID STATE NMR FINGERPRINT METHOD for MIMOSA EXTRACT

Solid State NMR (^{13}C) is well suited for fingerprinting organic compounds, particularly because spectra can be obtained from an actual solid powder product without any sample manipulation.

Procedure:

Solid State NMR spectra are obtained on a Bruker Avance 400 MHz spectrometer with the sample in a 4 mm rotor spinning at 14 kHz at the magic angle (54.7^{o}) to the primary 9.4 T magnetic field. The magic angle spinning frequency is chosen so that all spinning side bands fall outside the spectral region of interest at this field strength. A standard cross polarization technique is used to transfer magnetization from ^{1}H to ^{13}C, using 0.5 ms cross polarization, a spin lock field of 70kHz, and recycle time of 2s. High power broadband ^{1}H decoupling (field strength 100 kHz) is applied during signal acquisition. Other spectrometers and primary field strengths may be used but it must be remembered that the position of spinning side bands in the spectrum is spinning speed and field strength dependent. Chemical shifts are referenced to the methylene carbon signal of a previously acquired spectrum of solid glycine at a chemical shift of 43.1 relative to tetramethylsilane.

Chemical shifts are independent of spectrometer, field strength, cross polarization and decoupling methodology and recycle time, but the relative integrated intensity of signals may be dependent on some of these parameters especially cross polarization duration.

Assignments:

Typical chemical shifts encountered with Mimosa extract are:

5C, 7C, 8aC 155 ppm

3'C, 5'C 145 ppm

1'C, 4'C 130 ppm

4aC, 6C, 8C, 2'C,6'C 100 to 120 ppm

2C trans 80 ppm

2C cis 73 ppm

3C 62 ppm

4C internal 40 ppm

4C terminal 30 ppm

NP Slabbert

Mimosa Extract Company (Pty) Ltd.

12 May 2010

ANNEX B

INDEX of FIGURES, TABLES and PLATES

Figures:

Tables:

Plates: